

A multi-scale microscopic dynamical model of heavy ion interacts with biomolecules



Feng-Shou Zhang (张丰收)

College of Nuclear Science and Technology
Beijing Normal University
Beijing, China

Tel: 010-6220 5602

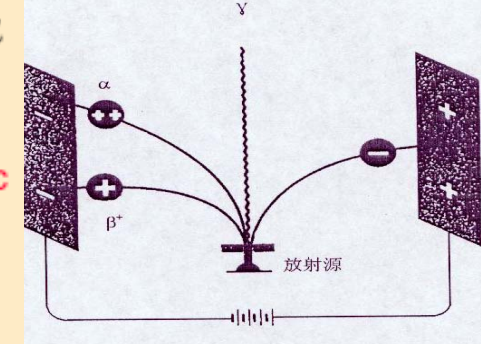
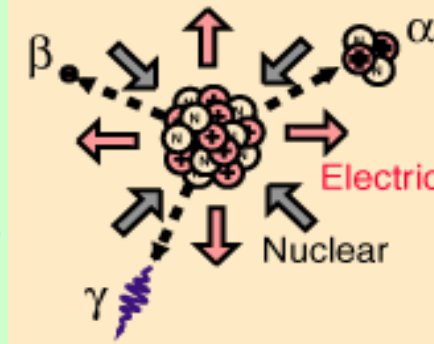
Fax: 010-6223 1765

E-mail: fszhang@bnu.edu.cn

<http://lenp.bnu.edu.cn/hkxyweb/zhangfengshou.htm>

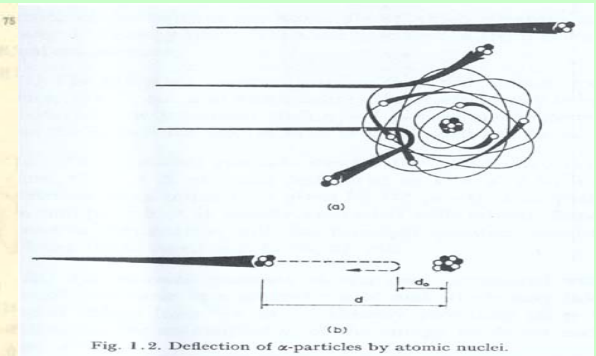


1896 H. Becquerel, from x-rays to
U rays? ($\alpha, \beta^\pm, \gamma, \text{Heavy Ion}$)



1898 M. and P. Curie,
Polonium and Radium, Radioactivity

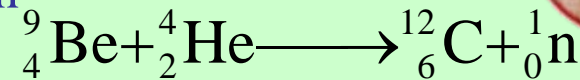
1911 Ernest Rutherford,
theoretical picture
of an atom



1919 E. Rutherford,
the first nuclear reaction in lab , $^{14}\text{N} + \alpha \rightarrow ^{17}\text{O} + p$

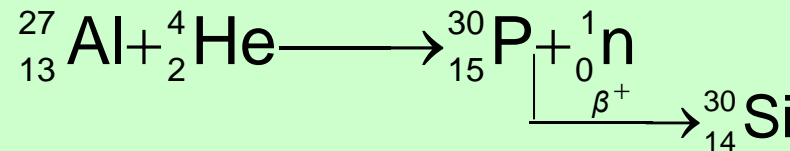
1931 W. Pauli proposed neutrino

1932 J. Chadwick discovered neutron



1932 J. Cockcroft and E. Walton accelerator

1934 I. and F. Joliot-Curie, artificial radioactive isotope

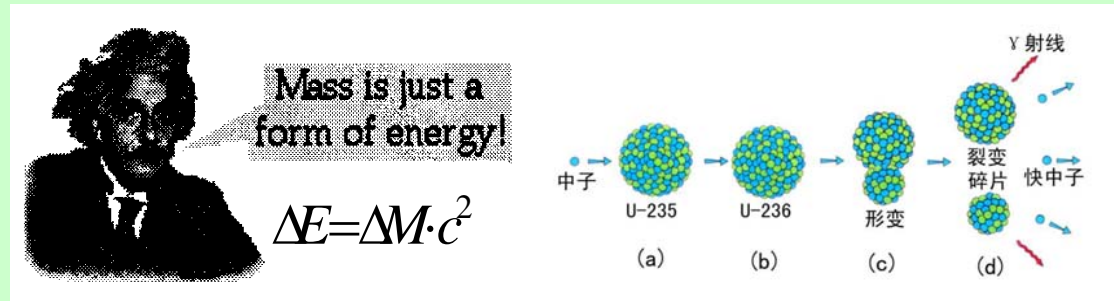


1935 H. Yukawa Pion meson theory

1936 N. Bohr Compound nuclei model

1938 O. Hahn and F. Starssmann, fission (energy: 200 MeV)

1 Kg (U)=
2.7x10⁶Kg (coal)



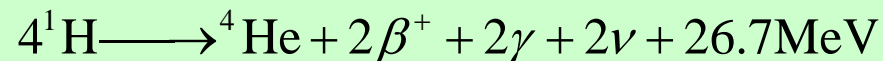
1939 N. Bohr and J. Wheeler, liquid drop model for fission

1942 E. Fermi Reactor, Nuclear energy (52 tons ²³⁵U)

1945 J. R. Oppenheimer, Atomic nuclear bomb

1948 M. Mayer and J. H. Jensen, Shell model

1952 E. Teller Hydrogen bomb

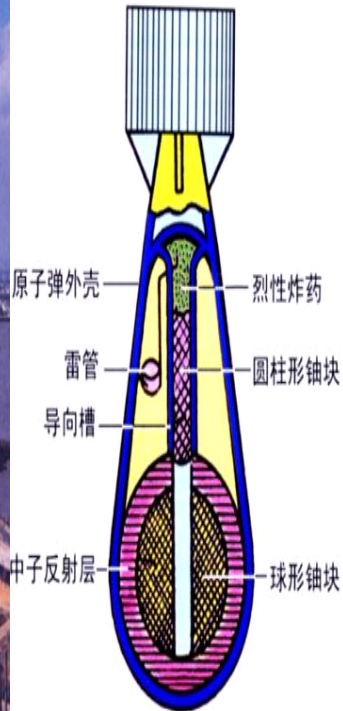


1953 A. Bohr and B. Mottelson, Nuclear collective Model

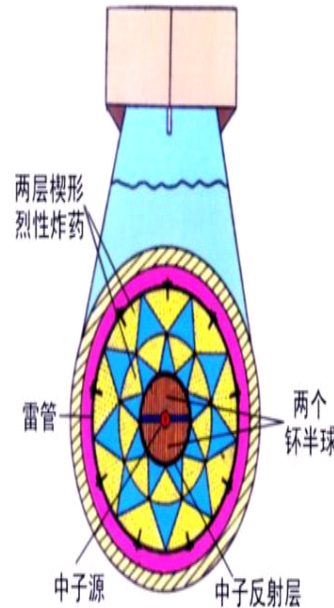
Nuclear Science and Technology



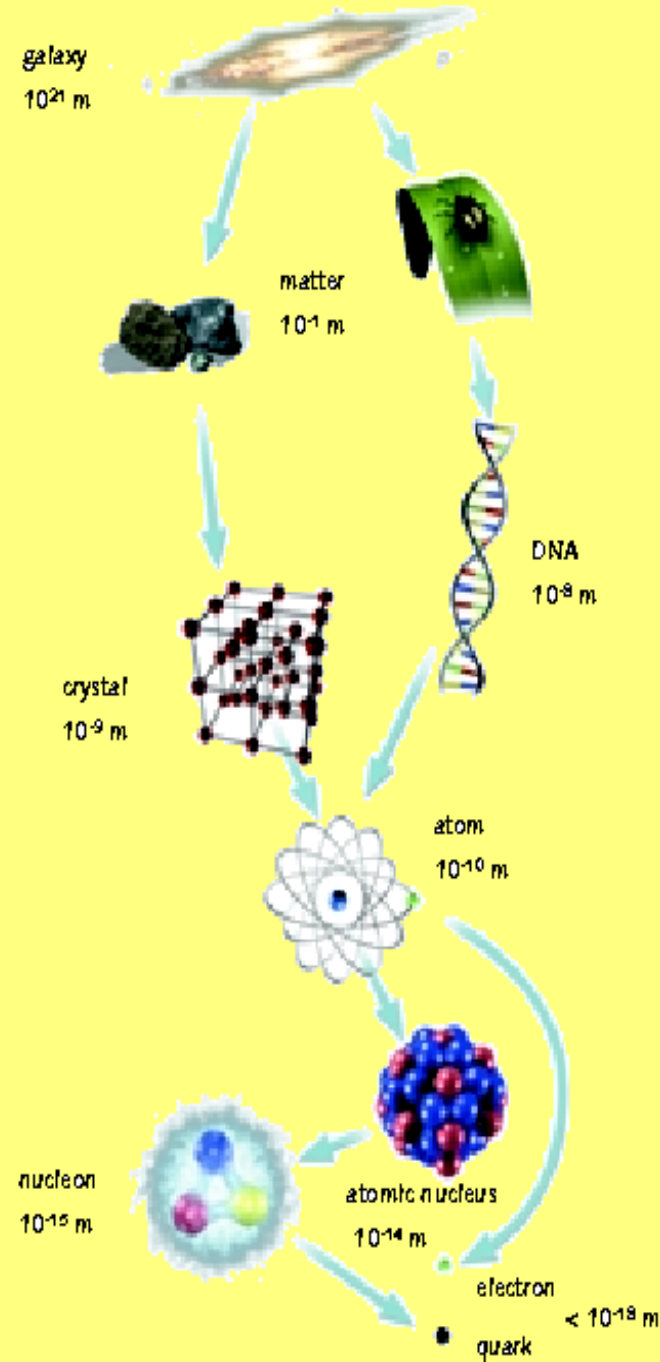
中国秦山核电站



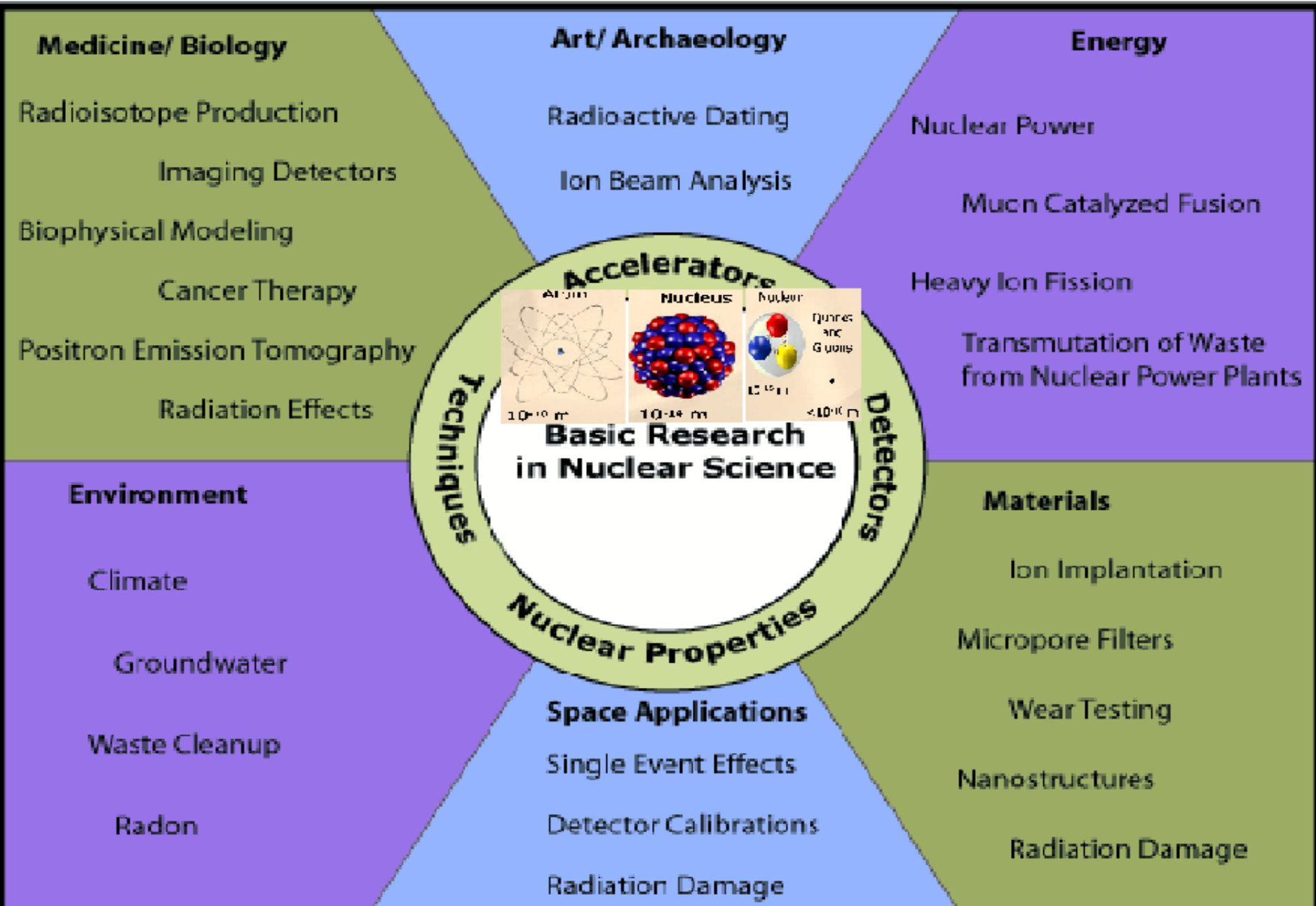
“枪式”原子弹结构原理图



“内爆式”原子弹结构原理图



Applications of Nuclear Science

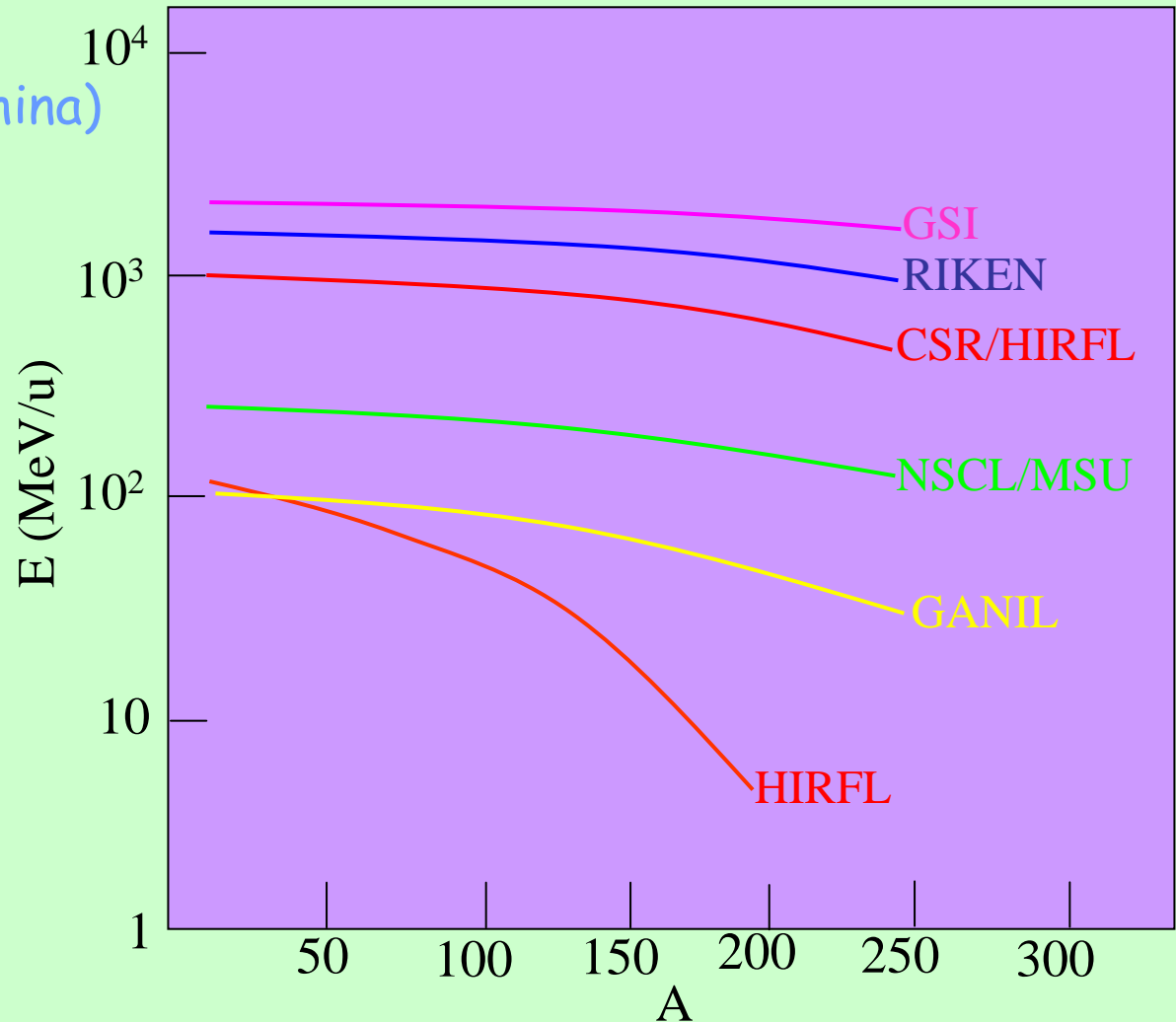


Heavy-Ion Accelerators at Intermediate Energies

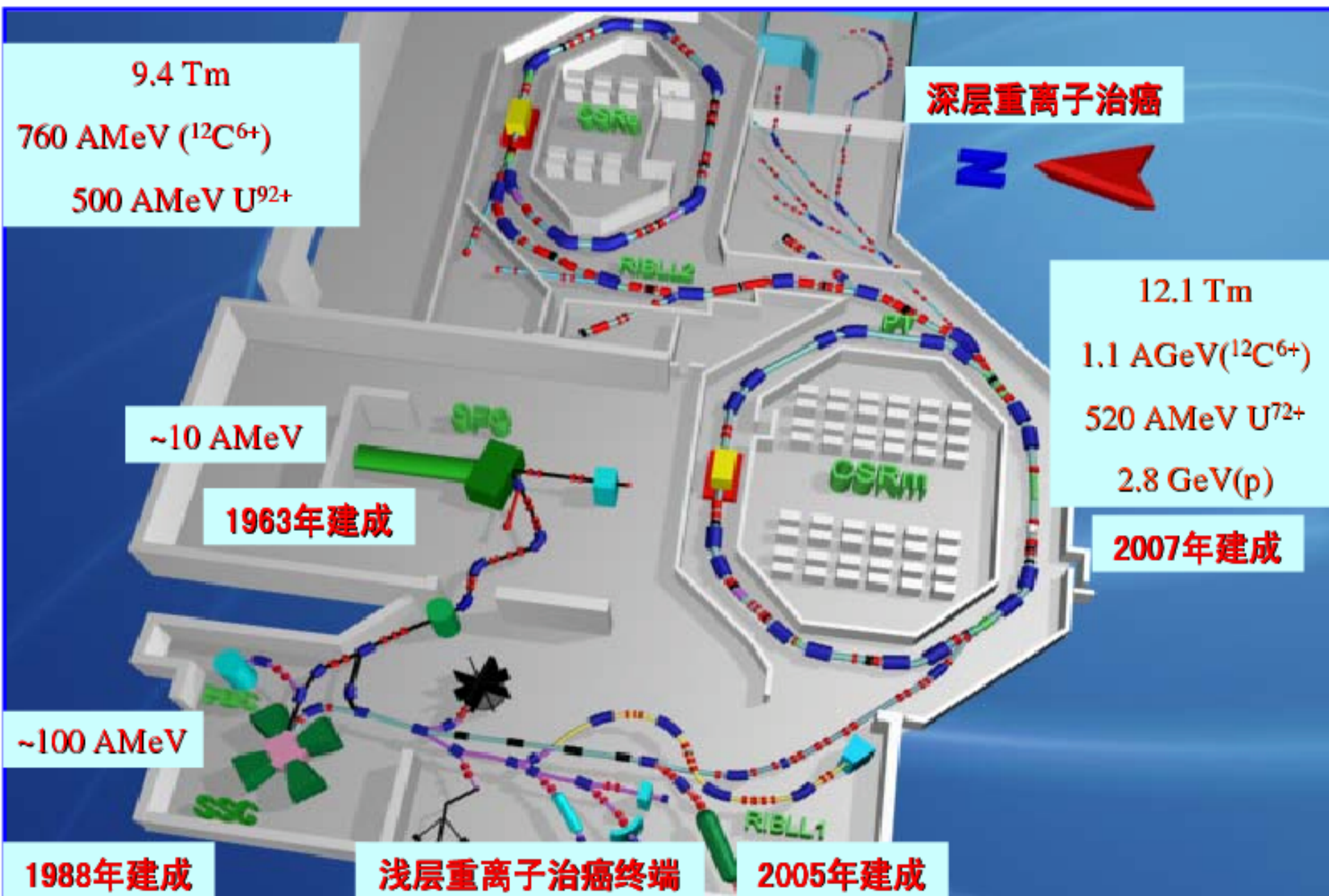
1. HIRFL, CSR/HIRFL (China)
2. GANIL (France)
3. GSI (Germany)
4. NSCL/MSU
5. RIKEN (Japan)

Dubna, LBL, ORNL, TAMU,
INFN, KVI,...

BNL, CERN



HIRFL-CSR



Outline

1. Introduction

2. Applications

2.1 Cancer therapy

2.2 Seed breeding

2.3 Space radiation

2.4 Problems

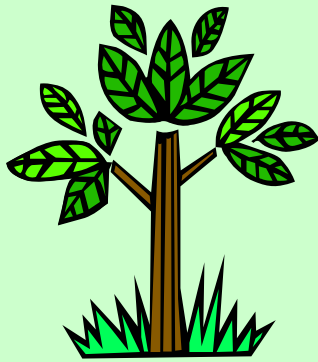
3. A Multi-scale microscopic dynamical model

4. Conclusions

Radiation is everywhere, all the time

Natural radiation from space and earth (15,000,000,000 years !)

medical examination (x-rays, neutron, ...)



plant



animal

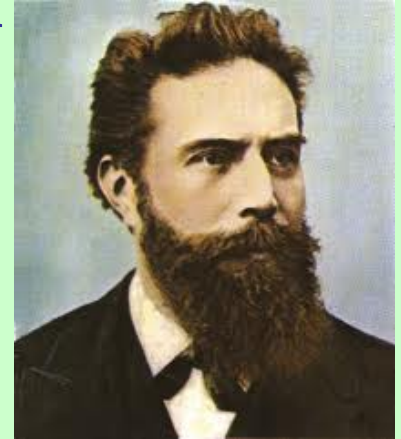


human being

Modification, evolution (Charles Robert Darwin), death...

A Simple history

1. 1895, Wilhelm Konrad Roentgen discovered x-rays, won a 1901 Nobel Prize

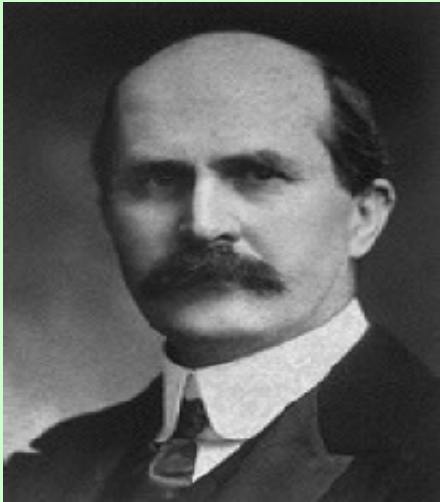


2. γ -rays, e^- , n , π , ...

3. Proton and heavy ions

In 1903, William Henry Bragg found a peak as α particle penetration in materials (Bragg peak), shared the 1915 Nobel Prize with his son

Bragg peak - discovered in 1904



William Henry Bragg

1. Bragg and Kleeman, On the ionization curves of radium, *Philosophical Magazine*, S.6, 8(1904)726
2. Bragg, Die alpha-Strahlen des Radiums, *Jahrbuch der Radioaktivitat und Elektronik*, 2(1905)4.
3. Bragg and Kleeman, On the alpha particles of radium, and their loss of range in passing through various atoms and molecules, *Philosophical Magazine*, S.6, 10(1905)318



William Lawrence Bragg

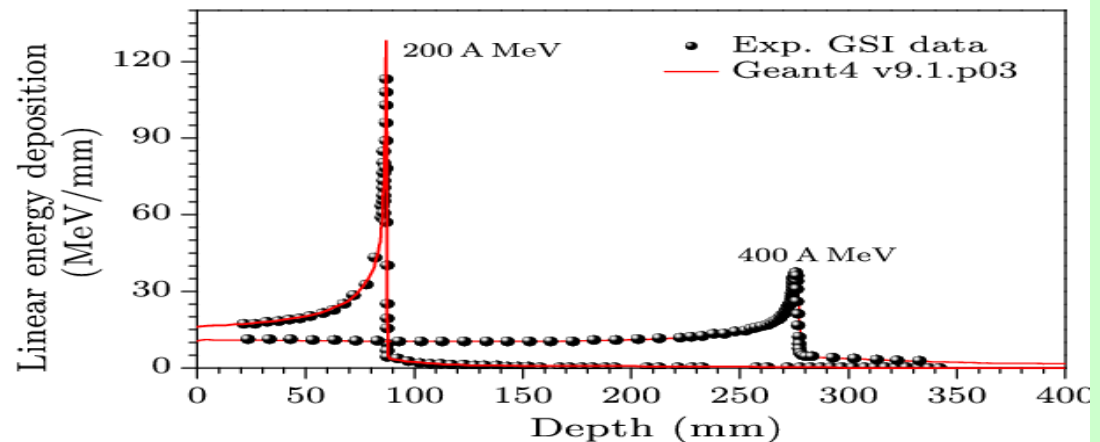


Fig. 1. Average linear energy deposition by ^{12}C ions in water. The beam energies are given in the boxes. GEANT4 calculations are shown by histograms; experimental data from GSI (Sihver *et al.* 1998)^[27] are shown by circles.

The Lawrence Brothers

Ernest Orlando Lawrence (1901-58)

1931 The first cyclotron was produced by Lawrence and Livingston. It was 4.5 inches in diameter and used 1800V to produce 80KeV protons.

1939 EOL was awarded the Nobel Prize for his invention of the cyclotron.



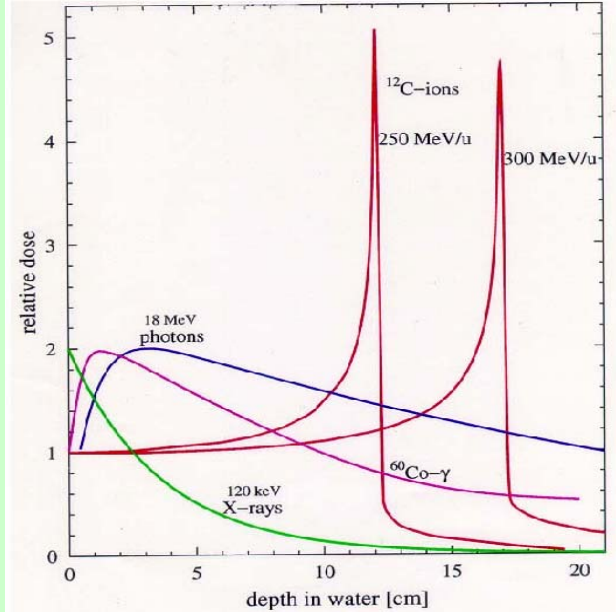
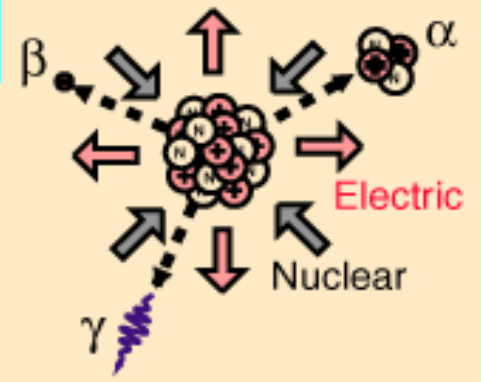
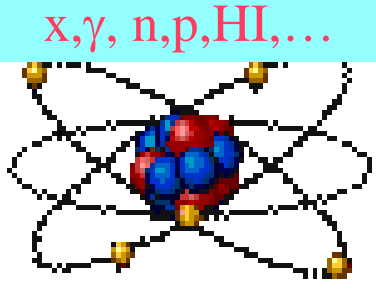
E.O. Lawrence (right) poses with his sixty inch cyclotron.

John H. Lawrence (1903-1991)

Ernest's younger brother John was a Doctor of Medicine. He came to the Radiation Laboratory in '35. John Lawrence was the first to treat cancer with cyclotrons when, in 1954, he began irradiating the pituitaries of patients with metastatic breast cancer.



John H. Lawrence using the 60 inch cyclotron to treat a patient with neutrons.



Strong electro-
magnetic radiation

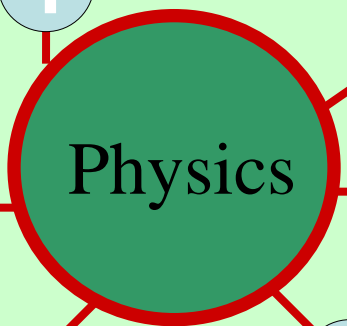
(inverse dose profile)
Bragg Curve

Beam verification

Small range-
straggling

Determinate range

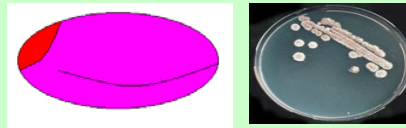
Small lateral
scattering



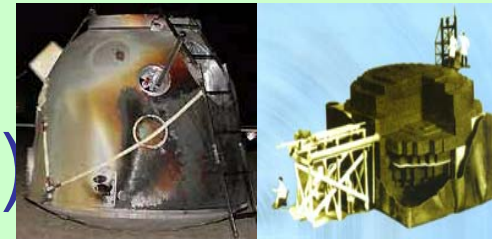
Physical advantages

1. Proton and HI therapy
EU, Japan, China, USA,...

2. Seed breeding



3. Radioprotection
(Space, power stations, hospitals)



4. Origin of human beings, evolution
of species (to understand it
from nuclear level)



Outline

1. Introduction

2. Applications

2.1 Cancer therapy

2.2 Seed breeding

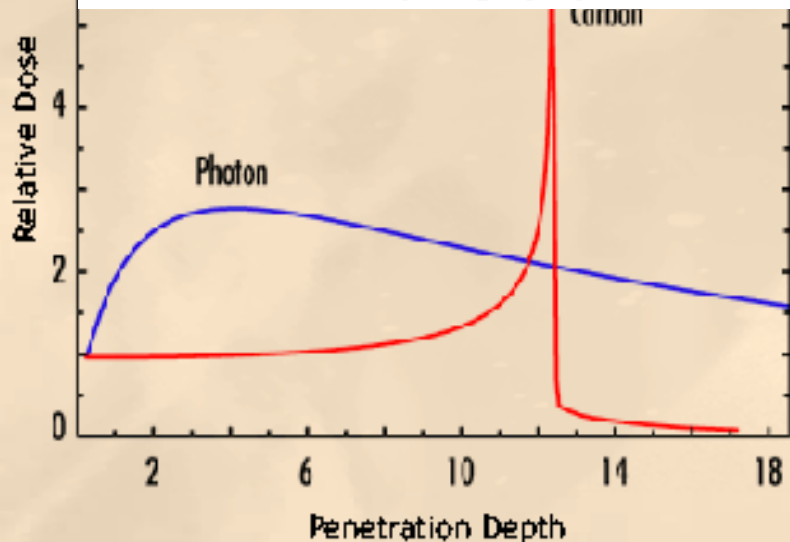
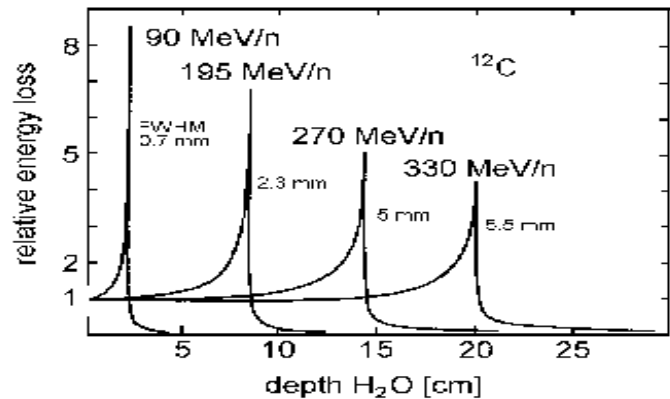
2.3 Space radiation

2.4 Problems

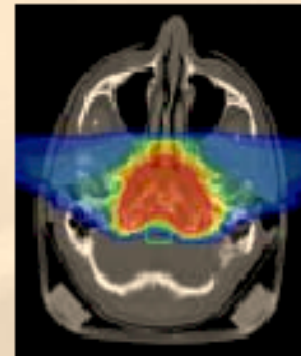
3. A Multi-scale microscopic dynamical model

4. Conclusions

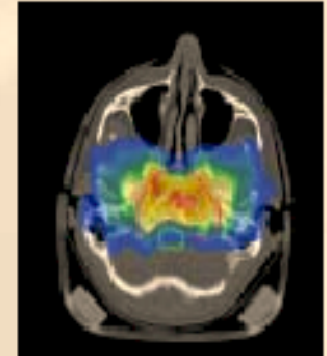
Cancer Therapy with Ion Beams



Patient
treatment plan



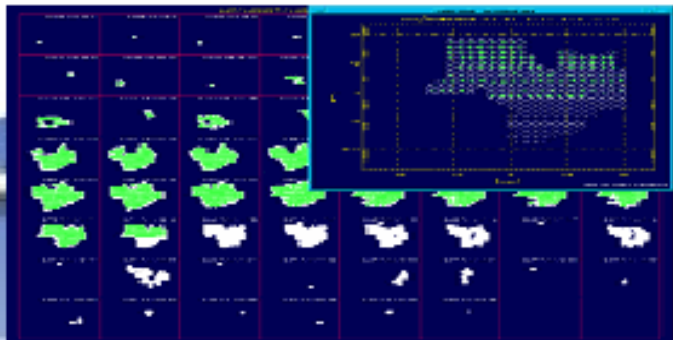
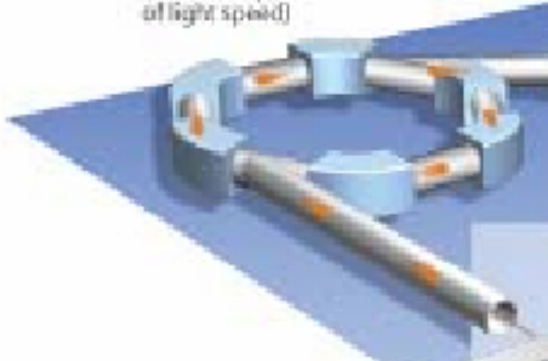
Verification
by PET



- 67 patients (2200 irradiations)
- no side effects
- no reoccurrence in treated volume

Cancer Therapy

Synchrotron
(Particles up to 60%
of light speed)

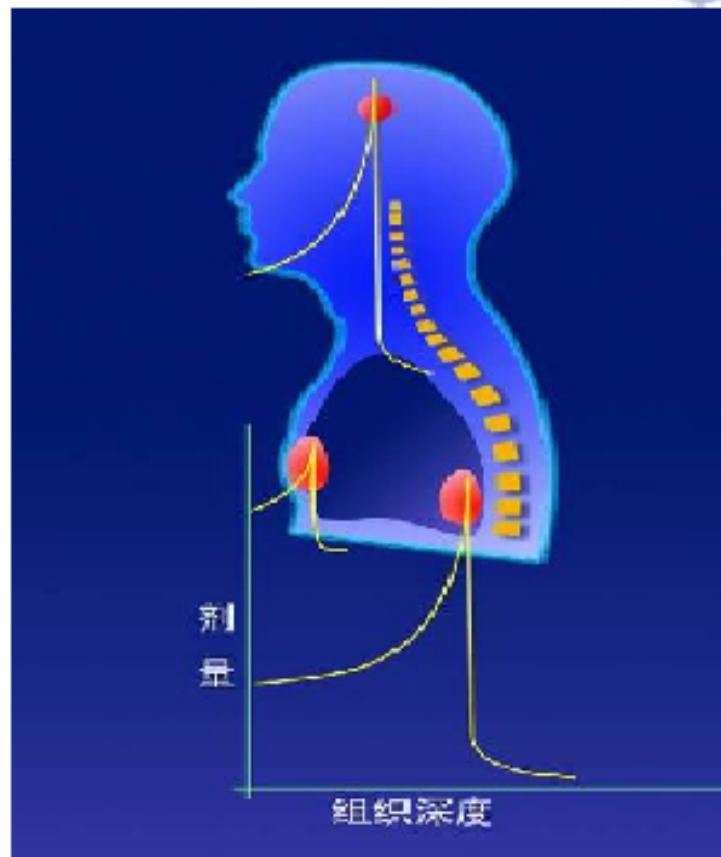
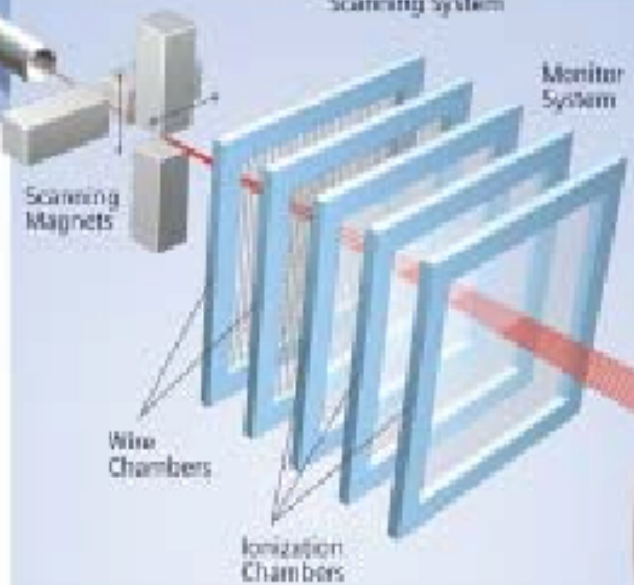


Online Monitoring



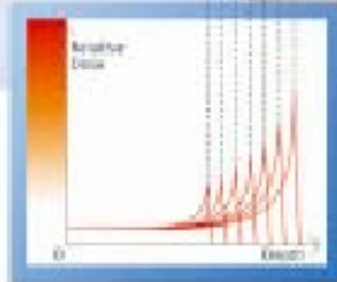
Scanning System

Monitor System

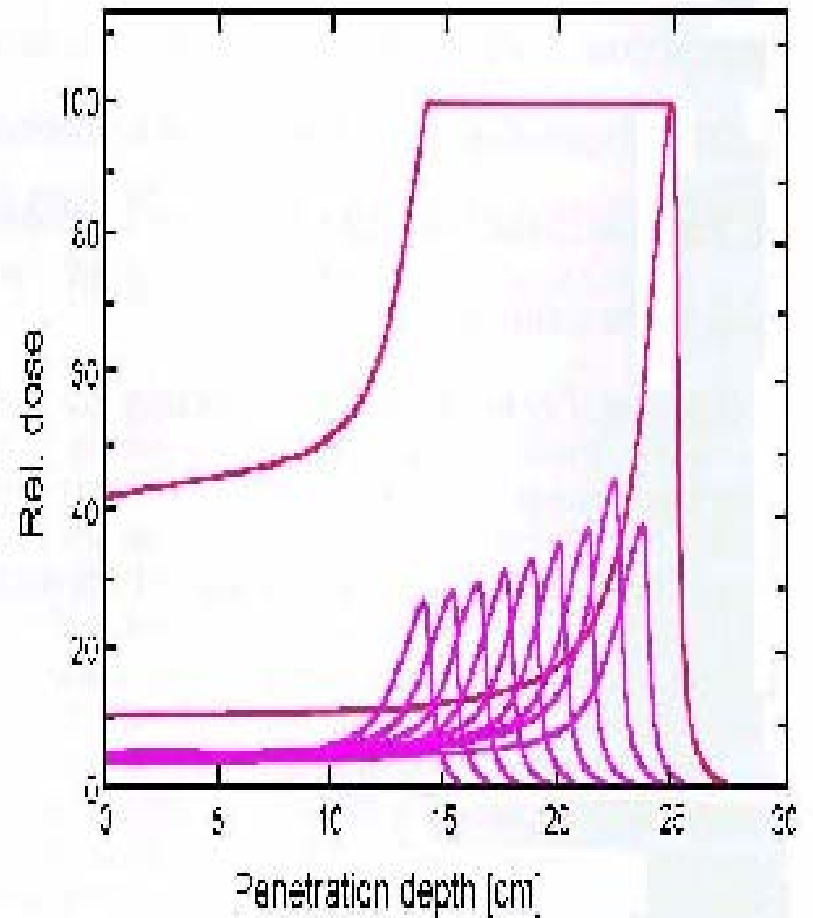
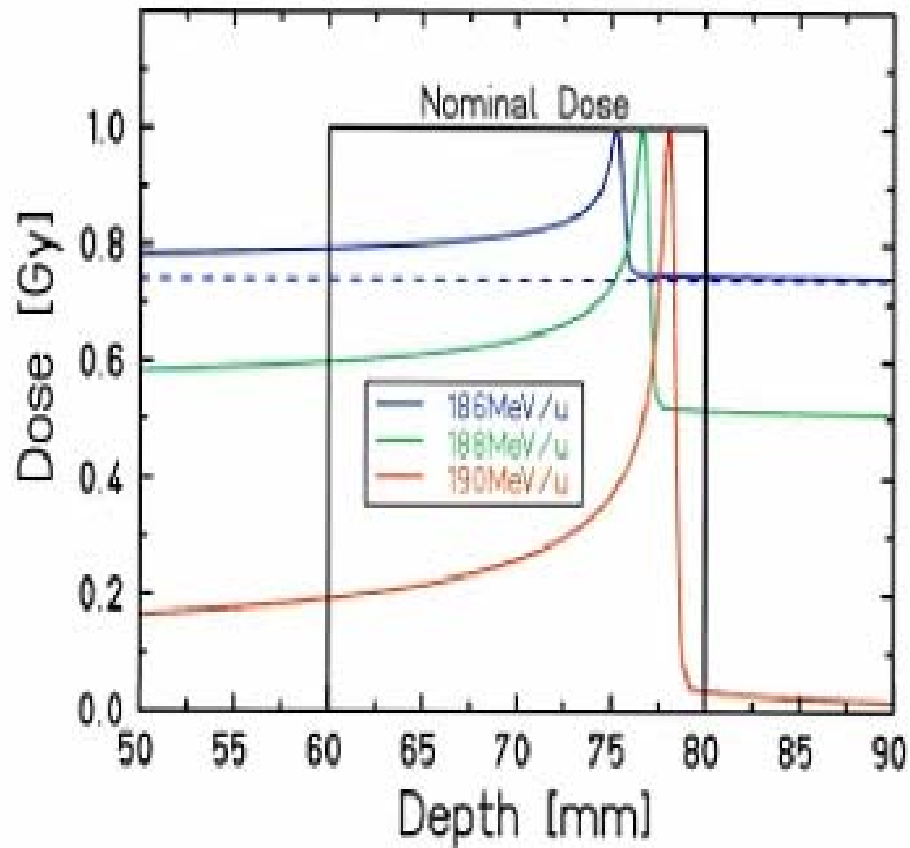


Depth 5 cm:
Proton 80 MeVw
Carbon 145 MeVw

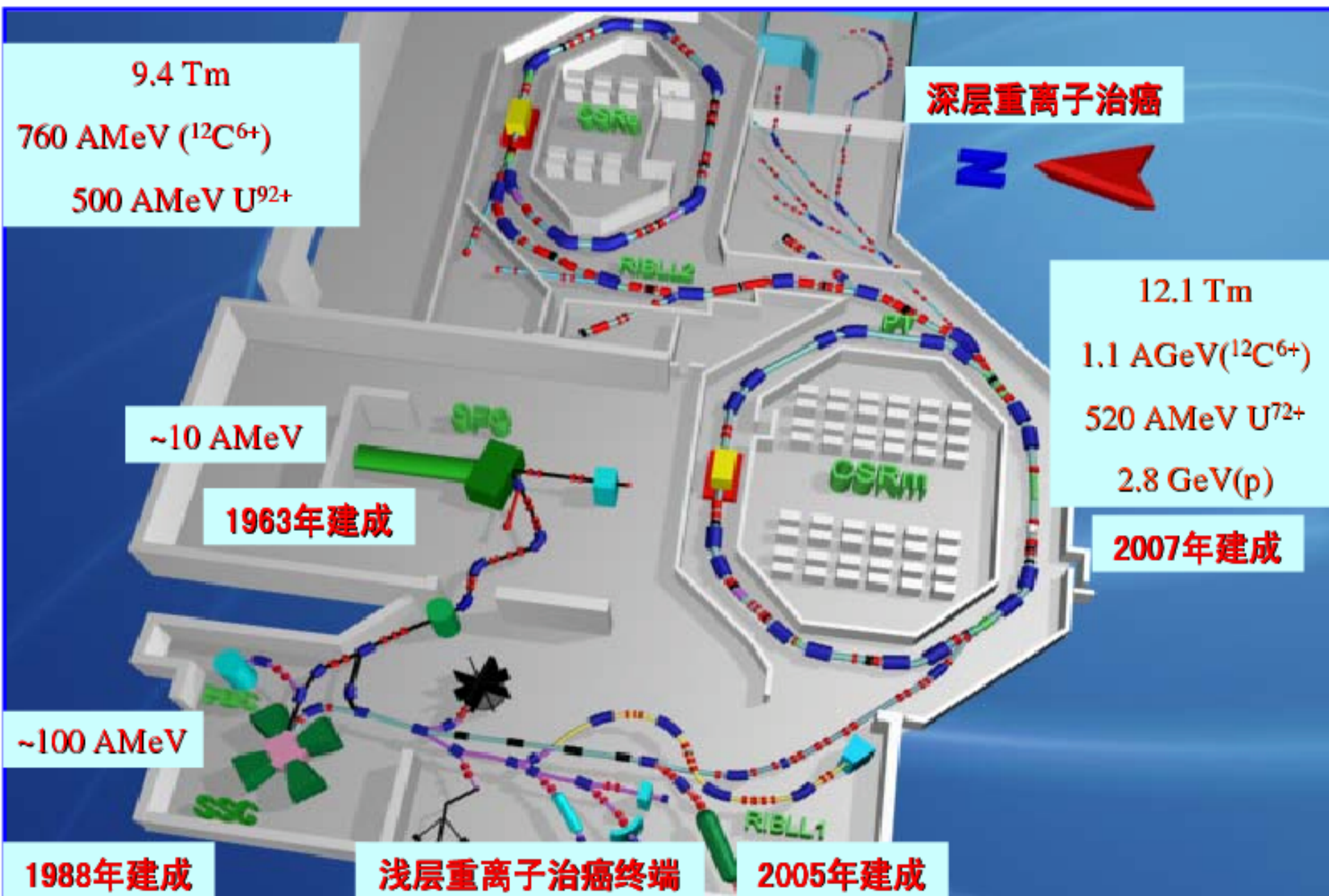
Depth 25 cm:
Proton 195 MeVw
Carbon 375 MeVw



Cancer Therapy



HIRFL-CSR



Outline

1. Introduction

2. Applications

2.1 Cancer therapy

2.2 Seed breeding

2.3 Space radiation

2.4 Problems

3. A Multi-scale microscopic dynamical model

4. Conclusions



対照

カーネーション
原品種「ビタル」



花色変異: 桃
花型変異: 丸弁



花色変異: 赤
花型変異: 丸弁



花色変異: 複色(覆輪)
花型変異: 丸弁



花色変異: 条斑(ストライプ)



花型変異: ナデシコ弁

$^{12}\text{C}^{5+}$ implantation to the seeds of pink

Beijing Normal University, flowers (Balsamine)

对照



中国凤仙1号“春霞”
(辐射变异: 粉色)



中国凤仙2号“朝阳”
(辐射变异: 红色)

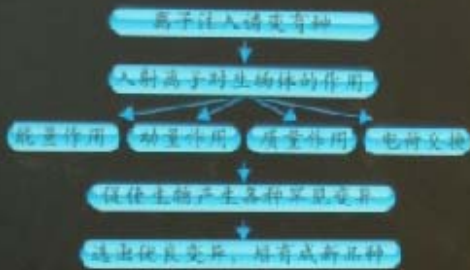


离子注入诱变育种

离子注入是近30年来国际上蓬勃发展和广泛应用的一种材料表面改性高技术。离子注入诱变育种就是利用离子注入进行生物诱变育种的一种新的育种技术。其基本原理是用能量为10-1000keV量级的离子束入射到植物中去，离子束与生物间既有物理和化学的相互作用，还会引起强烈的生物效应，促使生物产生各种变异，从中选出所期望的优良变异，培育成为一种植物新品种。离子注入诱变育种过程中，不仅离子束的能量对生物体有重要的作用，而且离子本身最终会停留在生物体内，对生物体变异产生重要的影响，这是它与一般用 γ 射线等进行的辐射育种和利用太空中强烈的宇宙射线进行的太空育种的主要区别。

离子注入诱变育种的特点

离子注入诱变育种技术简介



离子注入诱变育种的特点



离子注入诱变育种的优点

- 1、变异率高，一般要比自然变异率高1000倍以上；
- 2、变异谱宽，即变异的类型多，能够产生自然界里从未见过的新类型
- 3、变异快，可以大大缩短育种周期
- 4、离子注入诱变育种技术稳定可靠，简便易行。

北京市辐射中心暨北京师范大学核科学与技术学院，是国内最早开展低能离子束生物效应和育种研究的单位之一，对离子注入生物育种机理进行了研究，取得了重要科技成果，并发表相关学术论文百余篇。一些成果通过了北京市科技成果鉴定，为北京特色花卉等方面的发展做出贡献，已经形成紫玉米、紫花生、荷花、鸡冠花、凤仙花等新品种。2004年采用离子注入育种技术，培育出在花期、花形、株型、花色方面有明显改进的4个荷花新品种，申请实用新型专利2项。



北京市辐射中心主任王乃勇院士和课题组成员在野外考察离子辐射凤仙花、鸡冠花新品种生长情况

第七届中国花卉博览会
The 7th China Flower Expo

花卉与科技馆
FLOWER AND SCIENCE AREA



奖章、奖杯

(10) 其它进展



cockscombs (after radiations)





Beijing Lotus Flower Park (collaboration)



黄妃舞



仙女散花



时尚



初夏



露半唇



| 首页 | | 组织机构 | | 政策法规 | | 行政审批 | | 园林动态 | | 服务项目 | | 园林景观 | | 党风廉政建设 | 2009年9月12日 星期六 下午好!

园林动态

PARK DYNAMIC

- 工作动态
- 领导动态
- 局内动态
- 重点工程

工作动态

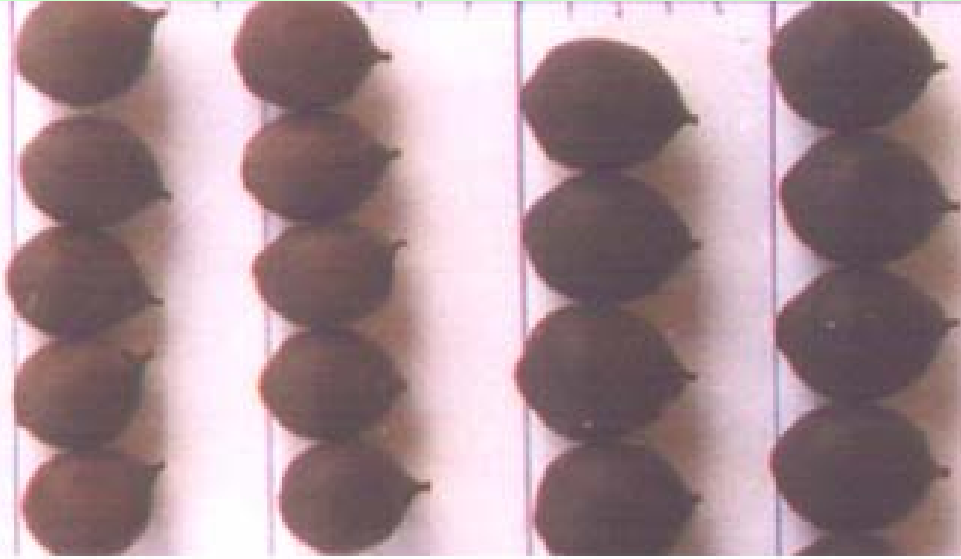
第九届北京莲花池荷花节盛大开幕

6/24/2009 17:10:37 莲花池公园 李雅丽



第九届北京莲花池荷花节于6月24日上午在莲花池公园东广场表演舞台举行了隆重的开幕仪式。原全国人大常委会副委员长何鲁丽、北京师范大学核科学与技术学院副院长张丰收、北京市园林绿化局科技处处长徐佳、北京市公园管理中心处长王鹏训、北京市园林绿化局公园林场风景名胜处副处长张亚红、太平桥街道工委书记都俊生、办事处主任何秋香、丰台区园林局局长申燕民、局长助理程朝晖等嘉宾出席了开幕仪式。

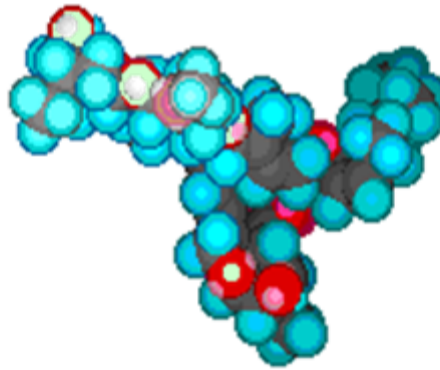
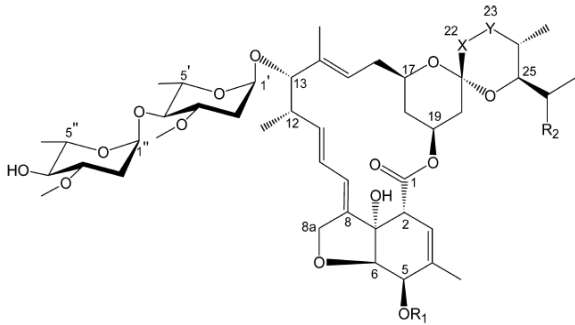
Lotus Seeds get larger



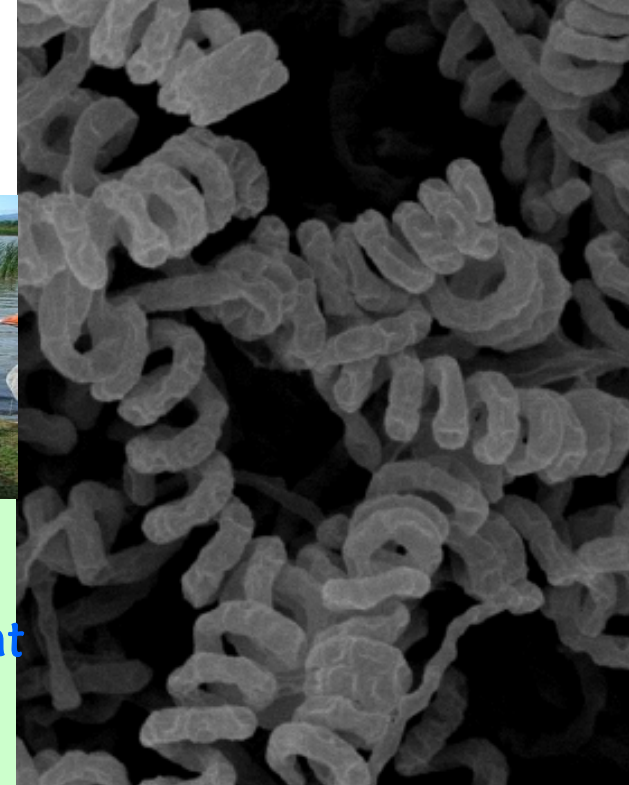
离子注入法
莲蓬形态变异



Green pesticide (Avermectilis, Spinosad)



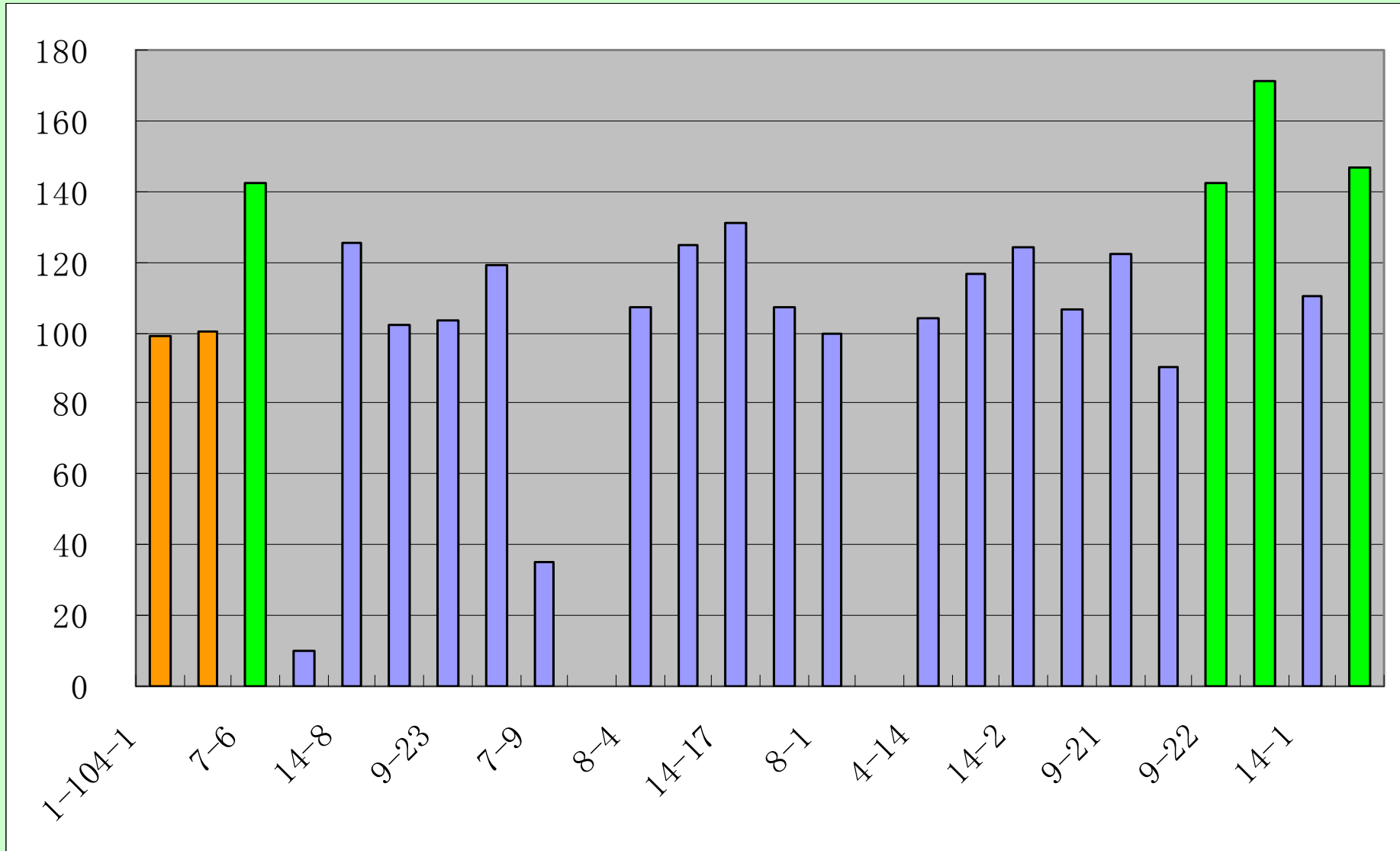
| | R1 | R2 | X-Y |
|----------------|-----------------|-------------------------------|-------------------------|
| Avermectin A1a | CH ₃ | C ₂ H ₅ | CH=CH |
| A1b | CH ₃ | CH ₃ | CH=CH |
| A2a | CH ₃ | C ₂ H ₅ | CH ₂ -CH(OH) |
| A2b | CH ₃ | CH ₃ | CH ₂ -CH(OH) |
| B1a | H | C ₂ H ₅ | CH=CH |
| B1b | H | CH ₃ | CH=CH |
| B2a | H | C ₂ H ₅ | CH ₂ -CH(OH) |
| B2b | H | CH ₃ | CH ₂ -CH(OH) |



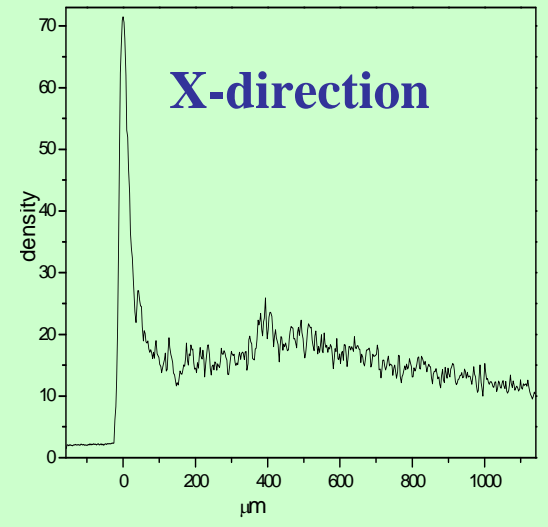
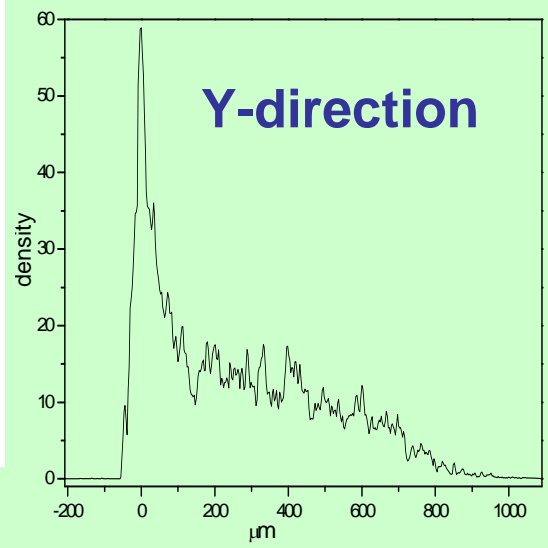
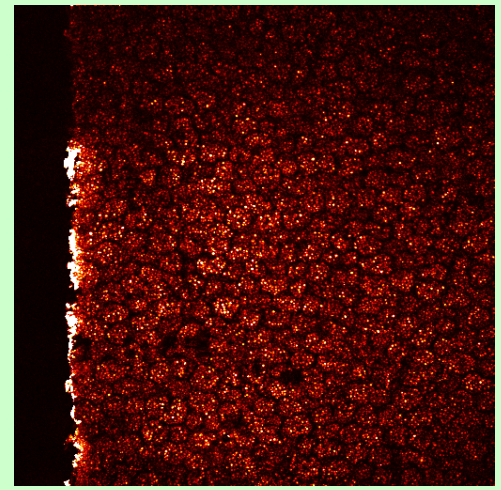
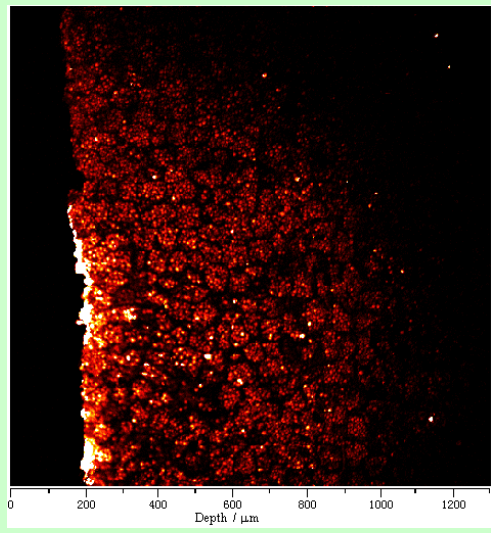
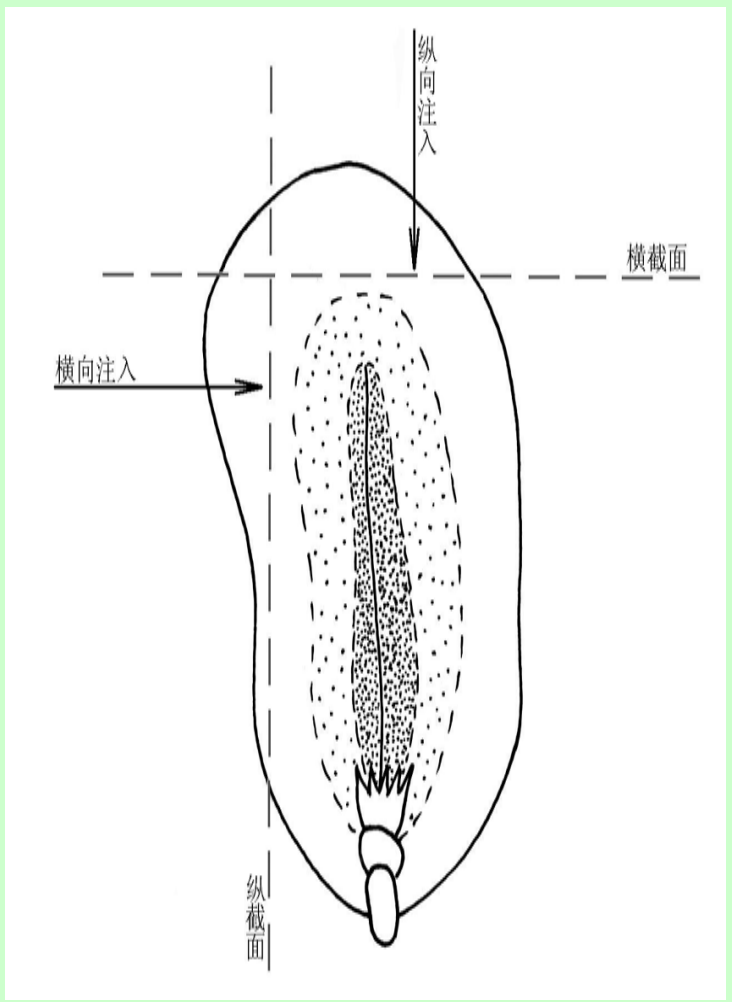
- Very low leave behind, easy decomposition with Sunlight, **friendly** for health and environment
- The **price** is high !

Preliminary results – Spinosad-

(collaboration with the Institute of Microbiology, CAS)



peanut



Profile of peanut seed

**Vanadium⁺($9 \times 10^{16}/\text{cm}^2$) at 200keV,
Concentration-d, (TPLSM method)**

Outline

1. Introduction

2. Applications

2.1 Cancer therapy

2.2 Seed breeding

2.3 Space radiation

2.4 Problems

3. A Multi-scale microscopic dynamical model

4. Conclusions

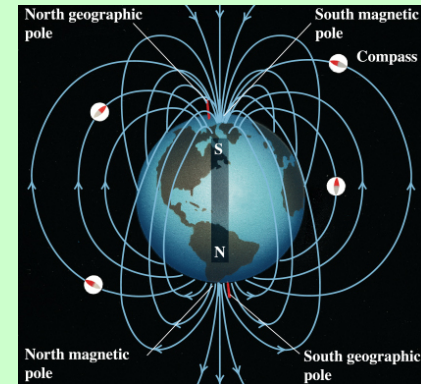
Three kinds of space radiations

high energy electrons and protons trapped by the Earth's magnetic field.

Cosmic Rays



solar protons



Chinese academy of agriculture: space seed breeding

南瓜身形如钟(Pumpkin)



彩棉是纯天然(Cotton)



太空佛手茄子(Eggplant)



Outline

1. Introduction

2. Applications

2.1 Cancer therapy

2.2 Seed breeding

2.3 Space radiation

2.4 Problems

3. A Multi-scale microscopic dynamical model

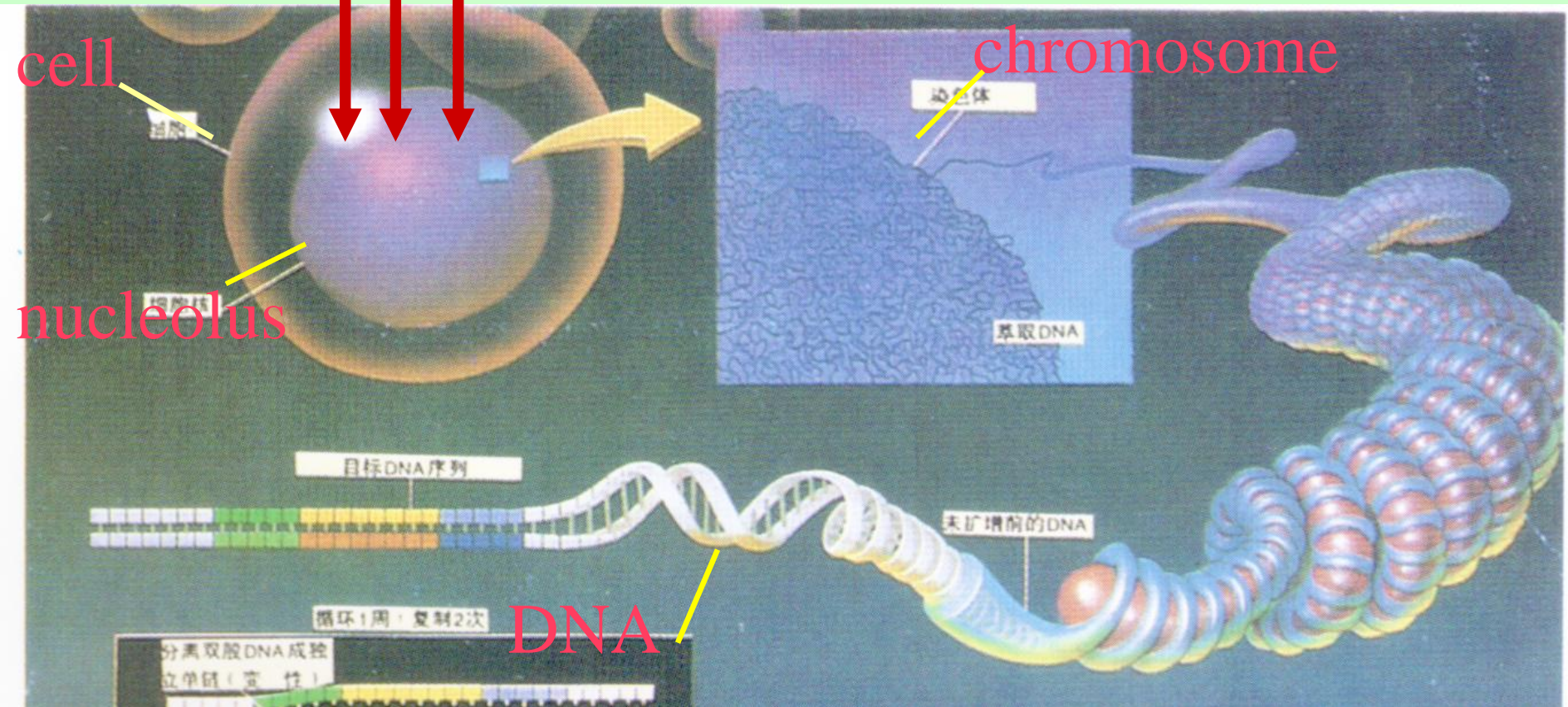
4. Conclusions

Common problem: *heavy ion interactis with biomolecules*

Heavy Ions

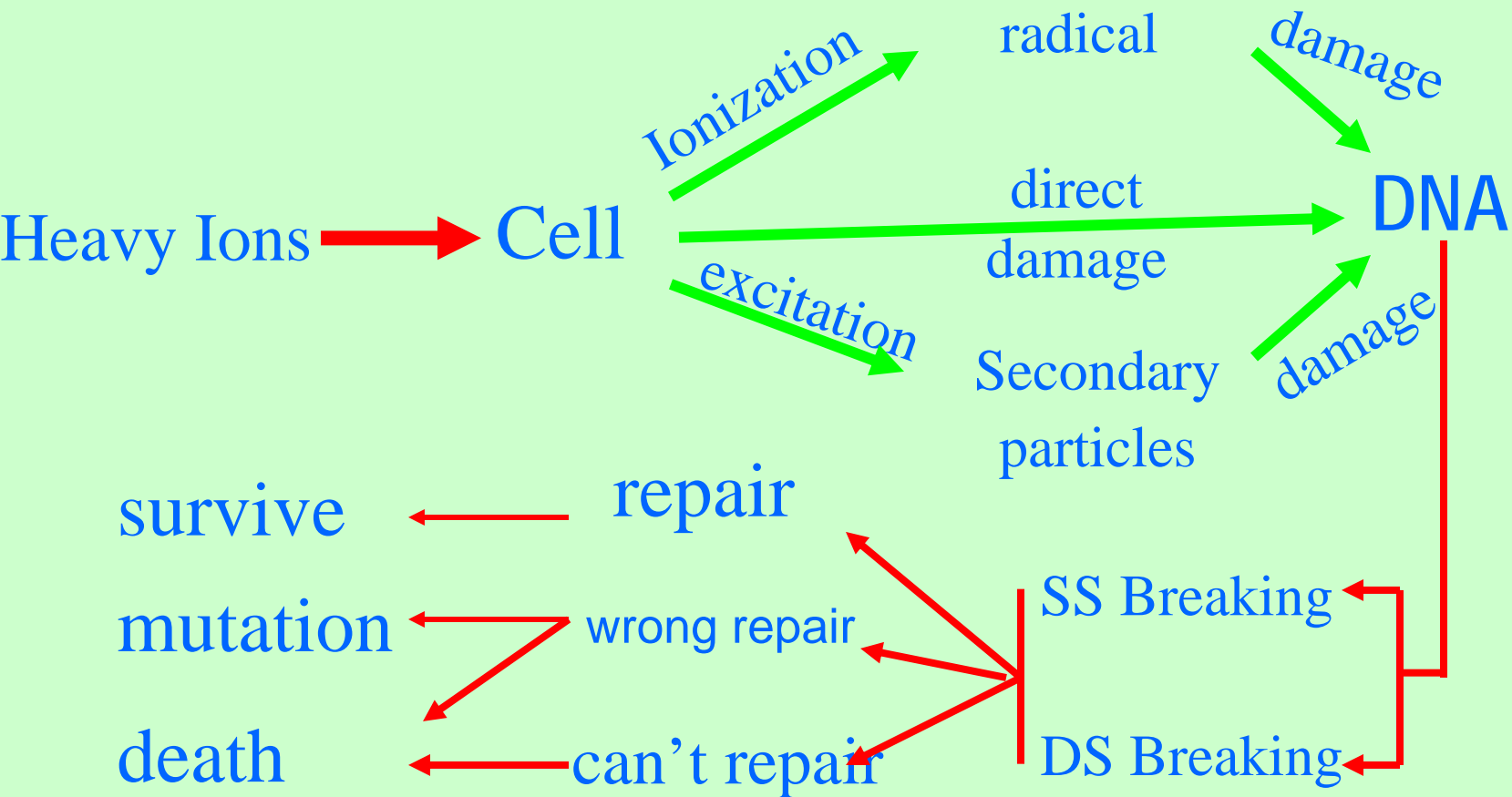
Nuclear Process, Electron excitation

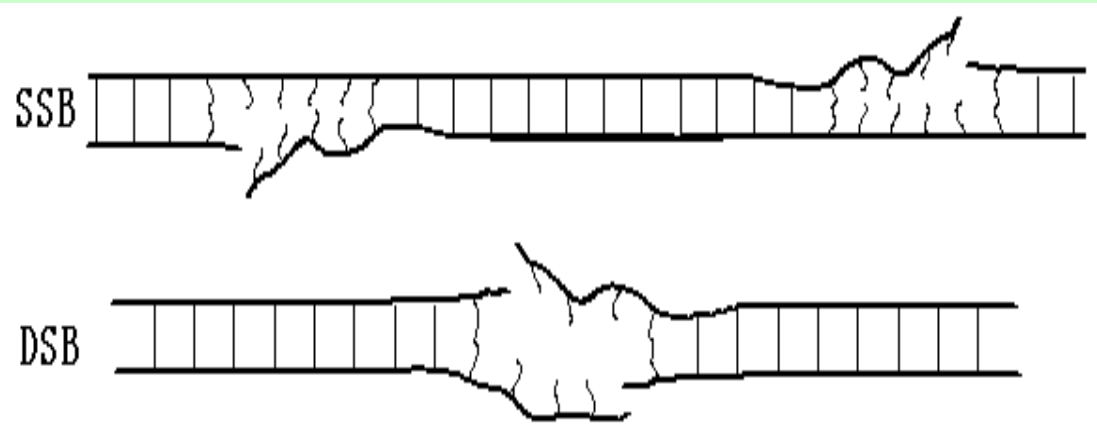
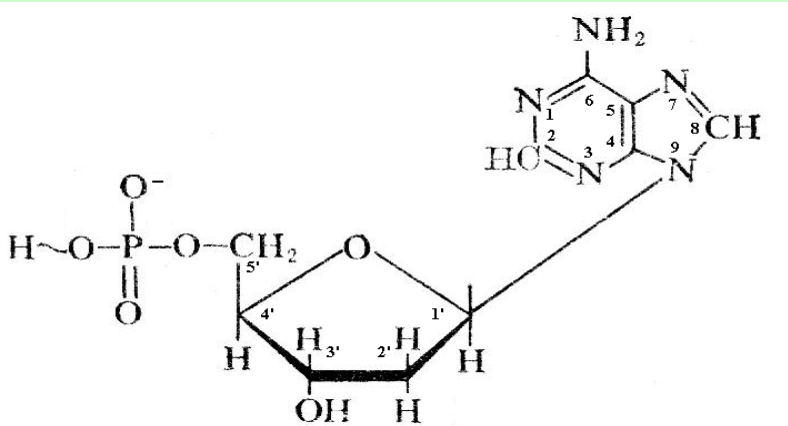
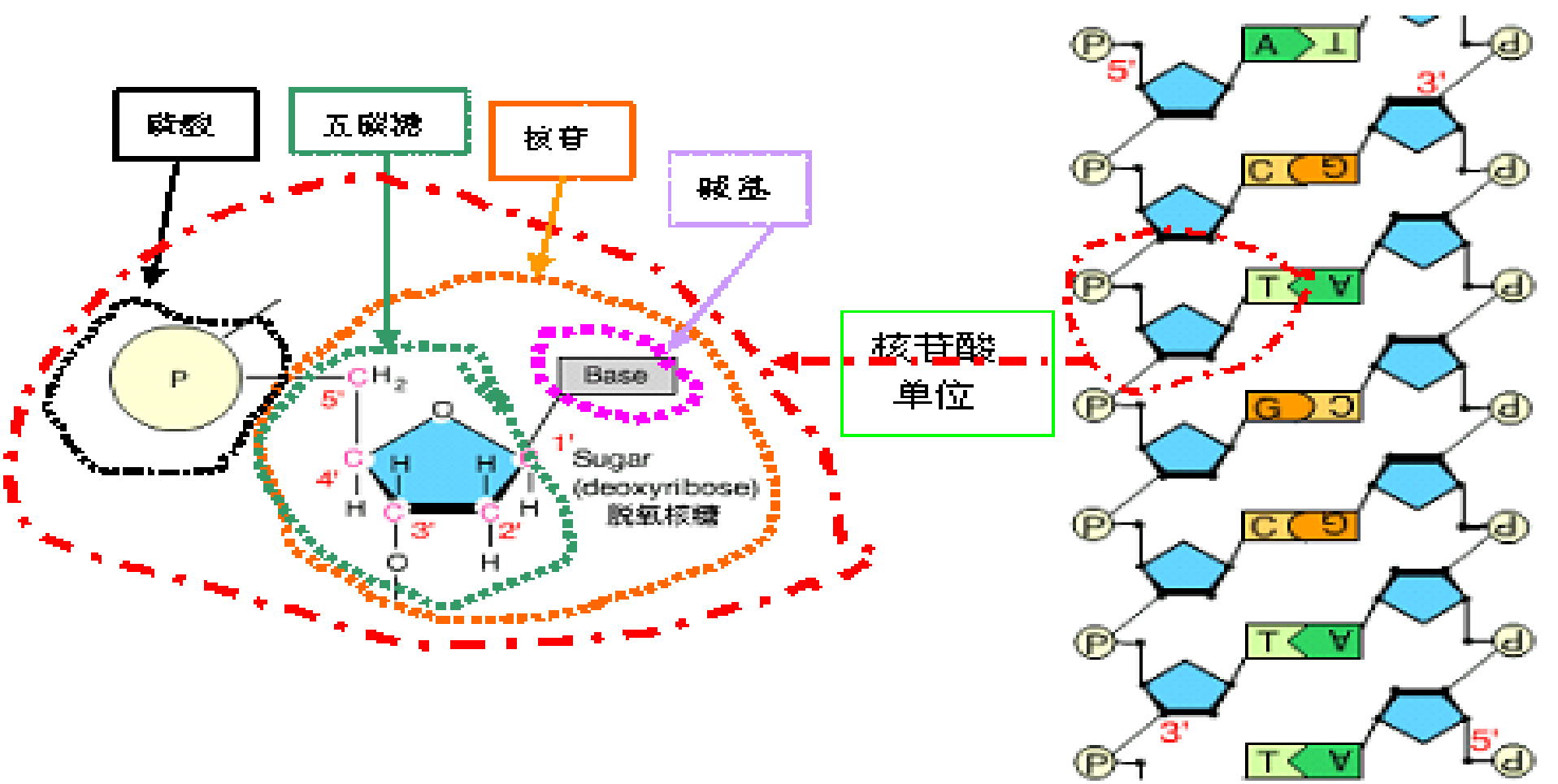
Relaxation, to a new structure



Cell, nucleolus, chromosome, DNA

mutation mechanism





Experiments: biological molecule therapy with heavy charged particles

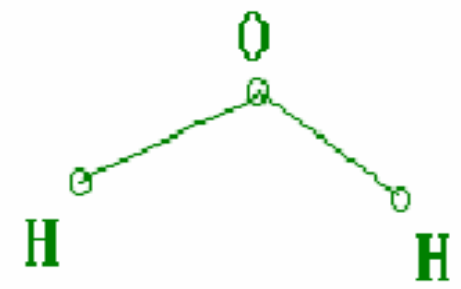
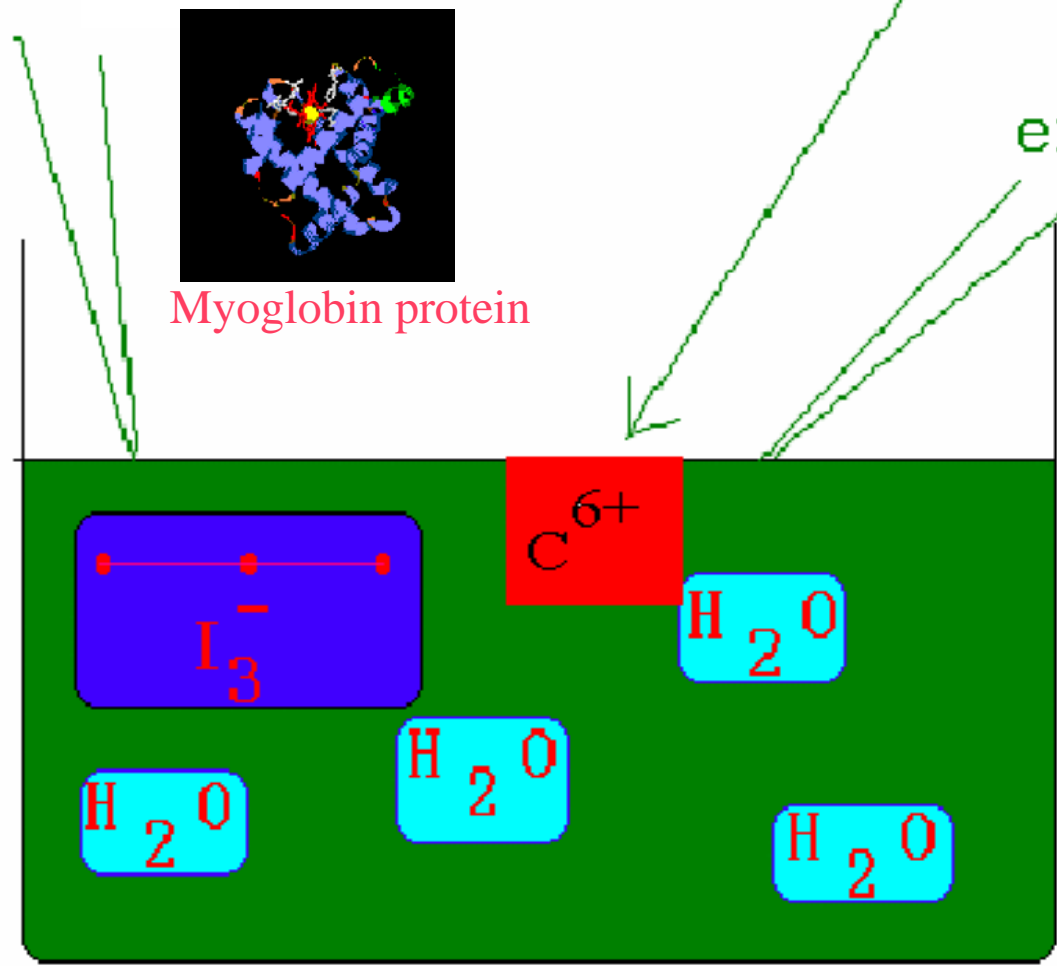
Object molecule:

Heavy charged particles, C^{6+}

protein, DNA, etc.

environment molecule

H_2O , ethanol, etc.



Physics analysis

- Object (Solute, protein, DNA, etc)
 - solvent molecules (water, etc.)
 - incident particles (heavy charged particles, x-rays, photons)
- ☺ Physical process: projectile fragmentation, ionization, electron transport and emission,
linear energy loss, strong potential energy and polarization, internal structure changes, etc.

Outline

1. Introduction

2. Applications

2.1 Cancer therapy

2.2 Seed breeding

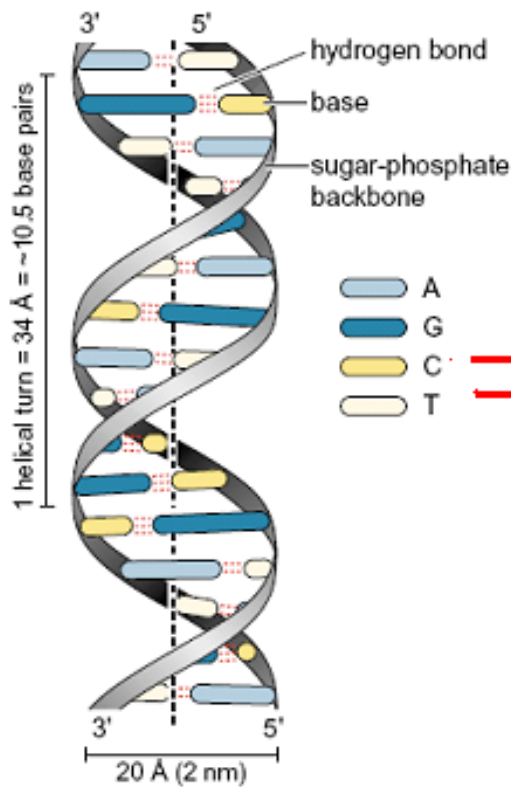
2.3 Space radiation

2.4 Problems

3. A Multi-scale microscopic dynamical model

4. Conclusions

A multi-scale microscopic dynamic approach to study interaction of heavy ions with biomolecules



New Structure !

Physical process ($10^{-24} \sim 10^{-8} \text{s}$)

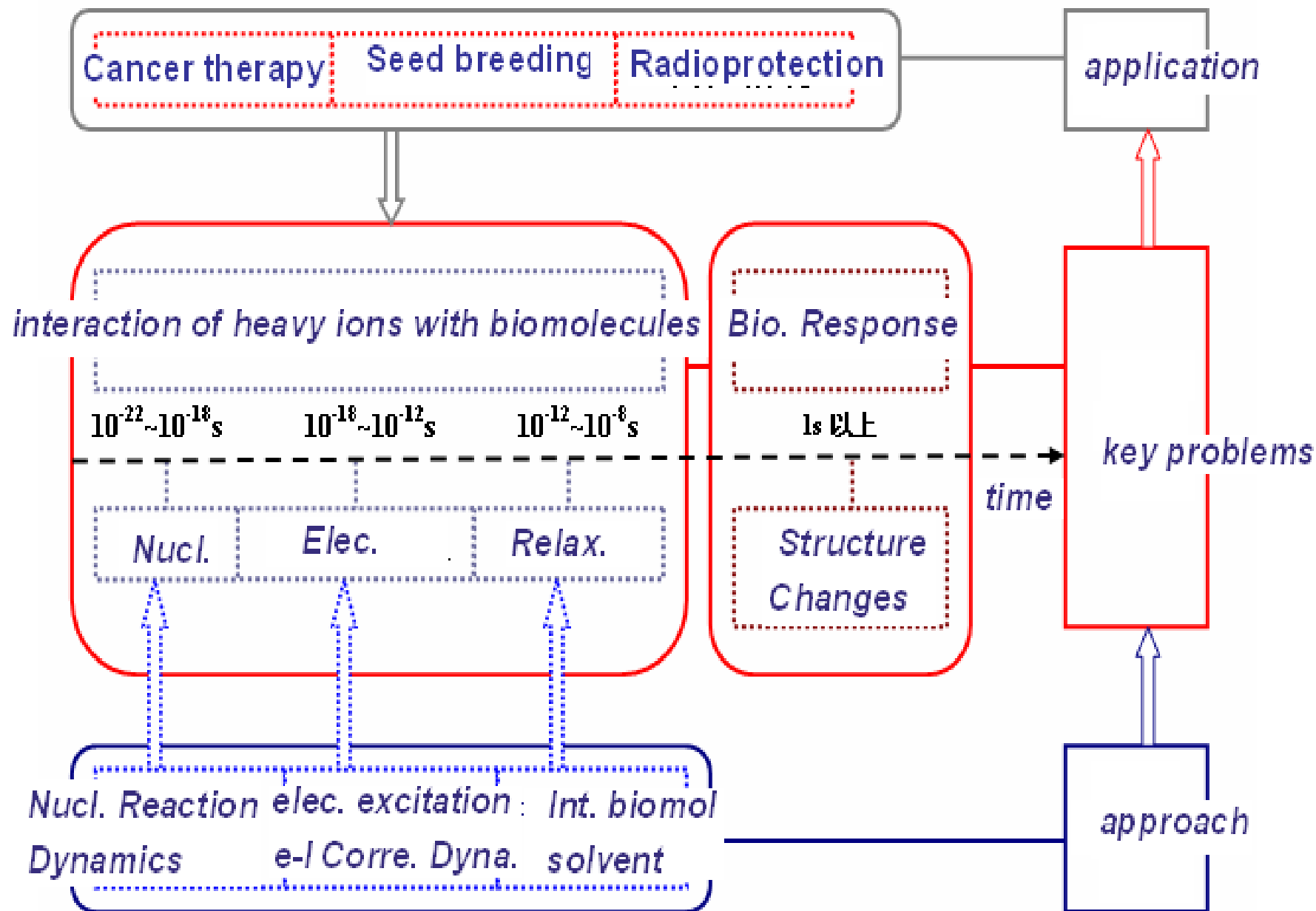
Chemical process (10^{-8}s)

Biological process (10^3s)

Nuclear process
($10^{-24} \sim 10^{-18} \text{s}$)

Electronic process
($10^{-18} \sim 10^{-12} \text{s}$)

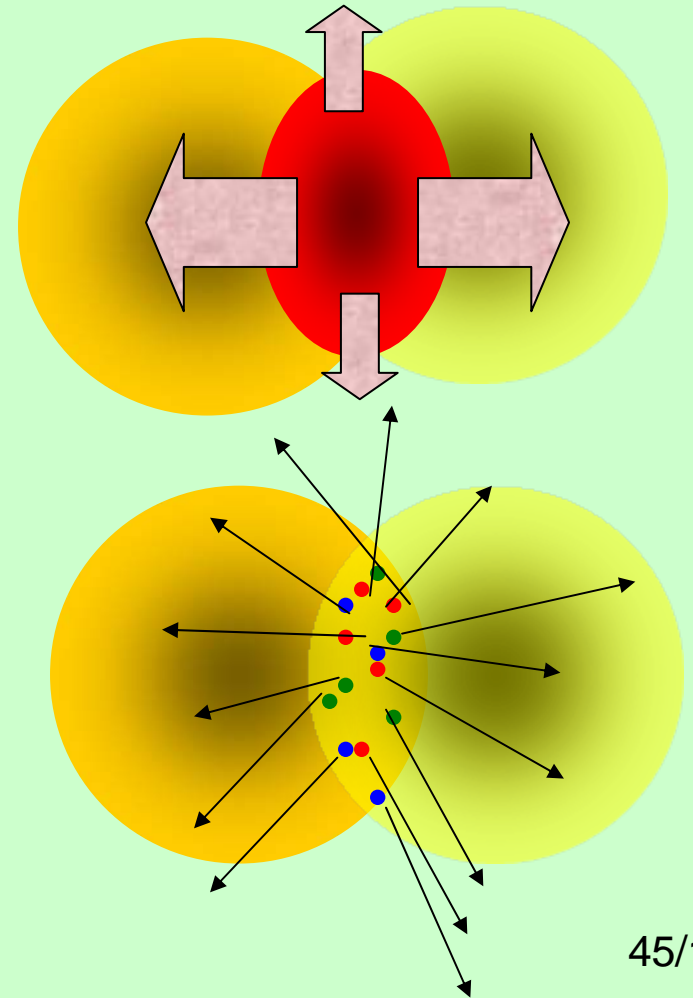
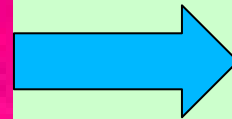
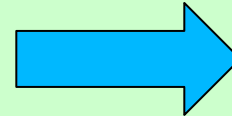
Relaxation process
($10^{-12} \sim 10^{-8} \text{s}$)



Decomposition of this approach

- (1). Nuclear multifragmentation (C, N, and Ne induced reactions)**
- (2). Electrons excitations during interactions of beam and/or fragments with molecules**
- (3). Dose distributions**
- (4). Properties of sub-unit of DNA, such as adenine(A), thymine(T), C,G,U**
- (5). Structure changes of DNA**
- (6). Structure-->biological functions ?**

(1) Nuclear Multifragmentation



Nuclear Multifragmentation,
F. S. Zhang and L. X. Ge,
Science Press, Beijing, 1998

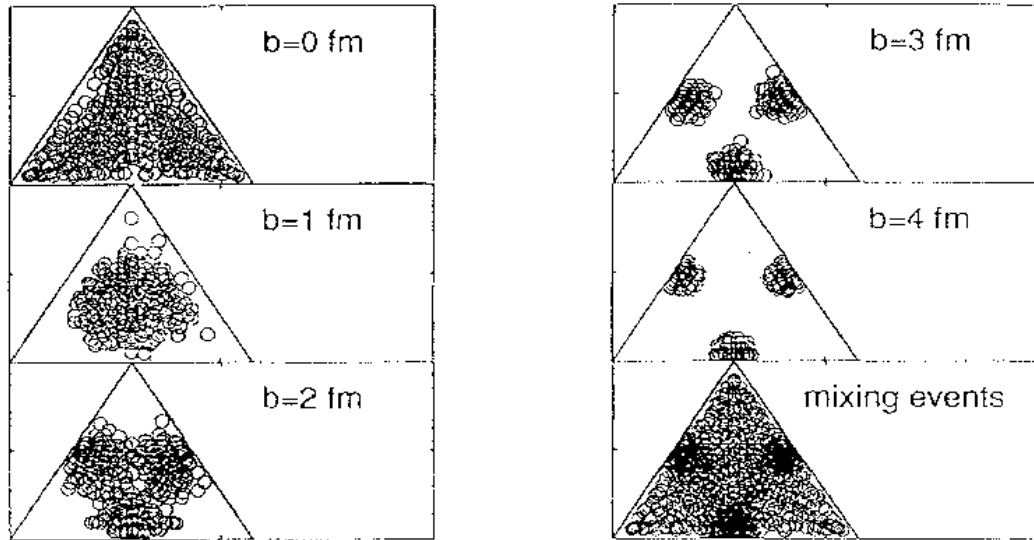


FIG. 8. The correlations between the three largest fragments of an event by a charge-Dalitz plot for the $^{40}\text{Ca}+^{40}\text{Ca}$ system at 90 MeV/nucleon with the events of impact parameters 0, 1, 2, 3, 4 fm and the mixing events with different impact parameters except $b = 0$ fm. The number of events is the same as in Fig. 5.

Zhang and Suraud,

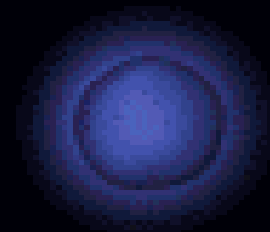
Phys. Rev. C51,1995,3201

$^{40}\text{Ca}+^{40}\text{Ca}$, 90 MeV/u

$$\sigma_{\text{tot}} \approx 1.5 \times 10^{-24} \text{ cm}^2$$

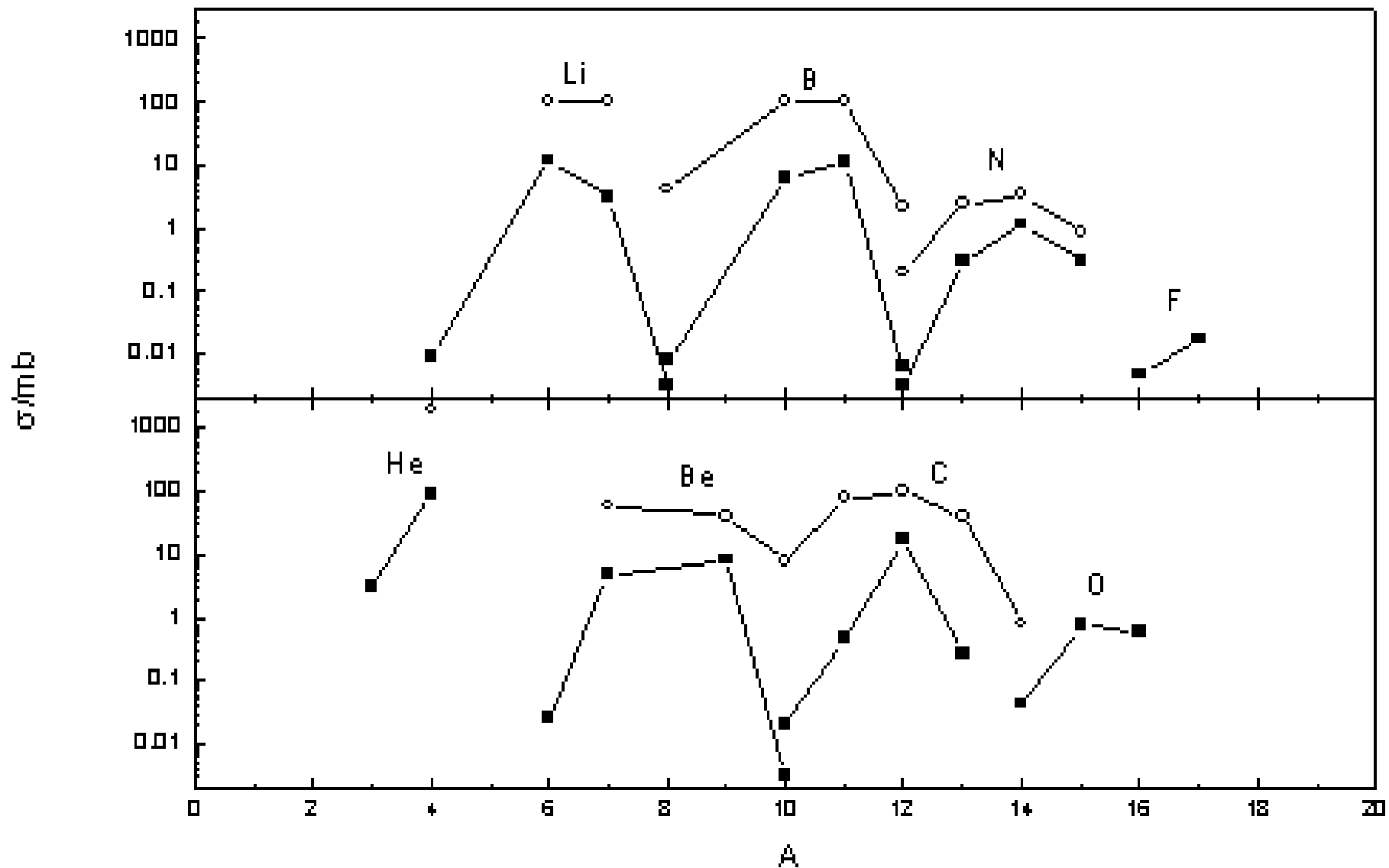
$$\sigma_{\text{frag}} \approx 1.2 \times 10^{-25} \text{ cm}^2$$

$$\sigma_{\text{frag}} / \sigma_{\text{tot}} \approx 8 \%$$

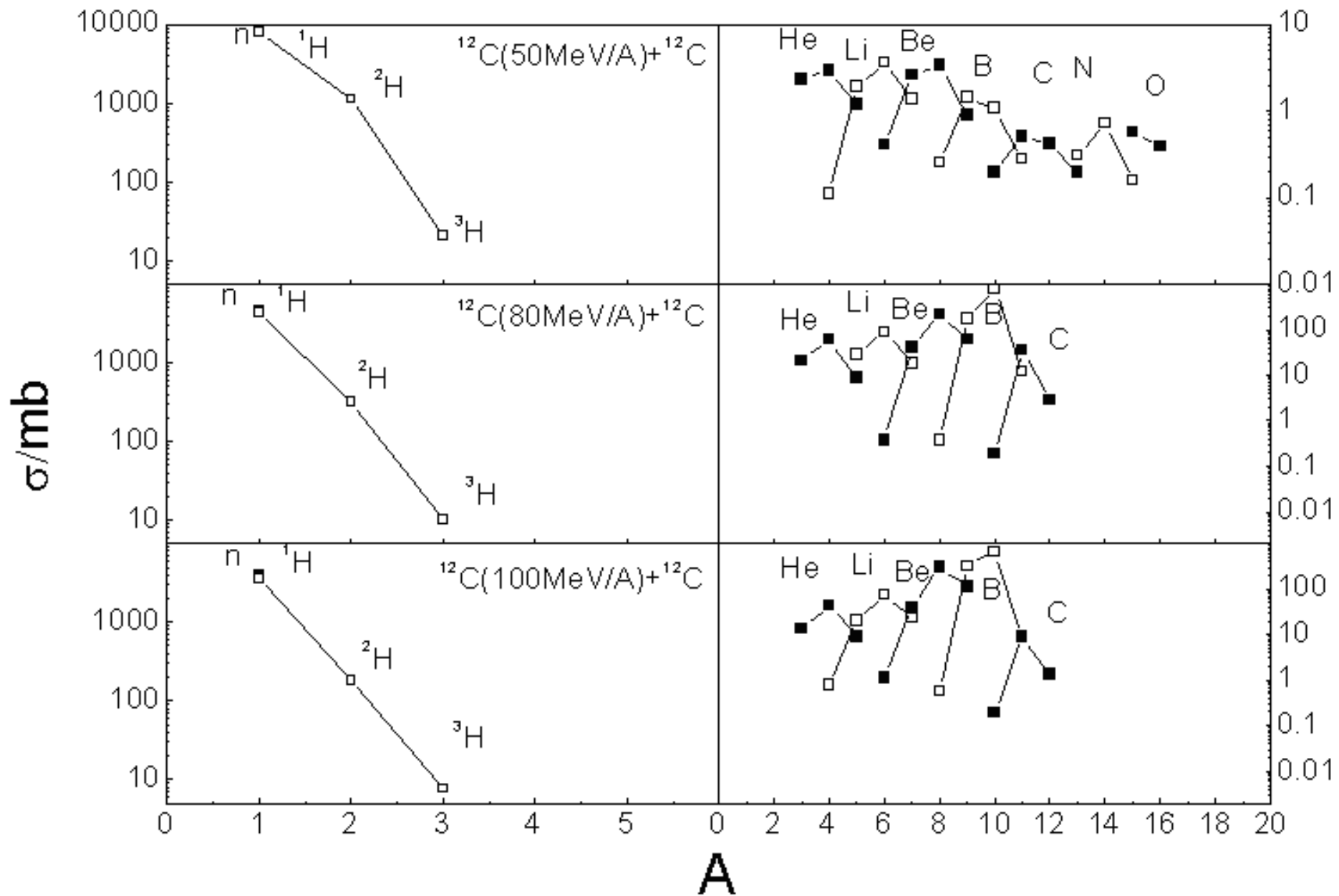


$^{12}\text{C}+^{12}\text{C}$, 28.7 MeV/u

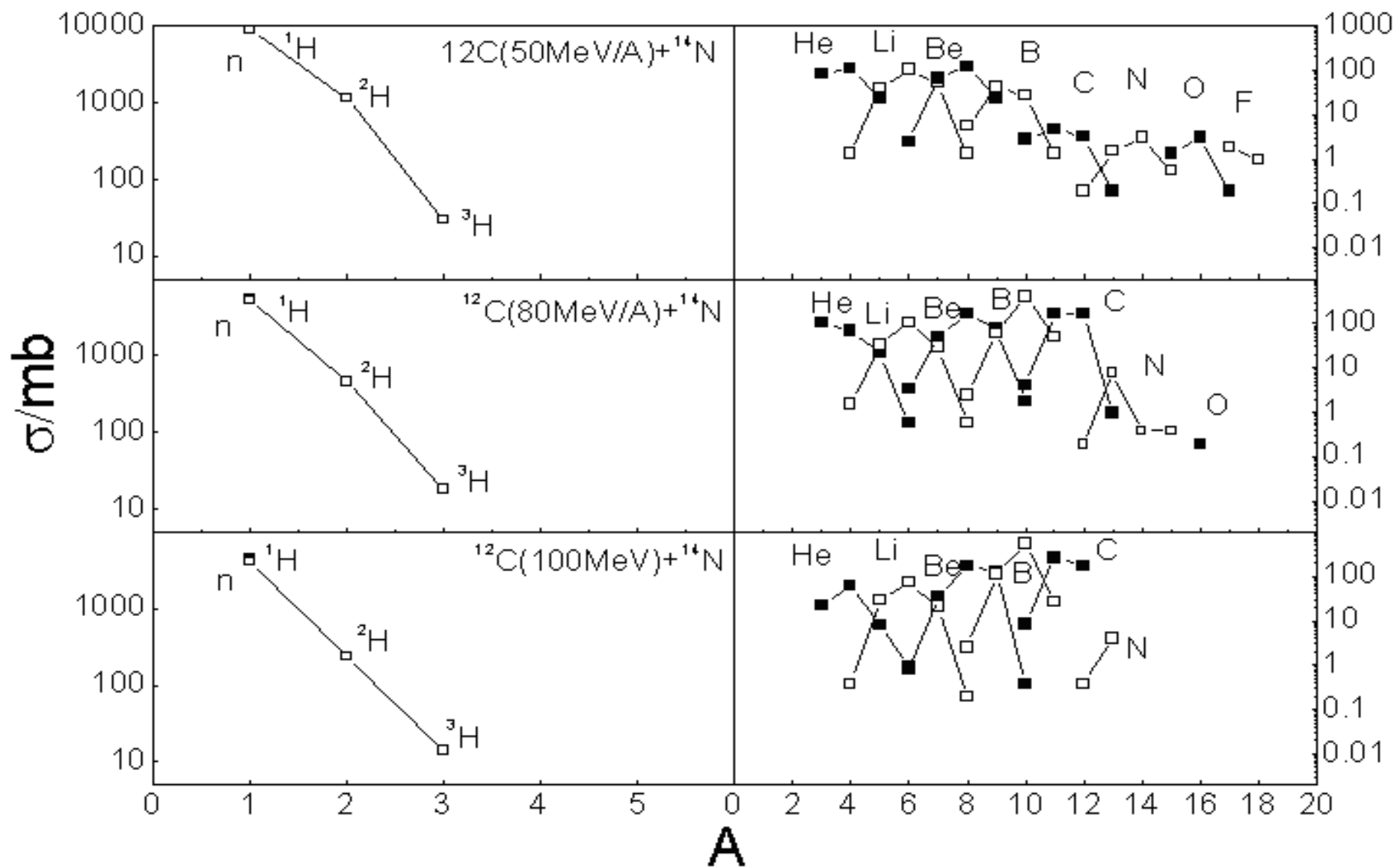
Exp. Czudek et al, *Phys. Rev. C*43(1991)1248)



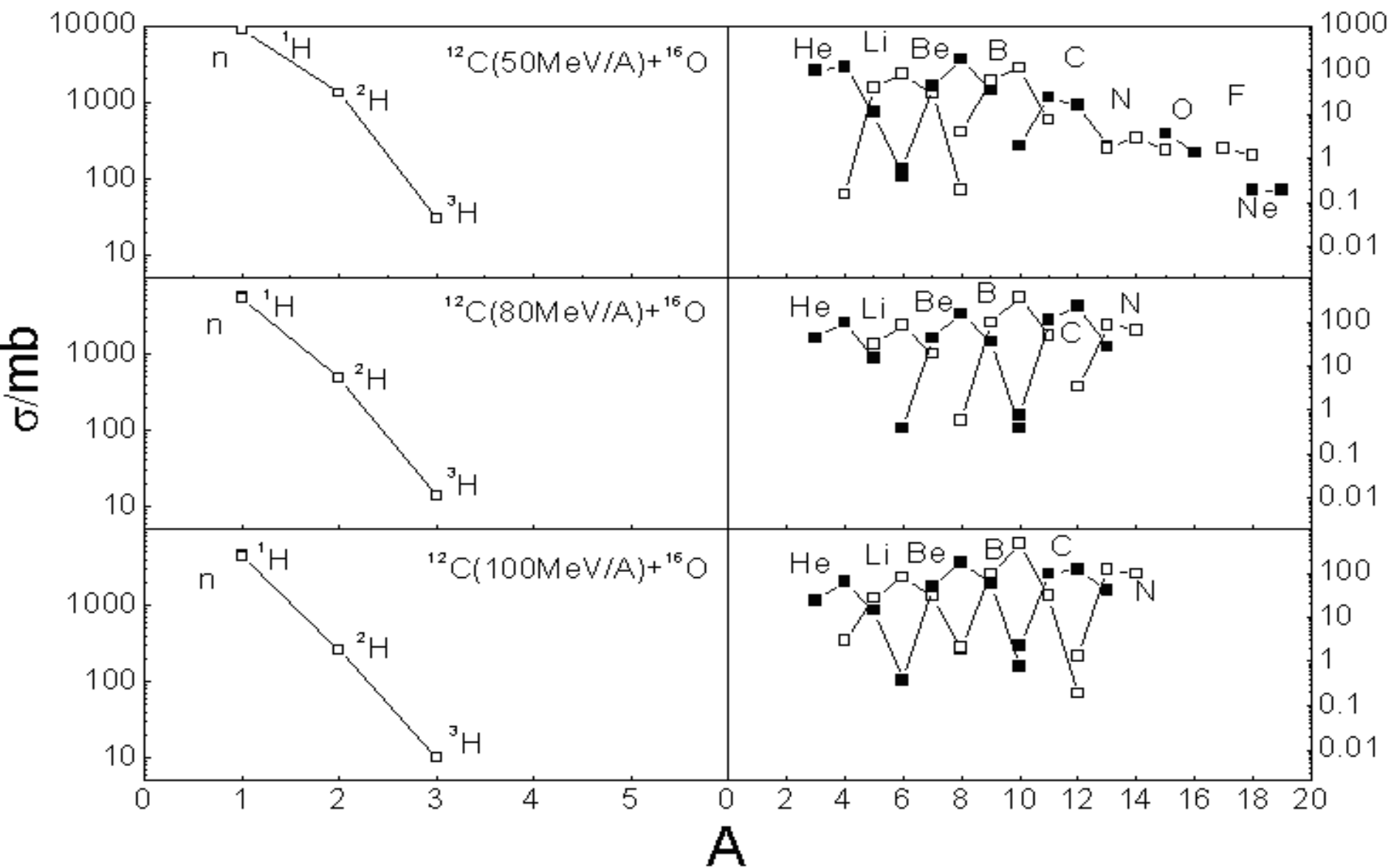
$^{12}\text{C}+^{12}\text{C}$



$^{12}\text{C}+^{14}\text{N}$



$^{12}\text{C}+^{16}\text{O}$



Fragmentation cross sections of ^{20}Ne collisions with different targets at 600 MeV/nucleon

Bao-An Bian^{a,b}, Feng-Shou Zhang^{a,b,c,*}, Hong-Yu Zhou^{a,b}

^a *The Key Laboratory of Beam Technology and Material Modification of Ministry of Education, Institute of Low Energy Nuclear Physics, Beijing Normal University, Beijing 100875, China*

^b *Beijing Radiation Center, Beijing 100875, China*

^c *Center of Theoretical Nuclear Physics, National Laboratory of Heavy Ion Accelerator of Lanzhou, Lanzhou 730000, China*

Received 5 February 2008; received in revised form 28 March 2008; accepted 30 March 2008

Available online 3 April 2008

Abstract

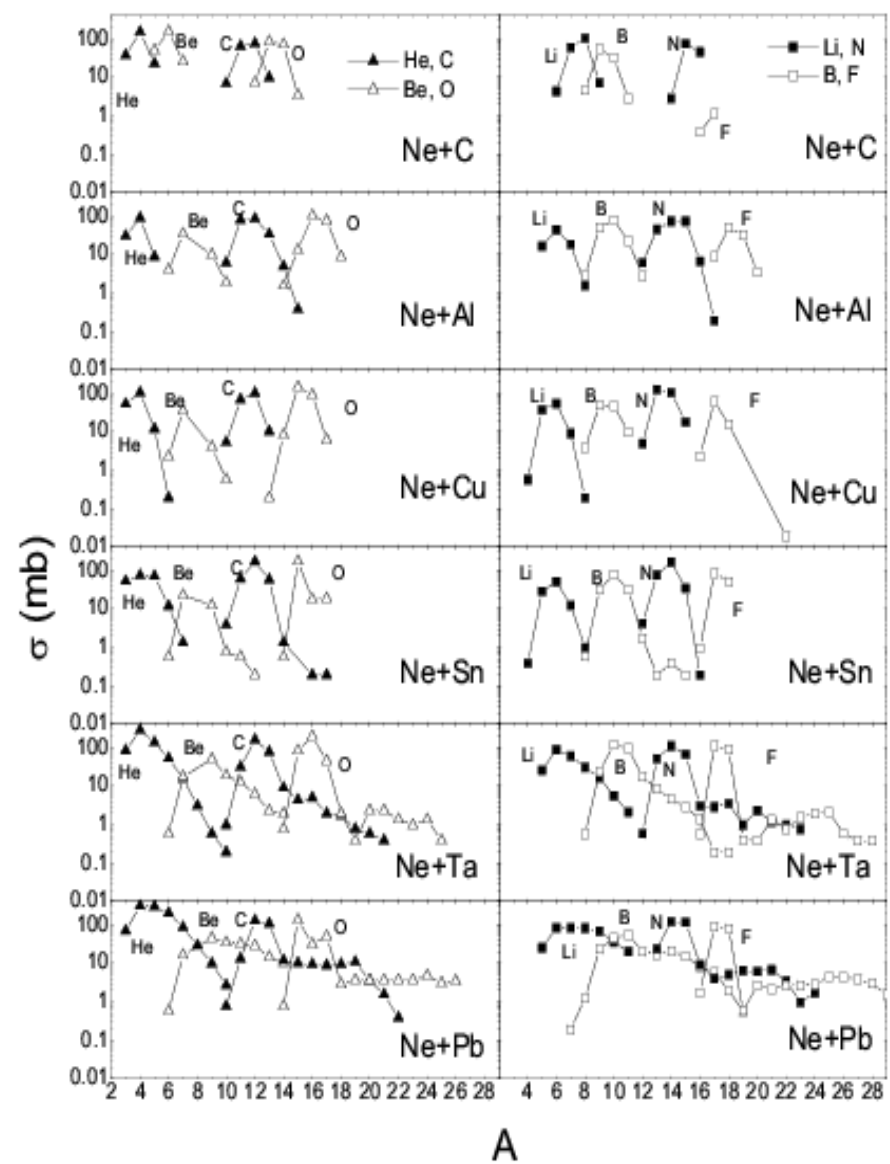
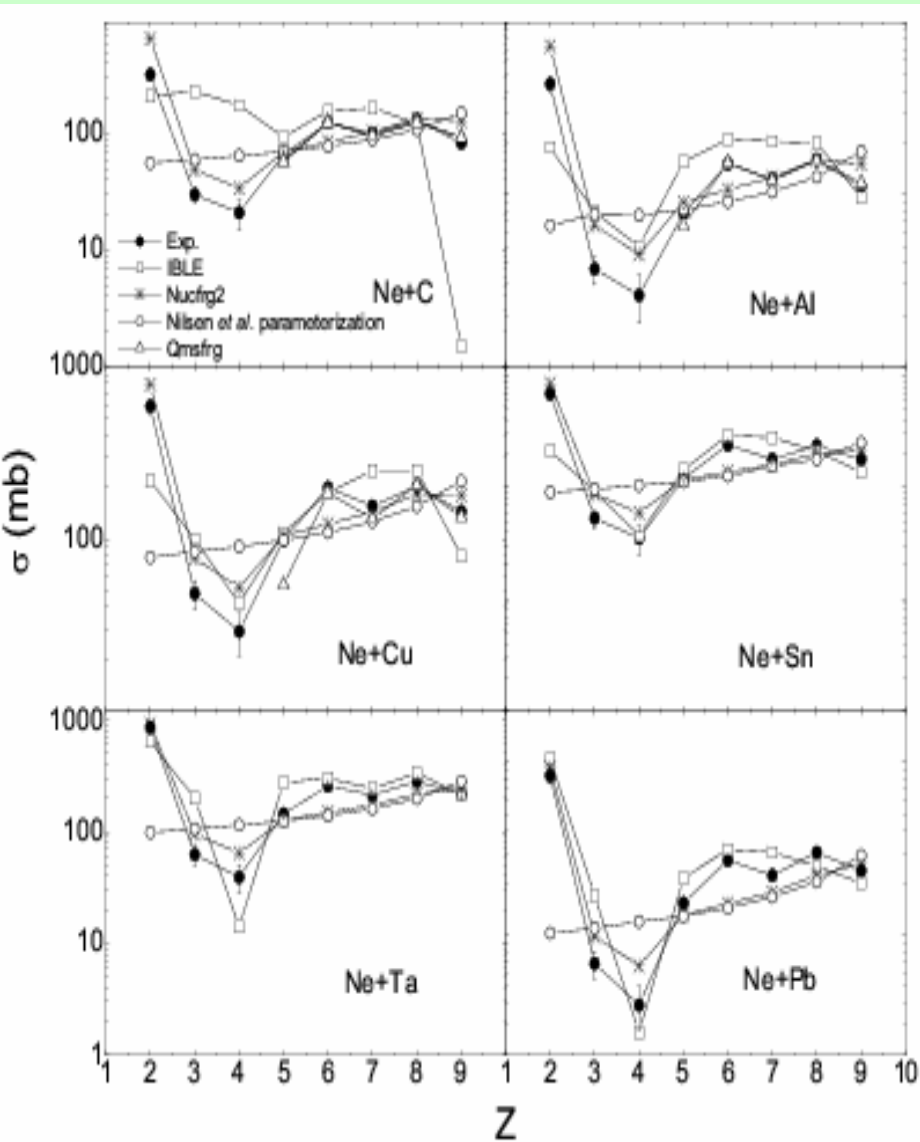
Within the framework of the isospin-dependent Boltzmann–Langevin equation, the production cross sections of fragments are calculated for reactions of Ne collisions with C, Al, Cu, Sn, Ta, and Pb targets at 600 MeV/nucleon. It is found that the production cross sections for fragments $Z = 2$ to 9 are qualitatively reproduced by the present calculations except for C target. The enhancement of even- Z fragments (C, O) cross sections shown in the experimental data is not well reproduced except for Ta target, however the observed suppression of the F fragment cross sections is described very well. The suppression of F production is discussed in terms of isotopic distribution of fragments. This is the first time to use the isospin-dependent Boltzmann–Langevin equation model to calculate the fragmentation cross sections for these reaction systems.

© 2008 Elsevier B.V. All rights reserved.

PACS: 25.70.-z; 25.70.Pq; 98.70.Sa

Keywords: Low and intermediate energy heavy-ion reactions; Multifragment emission; Cosmic rays

Isotope distributions



Odd-even effect in heavy-ion collisions at intermediate energies

Jun Su,^{1,2} Feng-Shou Zhang,^{1,2,3,*} and Bao-An Bian⁴

¹College of Nuclear Science and Technology, Beijing Normal University, 100875 Beijing, China

²Beijing Radiation Center, Beijing 100875, China

³Center of Theoretical Nuclear Physics, National Laboratory of Heavy Ion Accelerator of Lanzhou, Lanzhou 730000, China

⁴School of Science, Jiangnan University, Wuxi, Jiangsu 214122, China

(Received 7 December 2010; published 31 January 2011)

Heavy-ion collisions at intermediate energies are studied by the isospin-dependent quantum molecular dynamics model in the company of the GEMINI model. The isospin-dependent quantum molecular dynamics model is applied to describe the violent stage of the collisions, while the GEMINI model is applied to simulate the decays of the prefragments. The present study mainly focuses on the odd-even effect in the yields of the final fragments. We find that the odd-even effect appears in the deexcitation process of the excited prefragments, and is affected by the excitation energies and the isotope distributions of the prefragments. Both the projectile-isospin-dependent odd-even effect in the region of $-4 \leq T_z \leq 1$ and the role of the symmetry energy on the odd-even effect are studied. We find that the odd-even effect depends sensitively on the symmetry energy.

DOI: [10.1103/PhysRevC.83.014608](https://doi.org/10.1103/PhysRevC.83.014608)

PACS number(s): 25.70.Mn, 25.70.Pq, 24.10.Lx

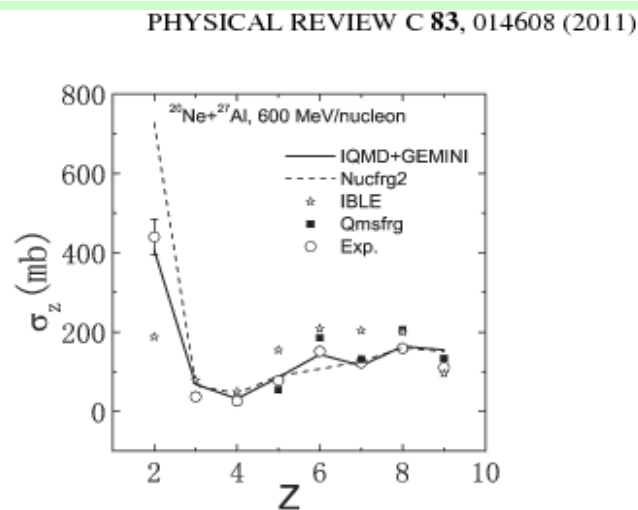


FIG. 1. Fragment cross sections presented as charge distribution for the reaction of $^{20}\text{Ne} + ^{27}\text{Al}$ at 600 MeV/nucleon. The experimental data [29] are shown as open circles. The calculations by the IQMD + GEMINI model are shown as a solid line. The calculations by other models are also shown: dashed line for Nucfrg2 [29], solid squares for Qmsfrg [29], and open stars for IBLE [35].

ODD-EVEN EFFECT IN HEAVY-ION COLLISIONS AT...

PHYSICAL REVIEW C 83, 014608 (2011)

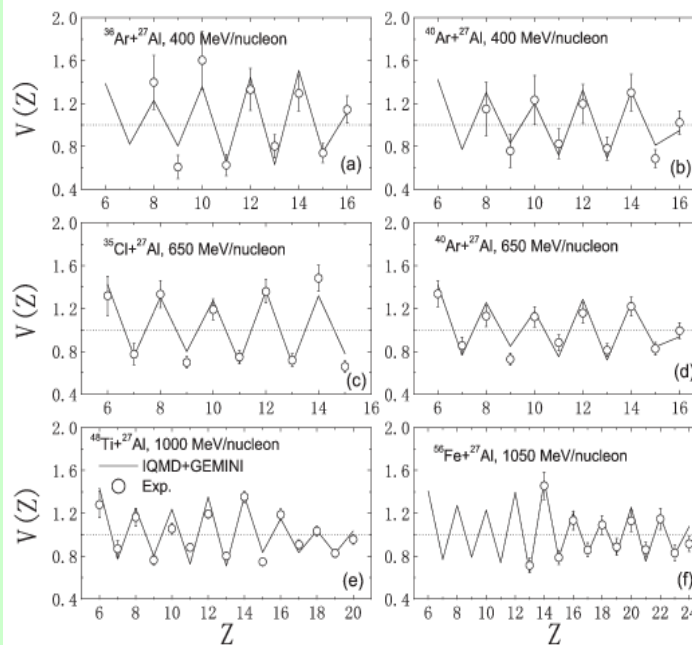


FIG. 4. Experimental $V(Z)$ (open circles) for fragments produced from the same reactions as in Fig. 2, plotted in comparison with the calculations by the IQMD + GEMINI model (solid lines).

Isotopic dependence of nuclear temperatures

Jun Su^{1,2} and Feng-Shou Zhang^{1,2,3,*}

¹The Key Laboratory of Beam Technology and Material Modification of Ministry of Education, College of Nuclear Science and Technology, Beijing Normal University, Beijing 100875, China

²Beijing Radiation Center, Beijing 100875, China

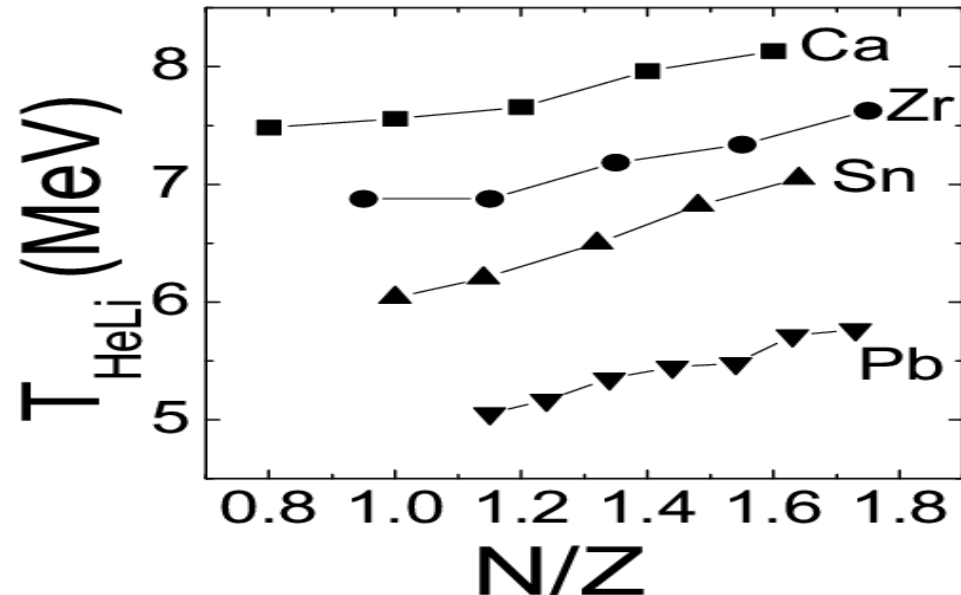
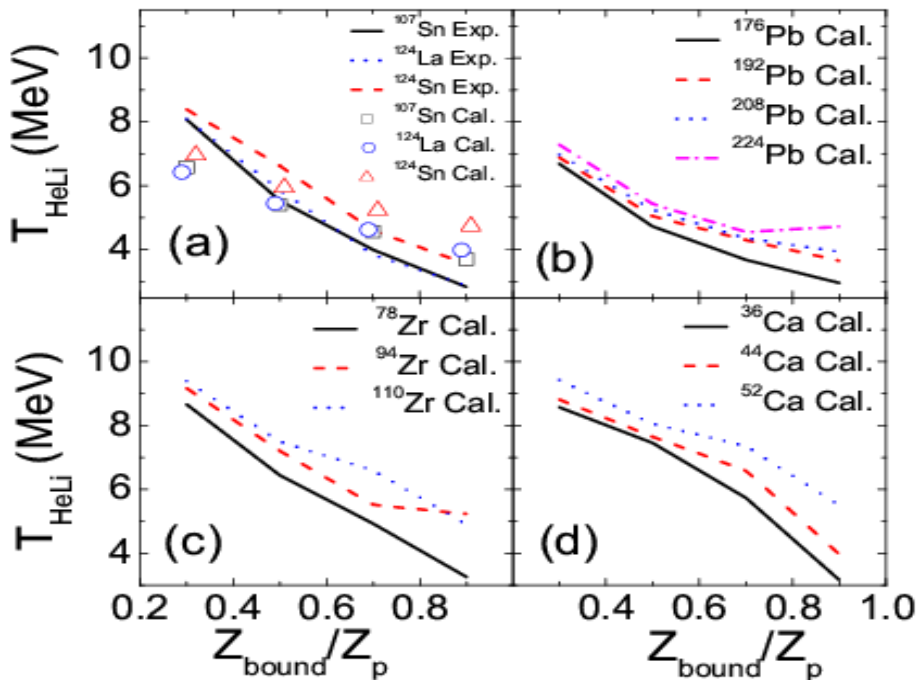
³Center of Theoretical Nuclear Physics, National Laboratory of Heavy Ion Accelerator of Lanzhou, Lanzhou 730000, China

(Received 28 June 2011; published 1 September 2011)

A systematic study of isotope temperatures has been presented for heavy-ion collisions at 600 MeV/nucleon via the isospin-dependent quantum molecular dynamics model in the company of the statistical decay model (GEMINI). We find that the isospin dependence of the isotope temperatures in multifragmentation is weak; however, this effect is still visible over a wide isotopic range. The isotope temperatures for the neutron-rich projectiles are larger than those for the neutron-poor projectiles. We also find that the isotope temperatures calculated by the model decrease with increasing nuclear mass.

DOI: [10.1103/PhysRevC.84.037601](https://doi.org/10.1103/PhysRevC.84.037601)

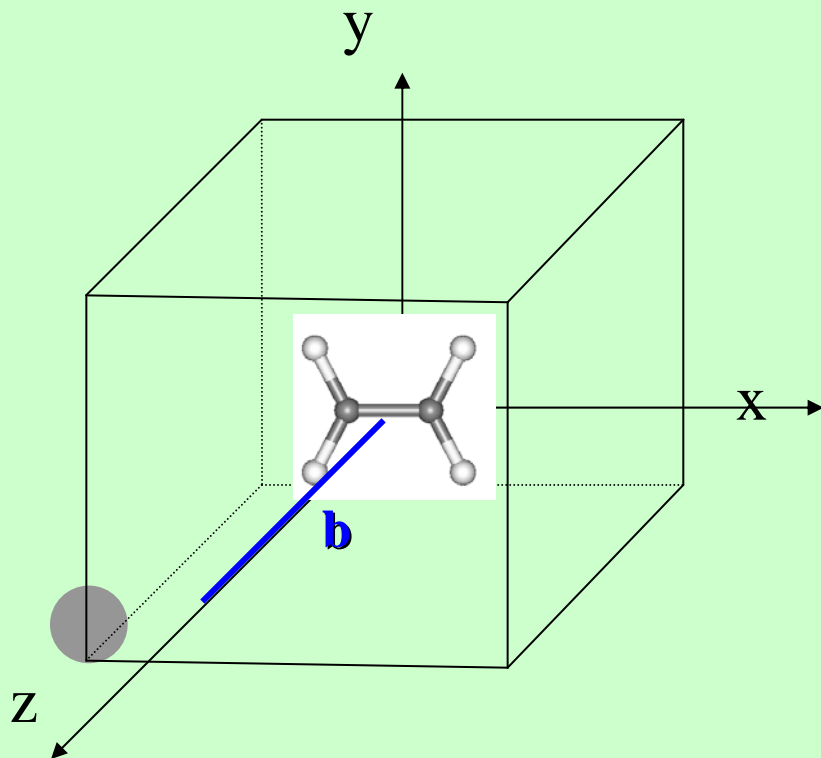
PACS number(s): 25.70.Mn, 25.70.Pq, 24.10.Lx



¹⁰⁷Sn, ¹²⁴Sn, ¹²⁴La (600MeV/u)+¹²⁴Sn

(2) Electron excitations and ionic motions

HI + C₂H₄ molecule



Energy (velocity)

Impact parameter

Charge

Orientation

Nonadiabatic Effects in the Irradiation of Ethylene

ZHI-PING WANG,^{1,2,3,4,5} PHUONG MAI DINH,^{4,5}
PAUL GERHARD REINHARD,⁶ ERIC SURAUD,^{4,5} FENG SHOU ZHANG^{2,3}

¹School of Science, JiangNan University, Wuxi 214122, China

²The Key Laboratory of Beam Technology and Material Modification of Ministry of Education, College of Nuclear Science and Technology, Beijing Normal University, Beijing 100875, People's Republic of China

³Beijing Radiation Center, Beijing 100875, China

⁴Université de Toulouse, UPS, Laboratoire Physique Théorique (IRSAMC), F-31062 Toulouse, France

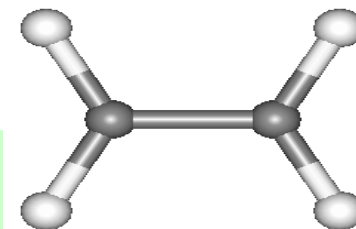
⁵CNRS, LPT(IRSAMC), F-31062 Toulouse, France

⁶Institut für Theoretische Physik, Universität Erlangen, Staudtstrasse 7, D-91058 Erlangen, Germany

Received 15 January 2010; accepted 9 February 2010

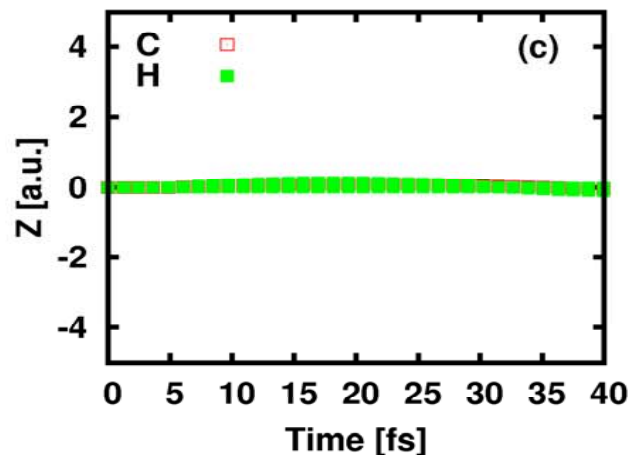
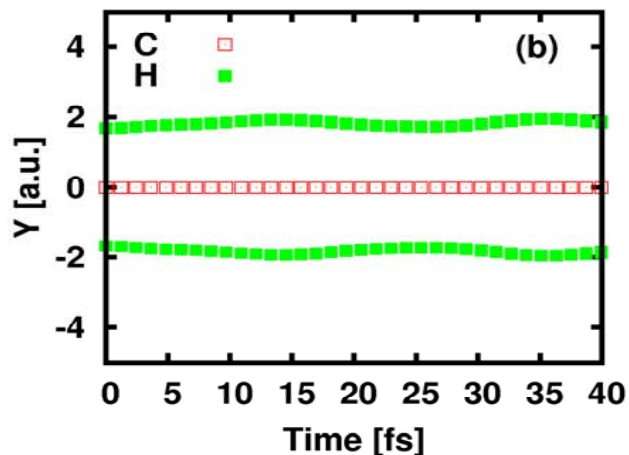
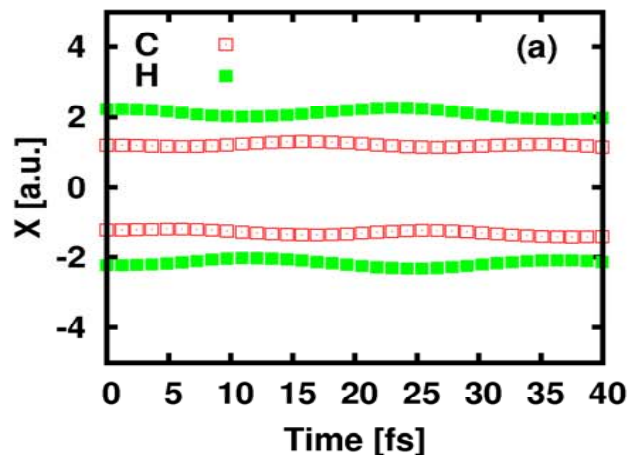
Published online 2 June 2010 in Wiley Online Library (wileyonlinelibrary.com).

DOI 10.1002/qua.22656



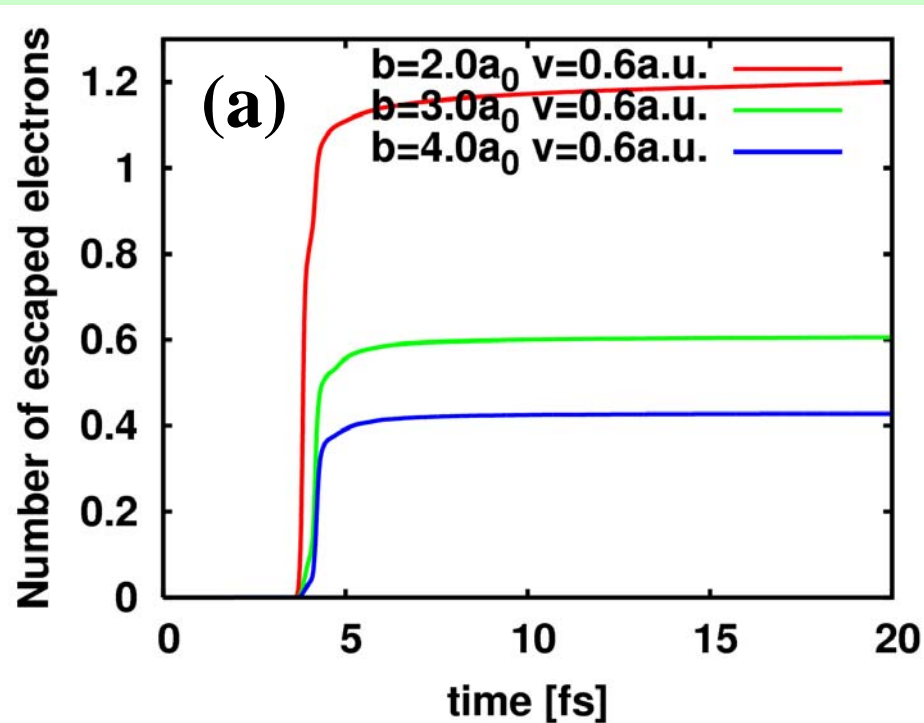
Collision process

$$Q=2, b=7a_0$$

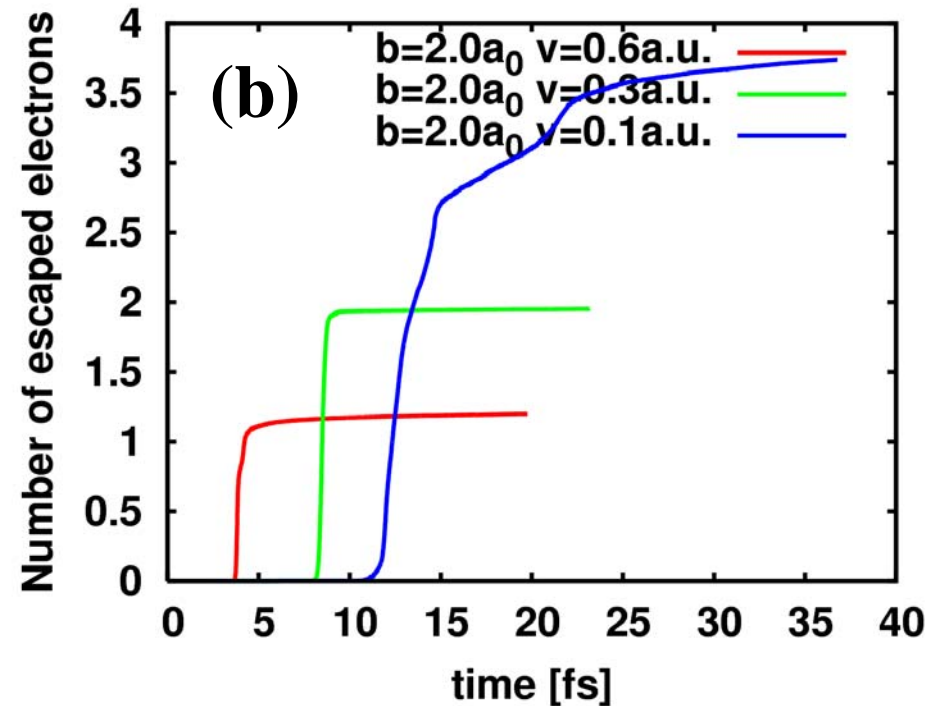


b and v dependence

(a) influence of impact parameter b

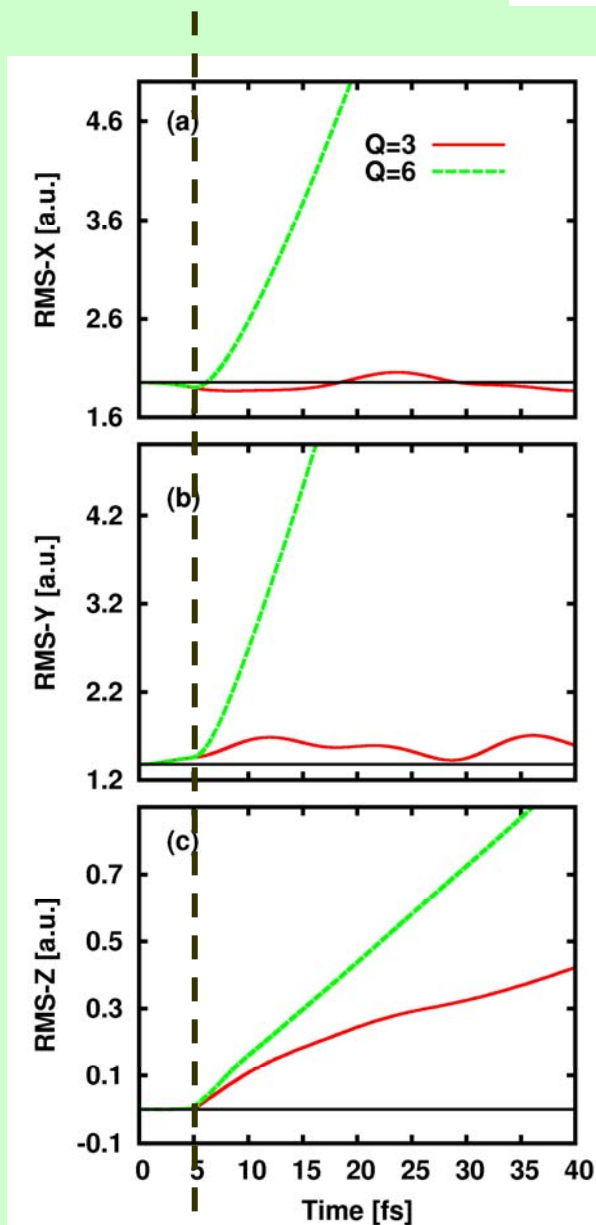
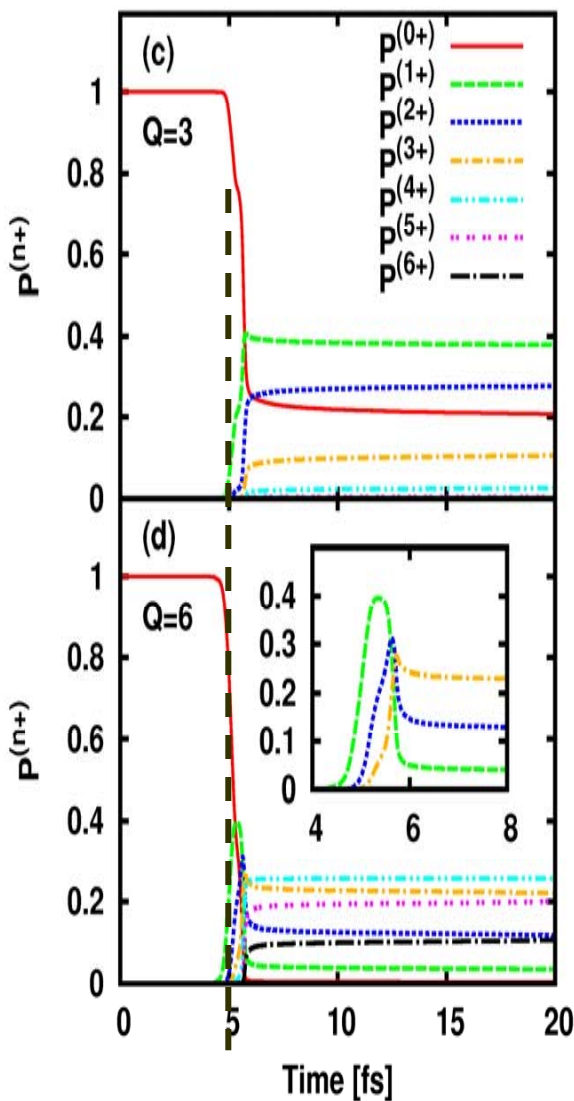
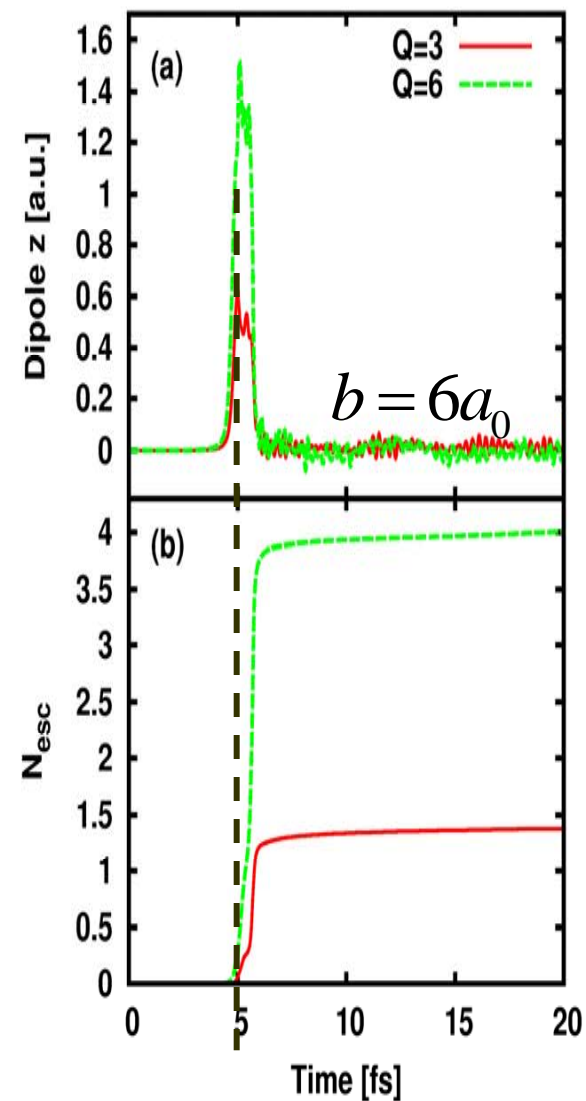
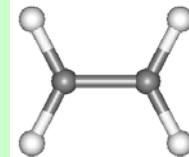


(b) influence of velocity v

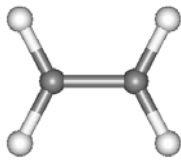


Different charges

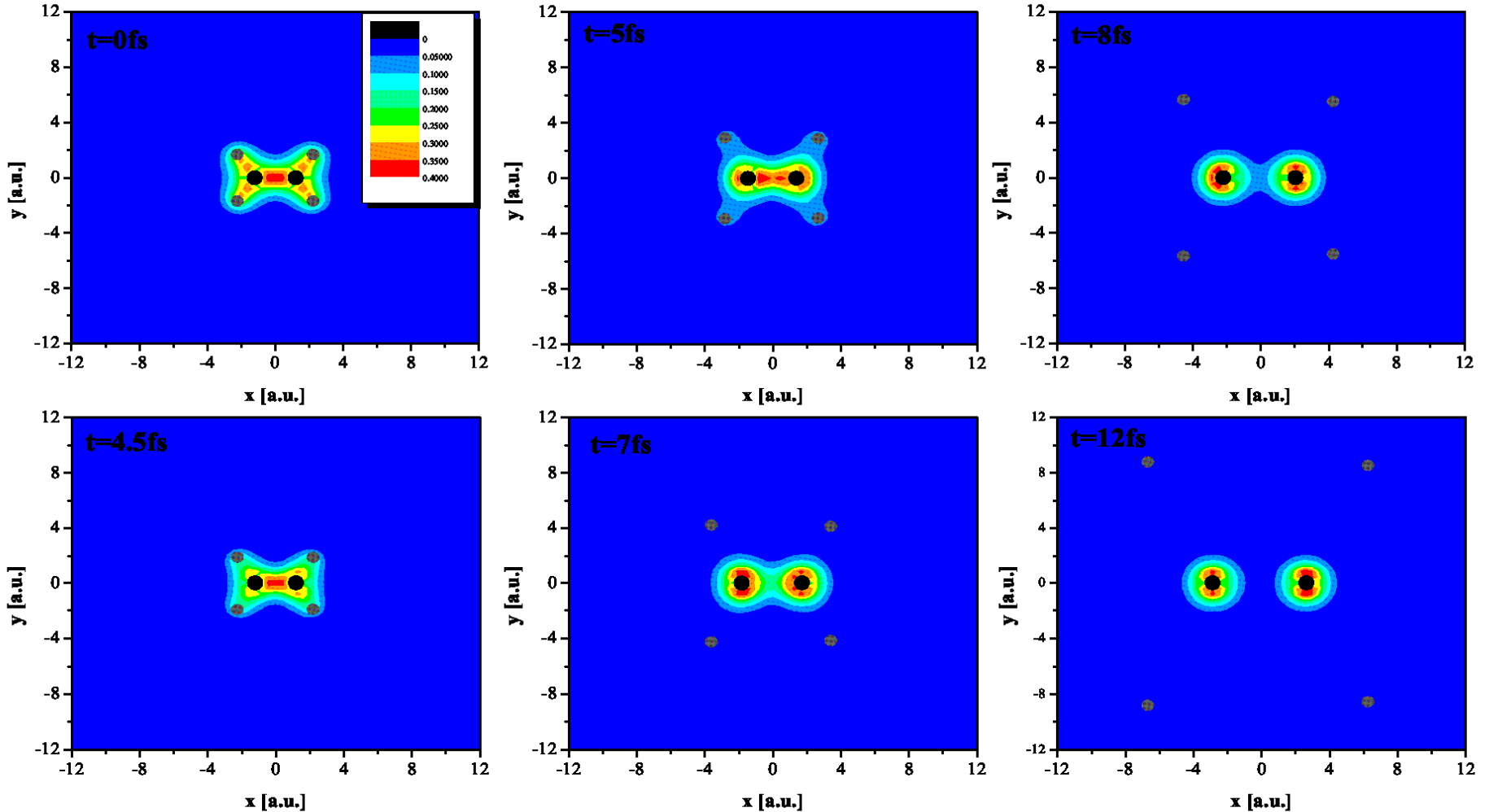
$Q=3$ $Q=6$



C_2H_4 Explosion at $Q=6$



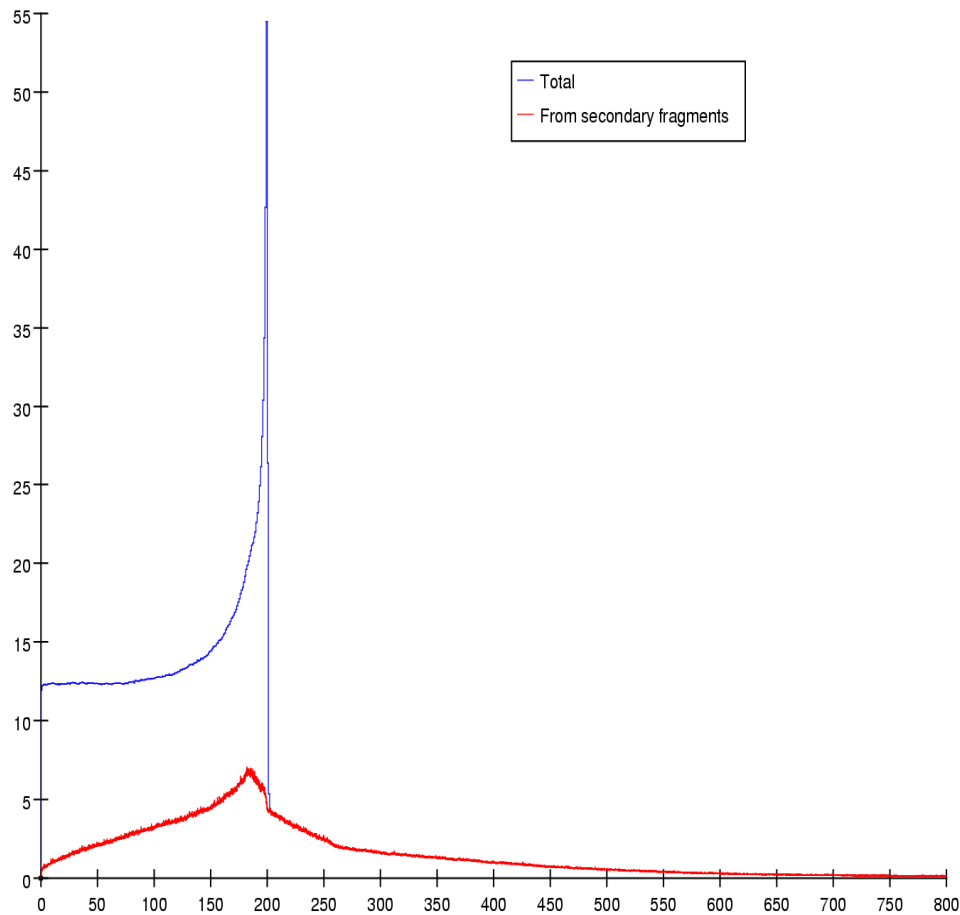
y



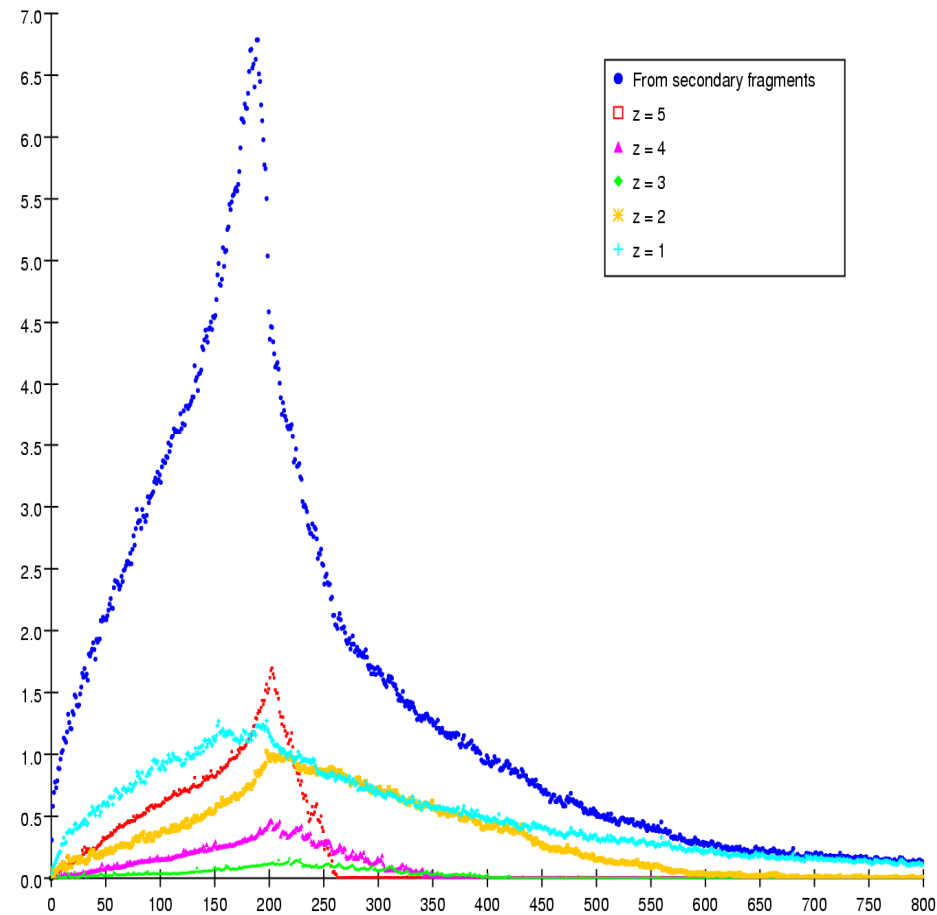
(3). Dose distributions

Contribution to the total energy deposition from secondary fragments produced in nuclear interactions of 330 MeV/u Carbon in water (Linear Energy Deposition as a function of penetration depth)

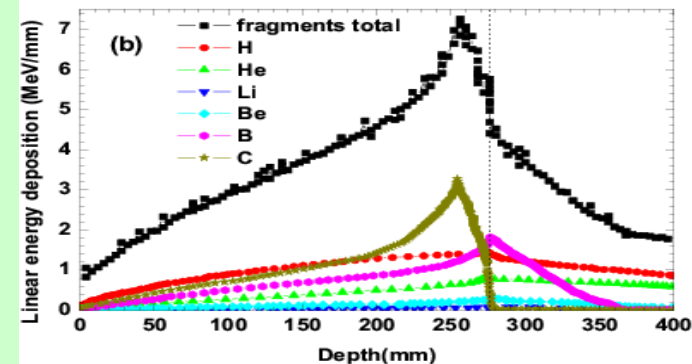
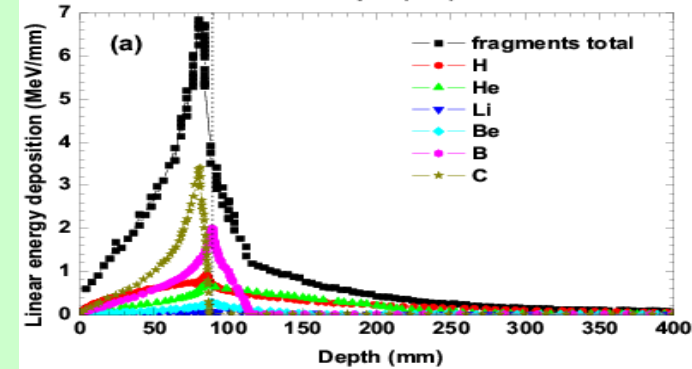
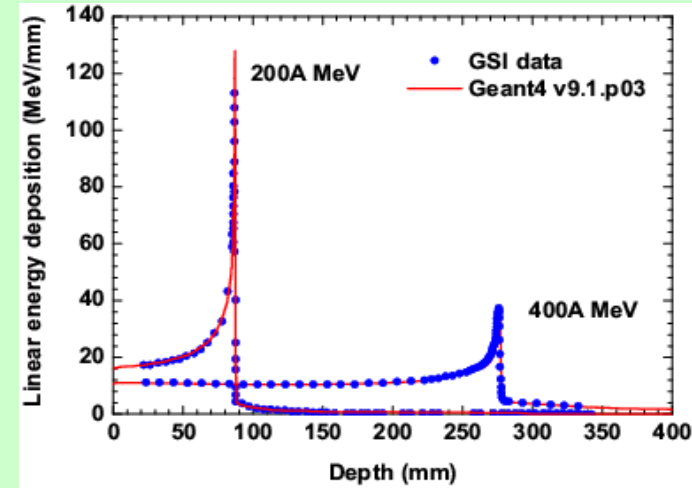
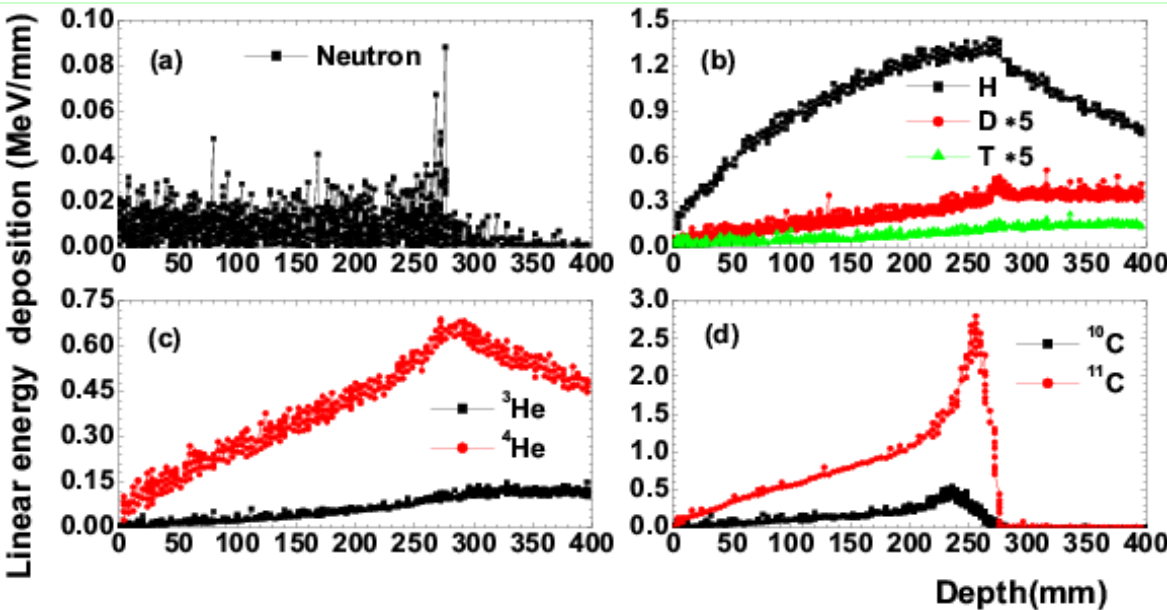
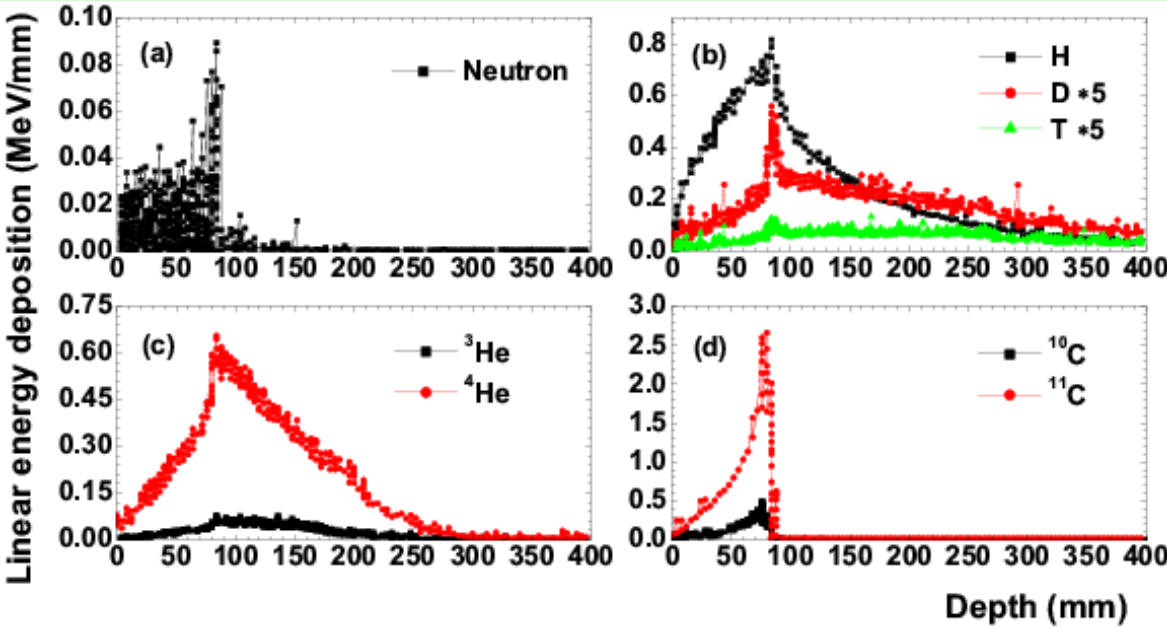
330A MeV 12C in water

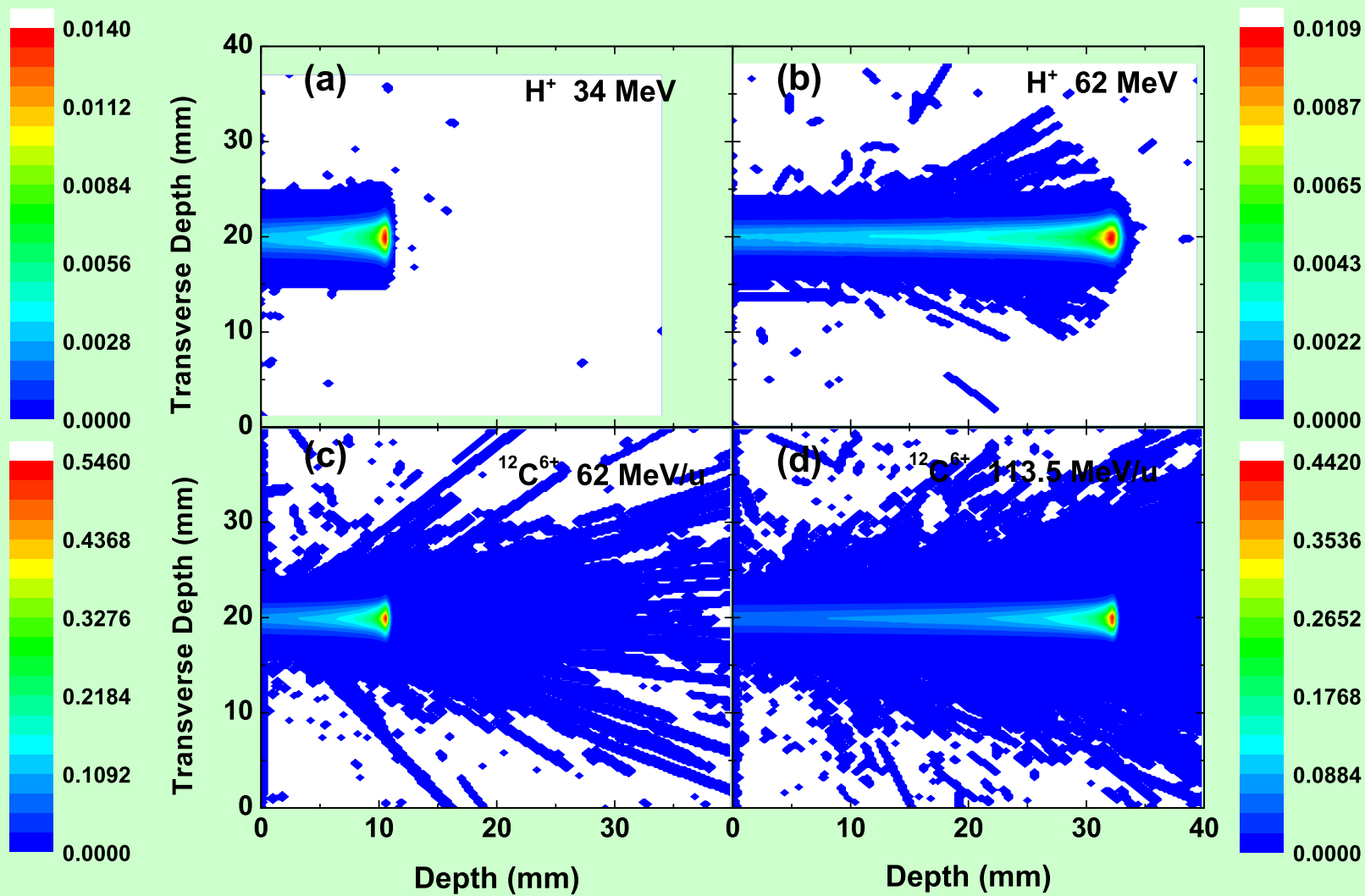


330A MeV 12C in water



Secondary beam fragments produced by 200 and 400 MeV/u C⁶⁺ ions in water



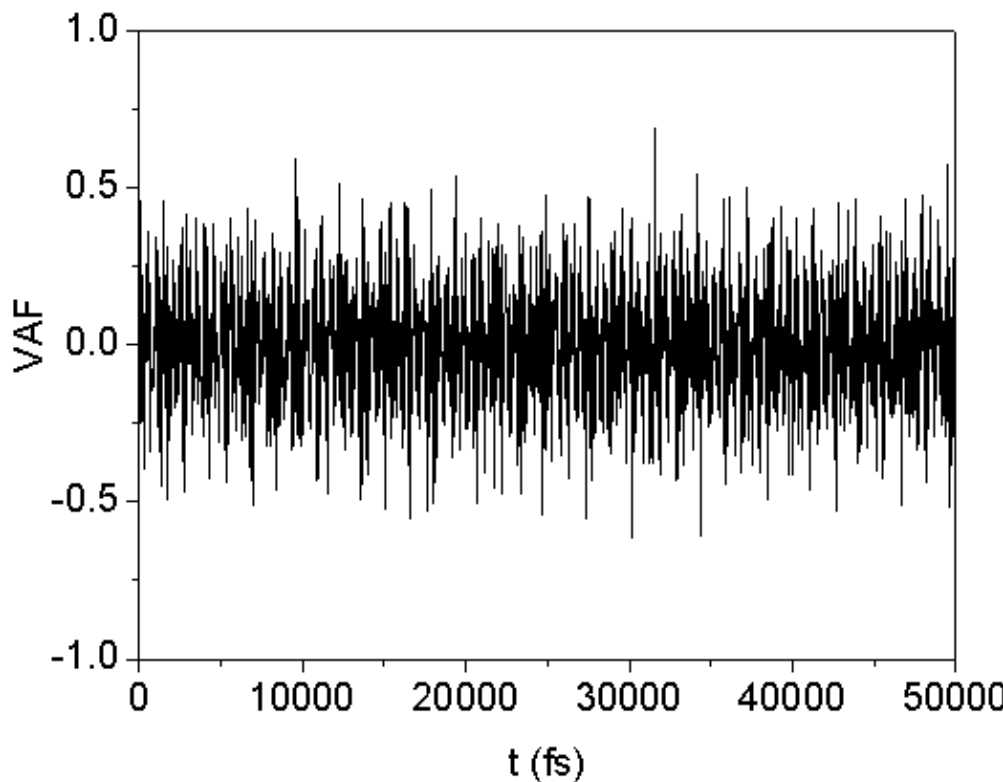
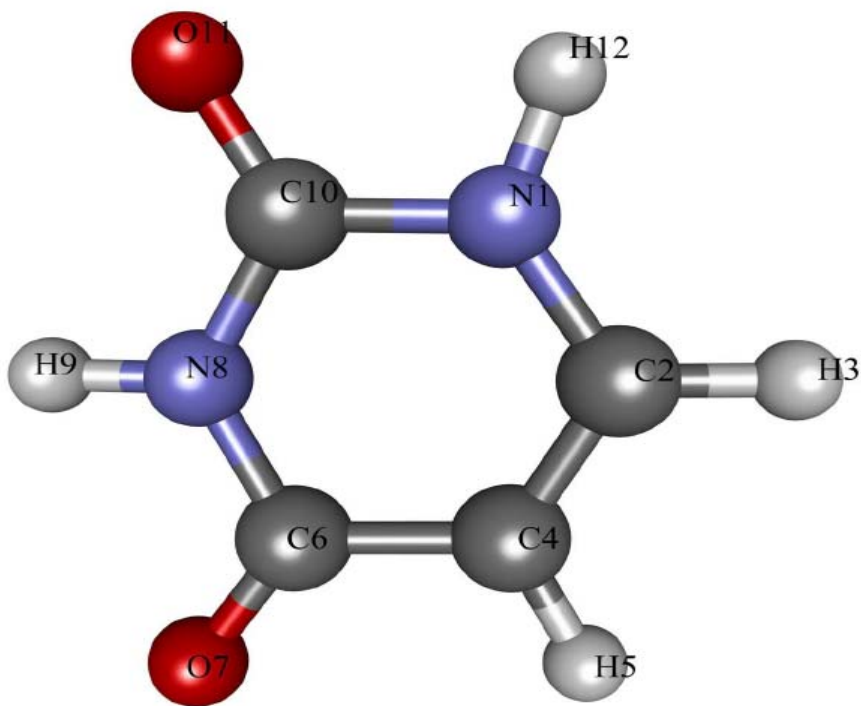


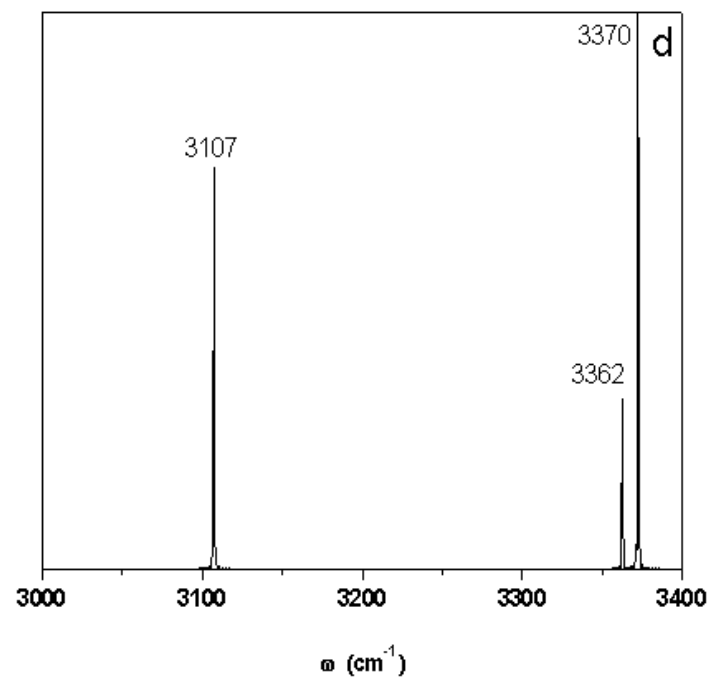
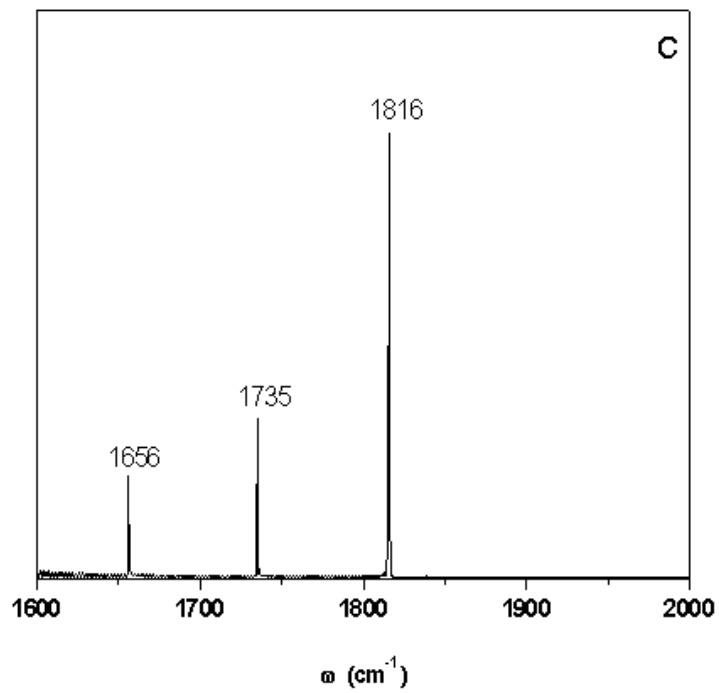
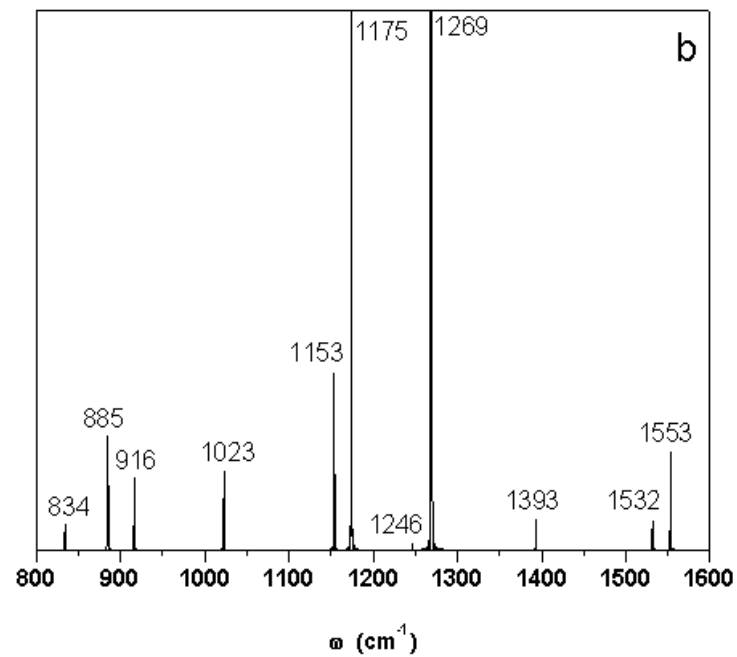
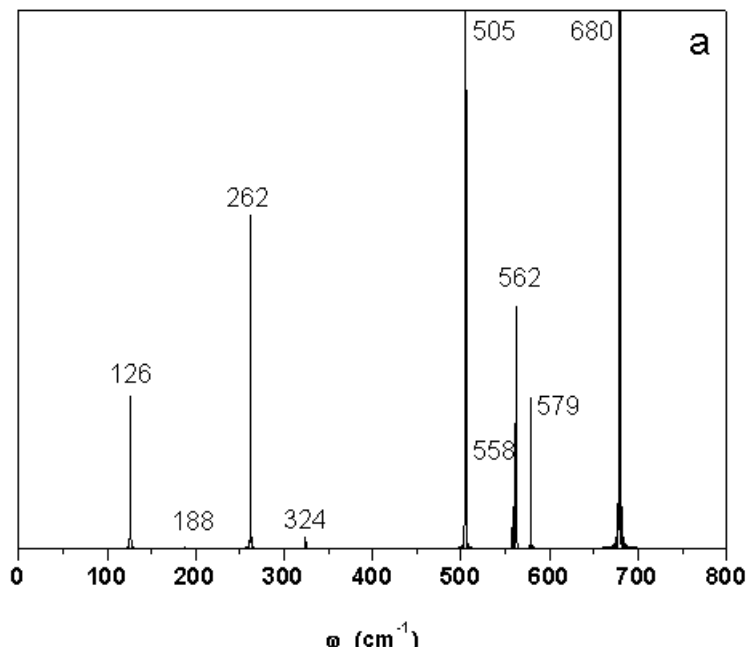
(4) Structure properties of biomolecule: U

(Wang, Zhang, Gu, Zhou ,

Chinese Science Bulletin 51(2006)1804)

Structure of Uracil



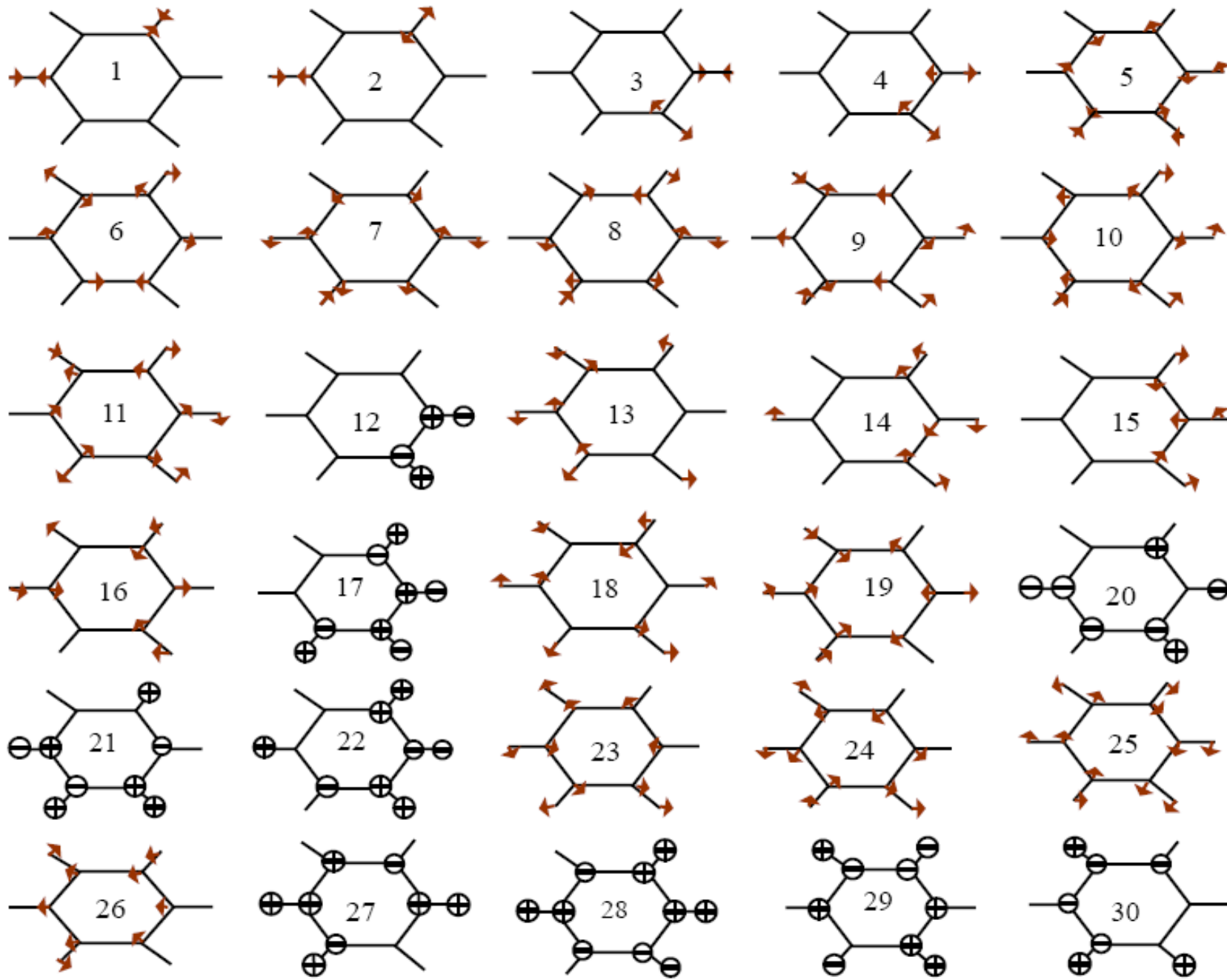


Vibrational frequencies of Uracil

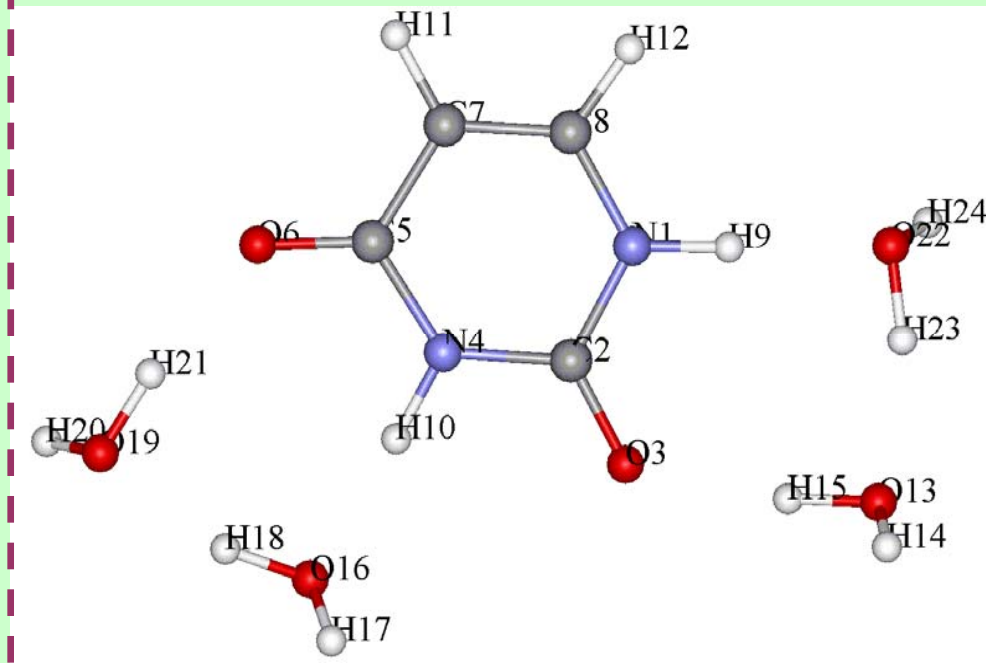
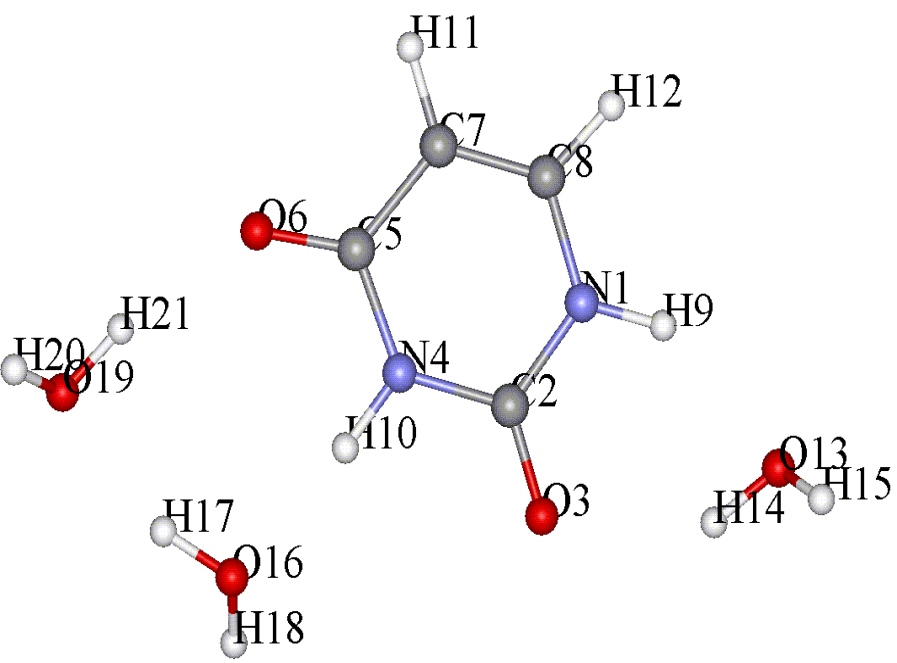
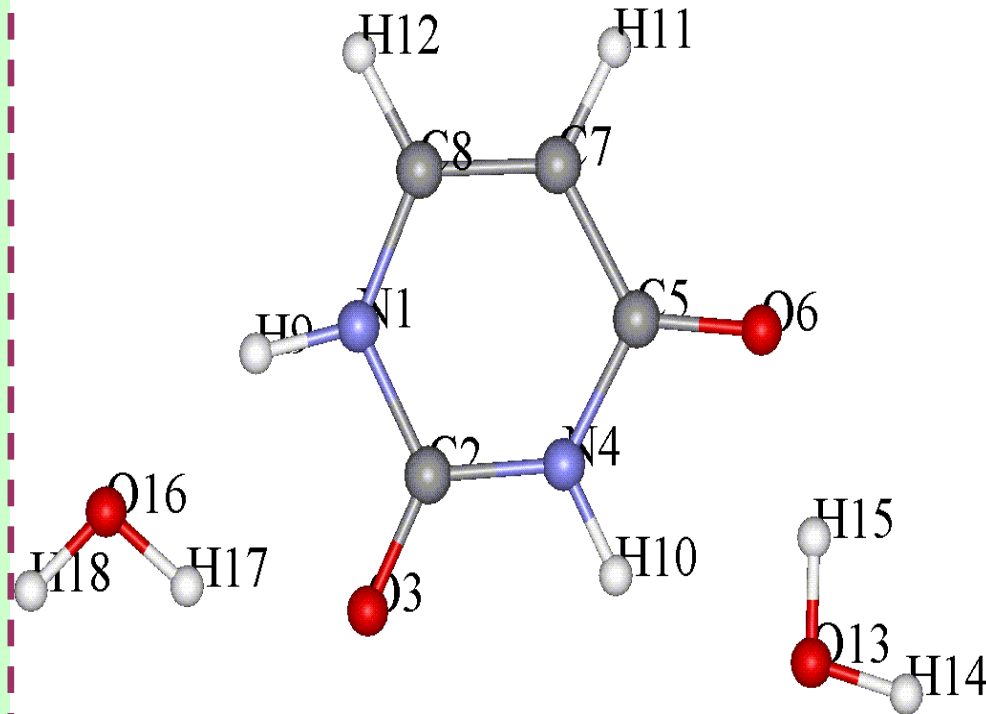
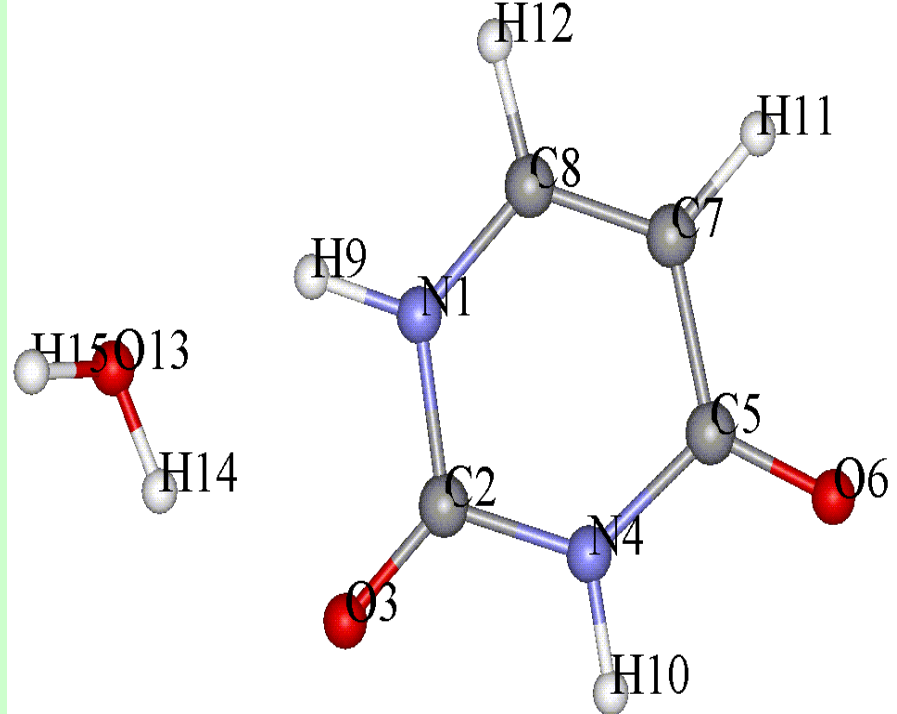
| Mode | FIR | VAF | Infra red | | Element | EXPERIMENTAL (cm^{-1}) | Mode | FIR | VAF | Infra red | | Element | EXPERIMENTAL (cm^{-1}) |
|------|------|------|-----------|------|---------|--------------------------------------|------|-----|-----|-----------|-----|---------|--------------------------------------|
| | | | ArMatrix | gas | | | | | | ArMatrix | gas | | |
| 1 | 3330 | 3370 | 3485 | 3484 | | 3658 | 16 | 916 | 916 | 980 | 972 | 994 | 970 |
| 2 | 3321 | 3362 | 3435 | 3436 | | 3620 | 17 | 888 | 885 | 958 | 952 | 928 | 965 |
| 3 | 3085 | | | 3124 | | 3264 | 18 | 835 | 834 | 804 | 802 | 860 | 813 |
| 4 | 3077 | 3107 | | 3076 | | 3221 | 19 | 713 | | 759 | | 824 | 772 |
| 5 | 1809 | 1816 | 1764 | 1756 | 1708 | 1845 | 20 | 683 | 680 | 757 | 757 | 804 | 752 |
| 6 | 1729 | 1735 | 1706 | 1703 | 1679 | 1808 | 21 | 582 | 579 | 718 | 717 | 786 | 729 |
| 7 | 1652 | 1656 | 1643 | 1641 | 1645 | 1690 | 22 | 564 | 562 | 662 | 660 | 761 | 687 |
| 8 | 1550 | 1553 | 1472 | 1461 | 1520 | 1506 | 23 | 559 | 558 | 562 | 545 | 579 | 563 |
| 9 | 1528 | 1532 | 1400 | 1400 | 1502 | 1422 | 24 | 530 | 529 | 551 | | 563 | 558 |
| 10 | 1393 | 1393 | 1389 | 1387 | 1456 | 1407 | 25 | 506 | 505 | 537 | | | 541 |
| 11 | 1270 | 1269 | 1359 | 1356 | 1392 | 1382 | 26 | 357 | 356 | 516 | 512 | 530 | 519 |
| 12 | 1249 | 1246 | 1217 | 1228 | 1260 | 1231 | 27 | 325 | 324 | 411 | 395 | | 396 |
| 13 | 1176 | 1175 | 1185 | 1172 | 1233 | 1198 | 28 | 263 | 262 | 391 | 374 | 429 | 385 |
| 14 | 1157 | 1153 | 1075 | 1082 | 1100 | 1091 | 29 | 189 | 188 | 185 | 185 | 195 | 170 |
| 15 | 1025 | 1023 | 987 | 990 | 1006 | 990 | 30 | 127 | 126 | 119 | | 145 | 150 |

Experimental data:

1. Graindourze, Grootaers, Smets, et al. J. Mol. Str.(Theochem), 237(1990)389
2. Palafox, Rastogi, Spectrochim Acta, A58 (2002)411
3. Florian, Hrouda, Spectrochim Acta, A49(1993)921



eigen modes of Uracil



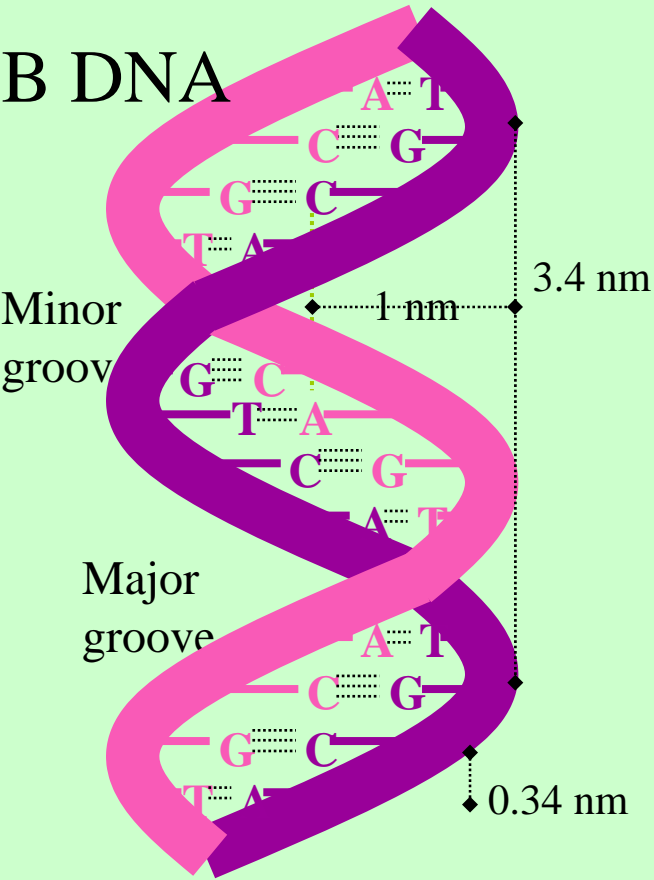
Vibrational frequencies of hydrated Uracil (in cm^{-1}) (only vibration of U molecule)

| Mode | uracil | Uw/s U | U2w/s U | U3w/s U | U4w/s U |
|------|--------|-----------|------------|------------|------------|
| 1 | 3330 | 3323 | 3322 | 3313 | 3299 |
| 2 | 3321 | 3313 | 3290 | 3286 | 3206 |
| 3 | 3085 | 3076 | 3061 | 3063 | 3008 |
| 4 | 3077 | 3068 | 3052 | 3053 | 2965 |
| 5 | 1809 | 1807 | 1814 | 1815 | 1860 |
| 6 | 1729 | 1729 | 1740 | 1740 | 1759 |
| 7 | 1652 | 1650 | 1656 | 1655 | 1656 |
| 8 | 1550 | 1548 | 1556 | 1552 | 1578 |
| 9 | 1528 | 1527 | 1533 | 1534 | 1515 |
| 10 | 1393 | 1388 | 1413 | 1414 | 1424 |
| 11 | 1270 | 1270 | 1316 | 1312 | 1392 |
| 12 | 1249 | 1230 | 1251 | 1251 | 1356 |
| 13 | 1176 | 1158 | 1213 | 1214 | 1309 |
| 14 | 1157 | 1137 | 1185 | 1184 | 1285 |
| 15 | 1025 | 1021 | 1054 | 1055 | 1262 |

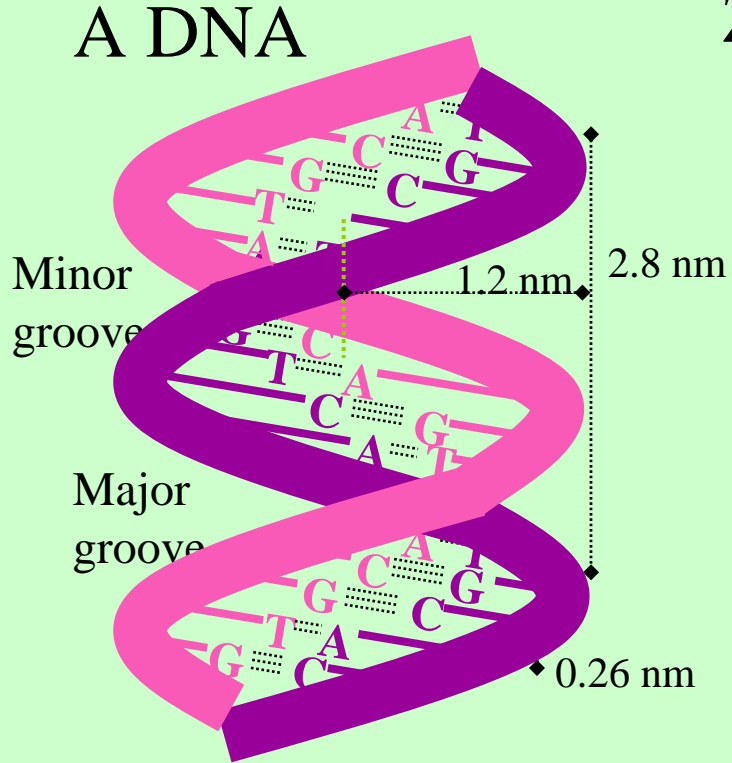
| Mode | uracil | Uw/s U | U2w/s U | U3w/s U | U4w/s U |
|------|--------|-----------|------------|------------|------------|
| 16 | 916 | 910 | 1005 | 1004 | 1219 |
| 17 | 888 | 873 | 937 | 938 | 1174 |
| 18 | 835 | 815 | 930 | 937 | 1139 |
| 19 | 713 | 741 | 881 | 912 | 1053 |
| 20 | 683 | 707 | 852 | 864 | 951 |
| 21 | 582 | 563 | 732 | 734 | 869 |
| 22 | 564 | 553 | 593 | 594 | 732 |
| 23 | 559 | 523 | 588 | 586 | 704 |
| 24 | 530 | 522 | 560 | 565 | 691 |
| 25 | 506 | 494 | 508 | 512 | 614 |
| 26 | 357 | 351 | 433 | 433 | 574 |
| 27 | 325 | 310 | 396 | 395 | 470 |
| 28 | 263 | 245 | 358 | 360 | 379 |
| 29 | 189 | 165 | 132 | 130 | 277 |
| 30 | 127 | 125 | 97 | 101 | 157 |

(5). Structure changes of DNA

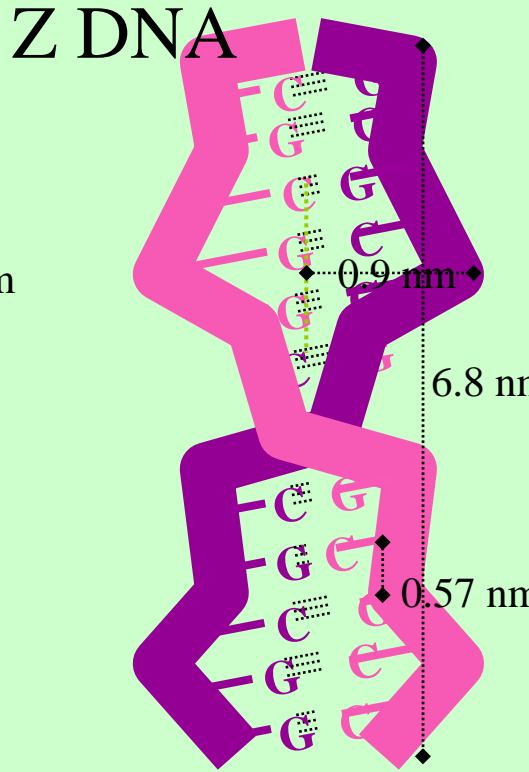
J.Chem.Phys.135 (2011) 034509, X. Shen et al



10.4 Bp/turn
+34.6° Rotation/Bp



11 Bp/turn
+34.7° Rotation/Bp



12 Bp/turn
-30.0° Rotation/Bp

Even More Forms Of DNA

- **C-DNA:**
 - Exists only under high dehydration conditions
 - 9.3 bp/turn, 0.19 nm diameter and tilted bases
- **D-DNA:**
 - Occurs in helices lacking guanine
 - 8 bp/turn
- **E-DNA:**
 - Like D-DNA lack guanine
 - 7.5 bp/turn
- **P-DNA:**
 - Artificially stretched DNA with phosphate groups found inside the long thin molecule and bases closer to the outside surface of the helix
 - 2.62 bp/turn

B-DNA appears to be the most common form *in vivo*. However, under some circumstances, alternative forms of DNA may play a biologically significant role.

DNA conformation transition ?

Factors to keep
helix of DNA

base stacking

hydrogen-bonds

solvent

counterions

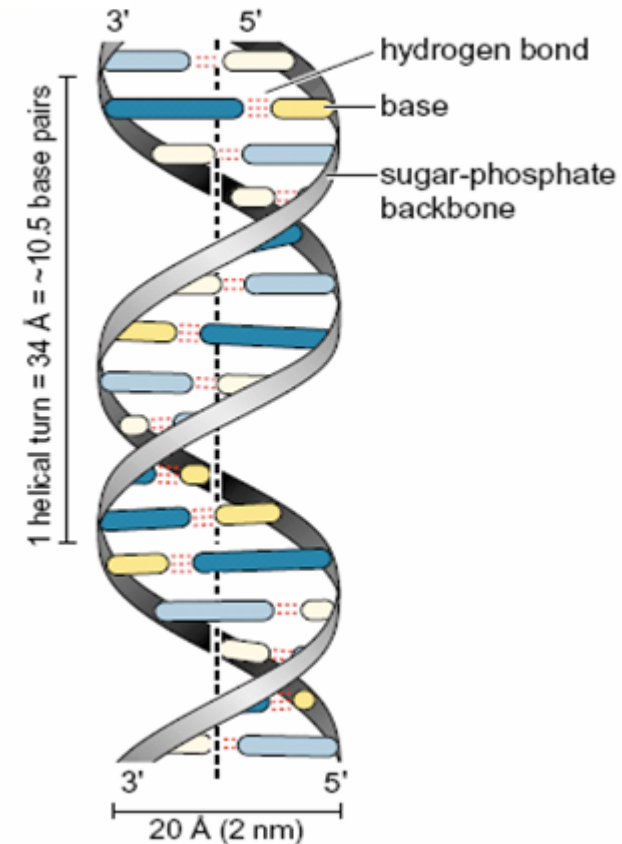
Water



Solvent environment

Temperature, pressure,
free radical, etc.

What we most care for?



“Knowing which properties of water are particularly sensitive to its structure can help to show how fine-tuned for life the liquid properties are”

NATURE Vol .436 25 August 2005

“water in changing”, “counterions in changing”,
“temperature in changing”

Solvent-Induced DNA Conformational Transition

B. Gu,^{1,2} F. S. Zhang,^{1,2,3,*} Z. P. Wang,^{1,2} and H. Y. Zhou^{1,2}

¹*The Key Laboratory of Beam Technology and Material Modification of Ministry of Education, Institute of Low Energy Nuclear Physics, Beijing Normal University, Beijing 100875, China*

²*Beijing Radiation Center, Beijing 100875, China*

³*Center of Theoretical Nuclear Physics, National Laboratory of Heavy Ion Accelerator of Lanzhou, Lanzhou 730000, China*

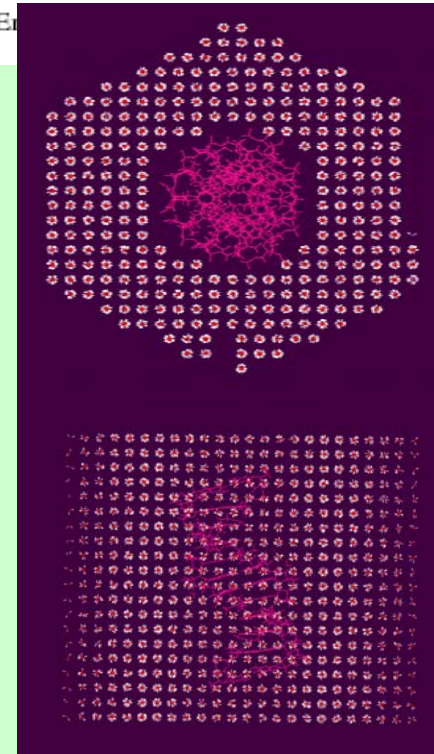
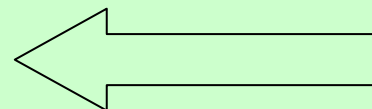
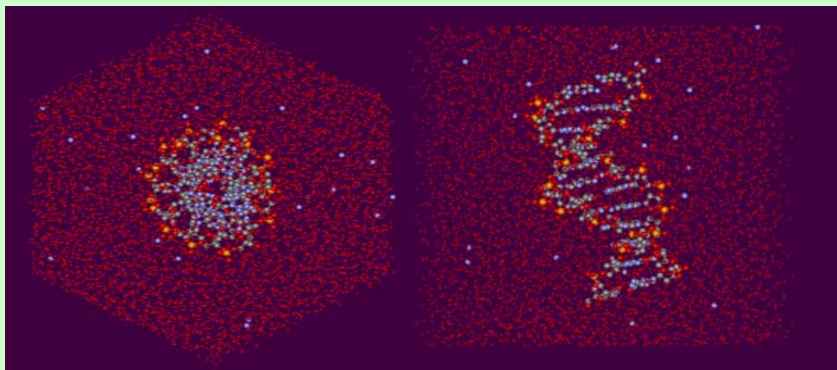
(Received 15 October 2007; published 29 February 2008)

Modified water models with scaled charges are used to investigate solvent polarity effects on DNA structure. Several intensive molecular dynamics simulations of the DNA EcoRI dodecamer d(CGCGAATTCGCG) in different model solvents are performed. When the polarity of the solvent molecule decreases, from overpolarized to less polarized, DNA experiences the conformational transitions of constrained $\rightarrow B$ form $\rightarrow (A-B)$ mix $\rightarrow A$ form. We demonstrate that one important cause of these structure changes is the competition between hydration and direct cation coupling to the free oxygen atoms in the phosphate groups on DNA backbones.

DOI: [10.1103/PhysRevLett.100.088104](https://doi.org/10.1103/PhysRevLett.100.088104)

PACS numbers: 87.14.G-, 61.25.E-

1 171d DNA
22 Na⁺ neutralizing ions
5800 charge-scaled water



Na⁺ interacts with DNA

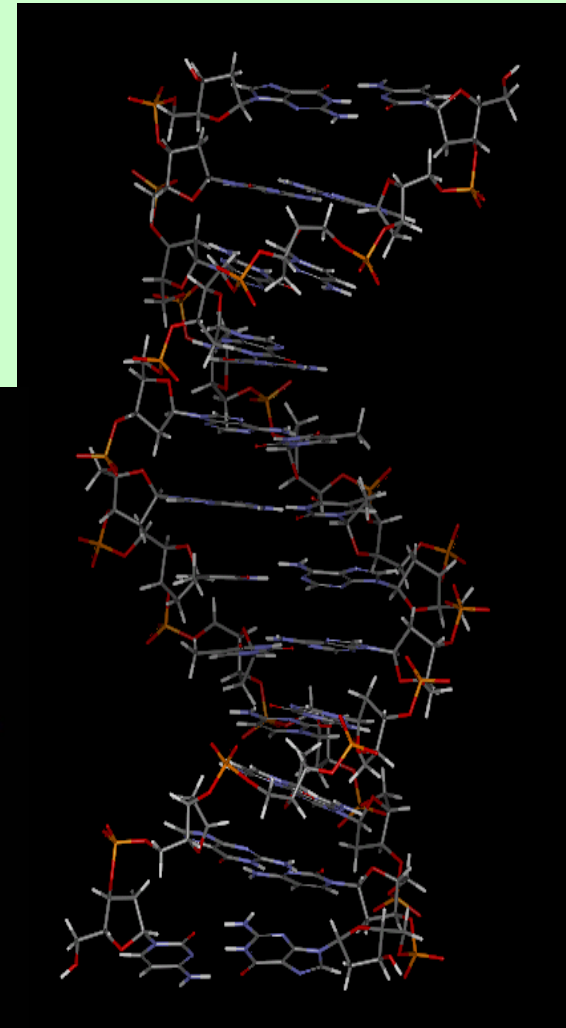
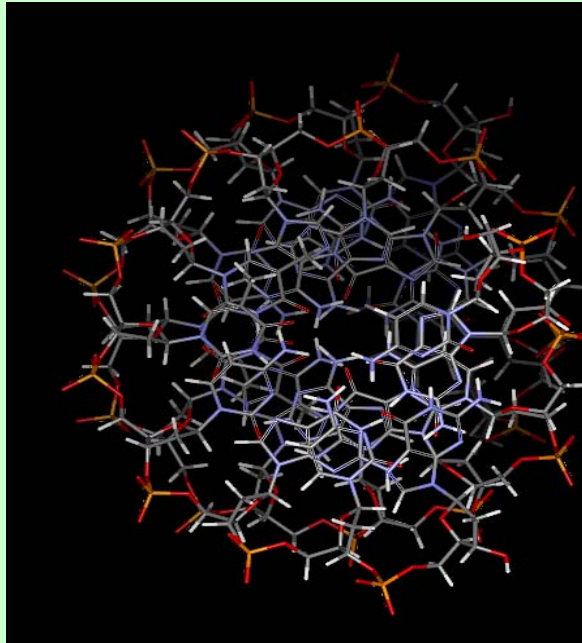
DNA : 171d PDB (Protein Data Bank)

NMR structure of a synthetic B-type dodecamer

d(CGCGAATTCGCG)

One cell: Hexagonal (~60 X 60 X 58 Å³), NVT, 298 K

171d DNA (1) + Na⁺ (22) neutralizing ions + H₂O (~5000)



Charge Scale

| Scale | Charges(e) O/H | Polarity(C·m×10 ⁻²⁹) |
|-----------------|---------------------|----------------------------------|
| 0.6 | -0.492/0.246 | 0.4551 |
| 0.7 | -0.574/0.287 | 0.5310 |
| 0.8 | -0.654/0.328 | 0.6068 |
| 1.0(SPC) | -0.820/0.410 | 0.7585 |
| 1.2 | -0.984/0.492 | 0.9102 |

Ions

| Ion | σ (Å) | ϵ (kJ/mol) |
|------------|--------------|---------------------|
| Li+ | 2.37 | 0.149 |
| Na+ | 2.73 | 0.358 |
| K+ | 3.36 | 0.568 |
| Ru+ | 3.36 | 0.568 |
| Cs+ | 3.57 | 1.602 |

Temperature Scale

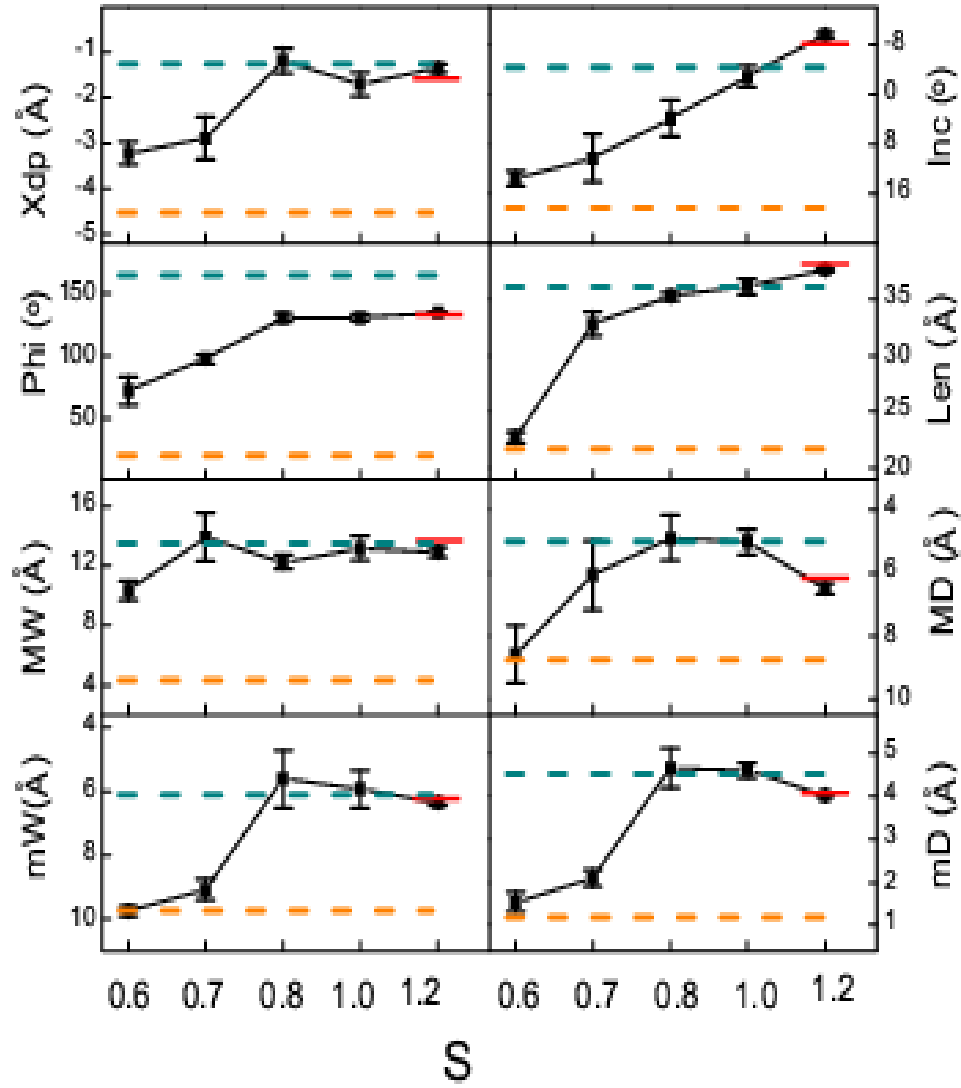
| | | | | | | | | |
|-------|-----|-----|-----|------------|-----|-----|--|-----|
| T (K) | 200 | 260 | 280 | 298 | 310 | 343 | | ... |
|-------|-----|-----|-----|------------|-----|-----|--|-----|

Averaged DNA structure parameters (2 ns)

typical A(orange), B(blue), and starting PDB(red)

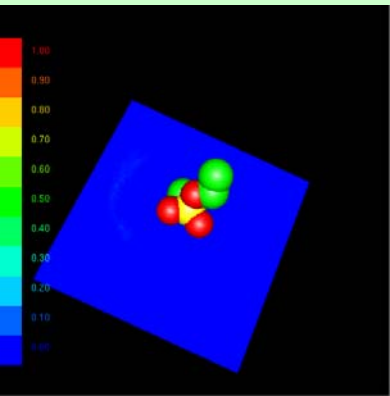
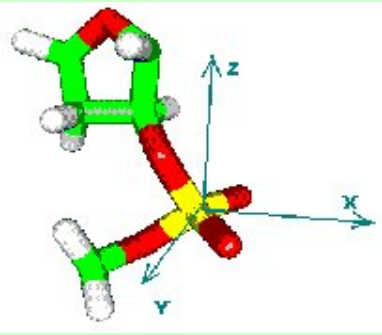
A,
B,
171d

- (1) x-displacement (Xdp)
- (2) inclination angle (Inc) of a base-pair from helical axis,
- (3) sugar pucker angle (Phi)
- (4) end to end length (Len)
- (5) width of Major groove MW
- (6) depth of Major groove MD
- (7) width of minor groove mW
- (8) depth of minor groove mD



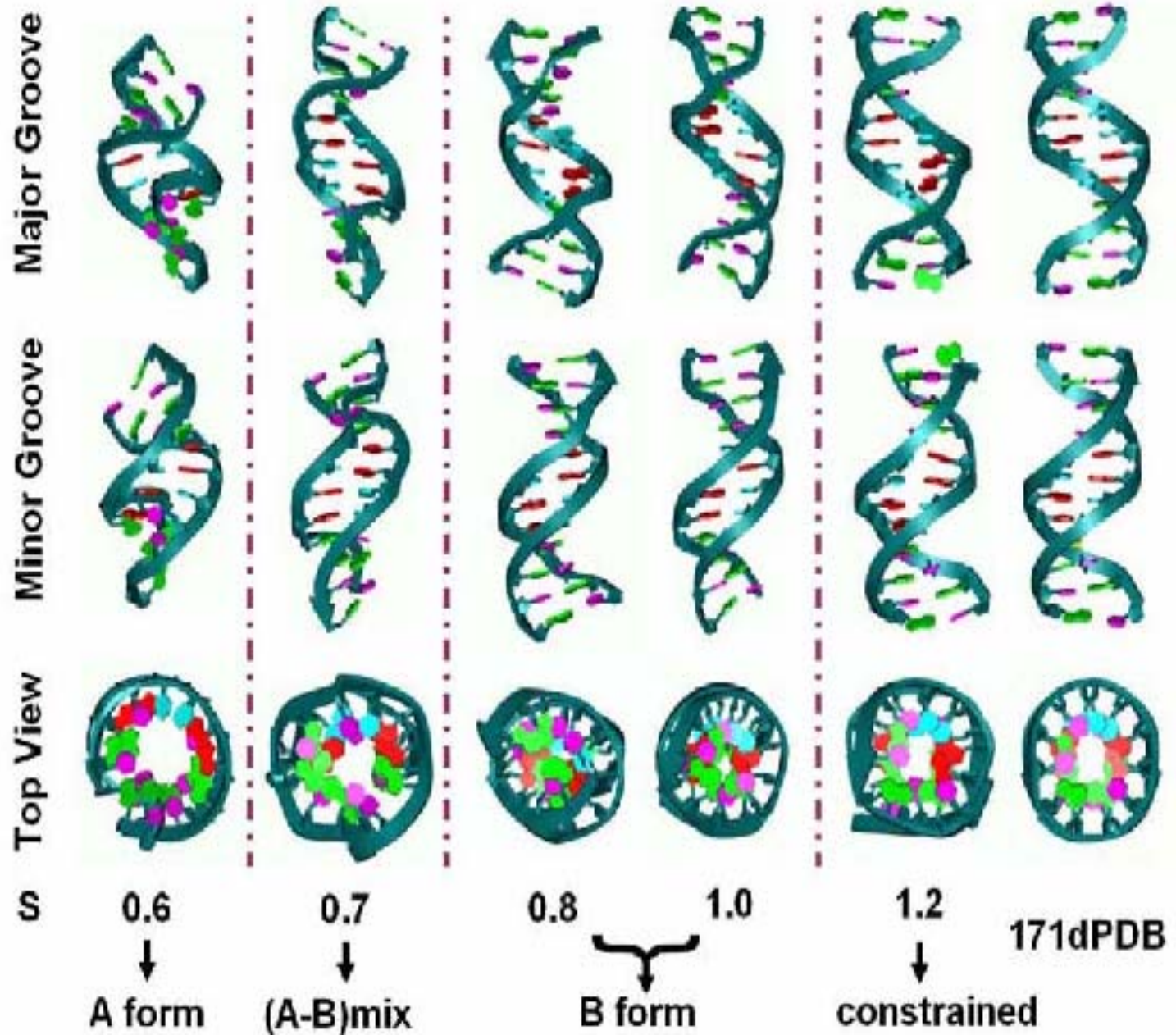
O(P)周围的Na⁺

B. Gu et al., PRL100 (2008) 088104

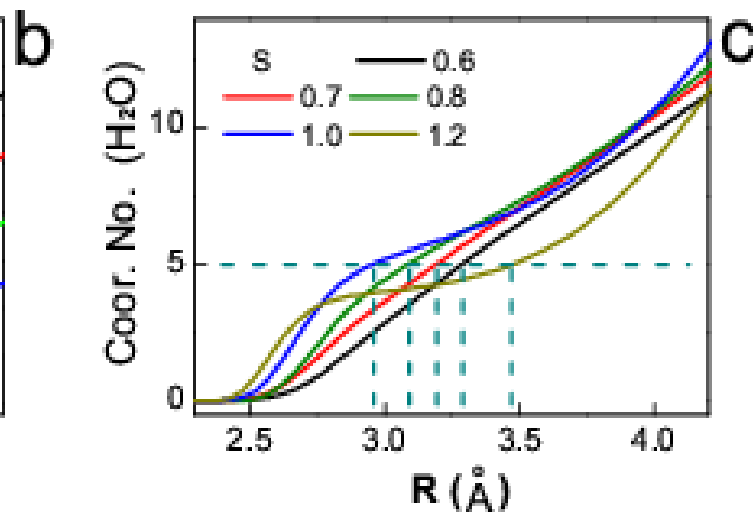
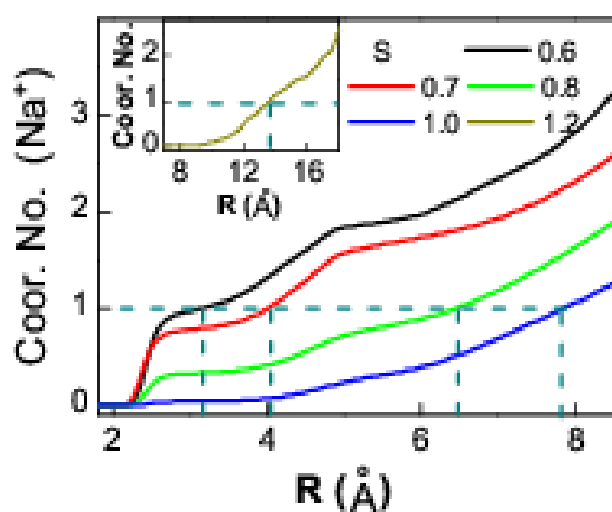
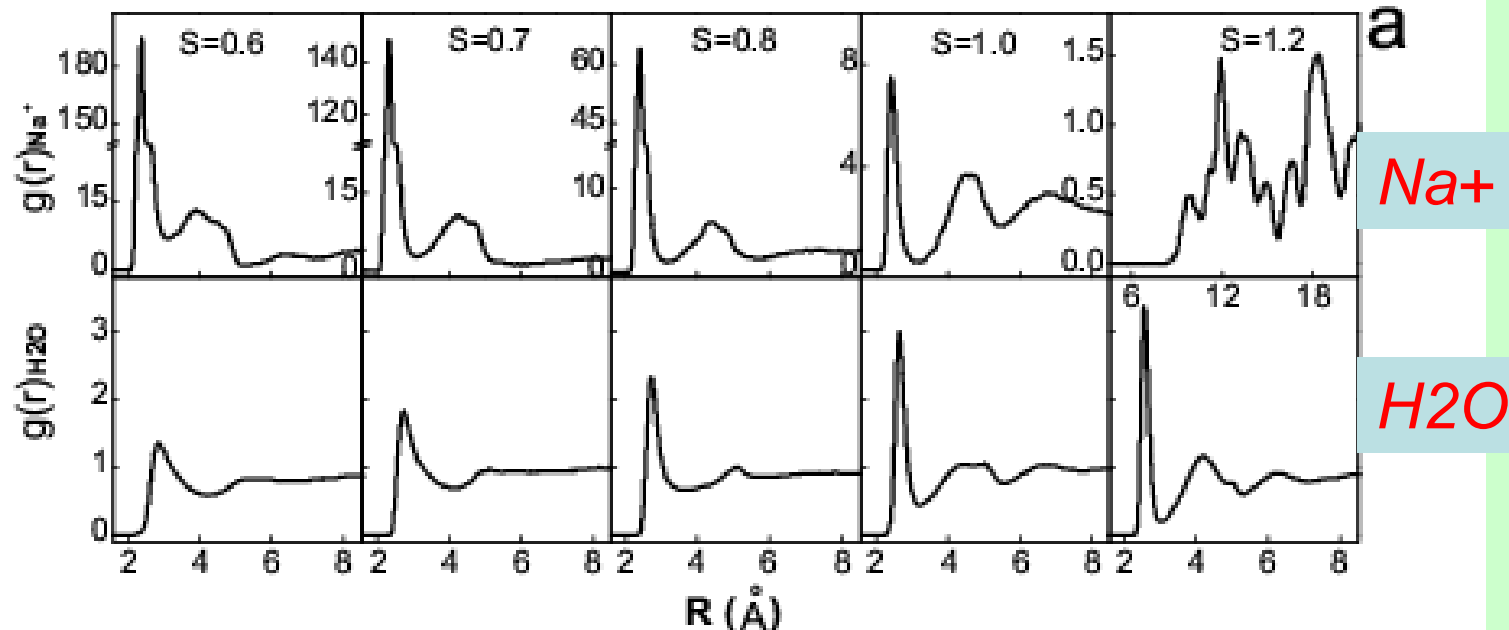


空间分布函数
x-y截面

Na⁺-O(P)



Radial distribution functions (RDF) and the coordination no. of Na^+ ions and H_2O



Solvent effects on the conformation of DNA dodecamer segment: A simulation study

X. Shen,^{1,2} B. Gu,³ S. A. Che,⁴ and F. S. Zhang^{1,2,5,a)}

¹The Key Laboratory of Beam Technology and Material Modification of Ministry of Education, College of Nuclear Science and Technology, Beijing Normal University, Beijing 100875, China

²Beijing Radiation Center, Beijing 100875, China

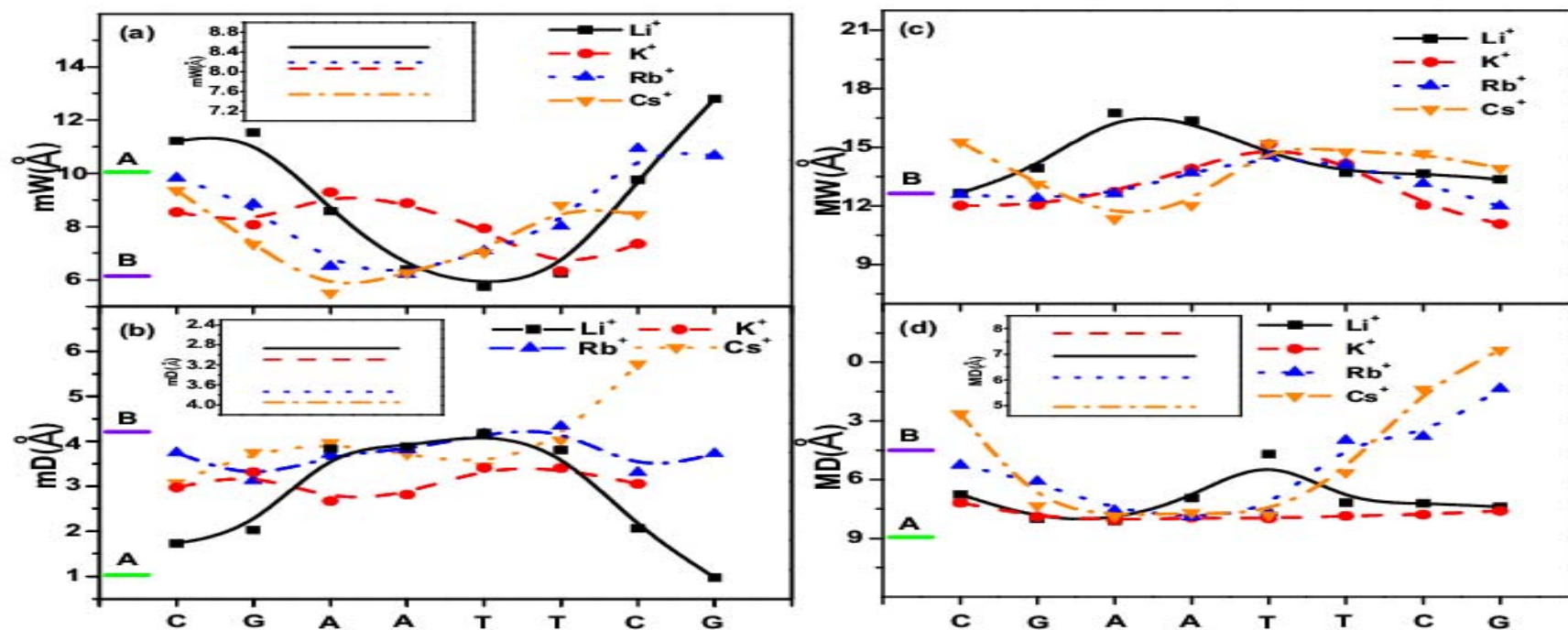
³College of Math and Physics, Nanjing University of Information Science and Technology, Nanjing 210044, China

⁴School of Chemistry and Chemical Technology, Shanghai Jiao Tong University, Shanghai 200240, China

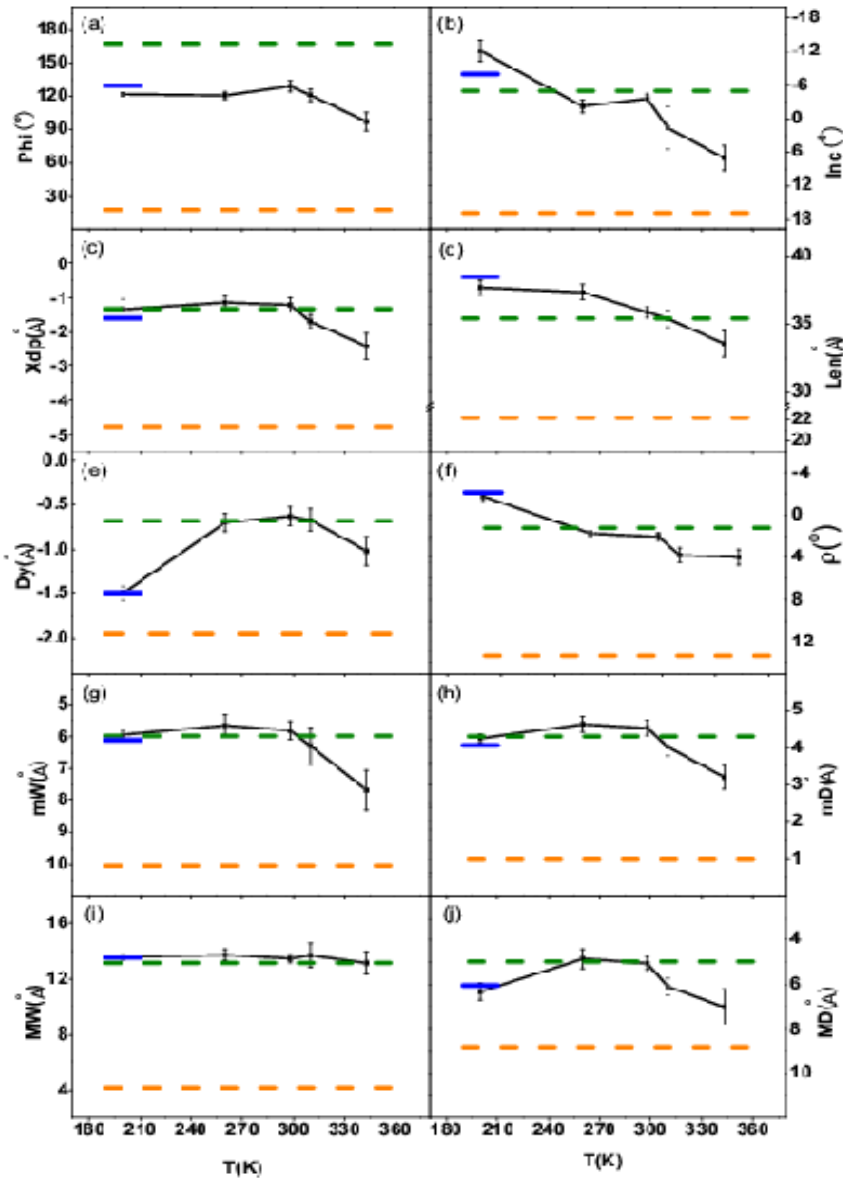
⁵Center of Theoretical Nuclear Physics, National Laboratory of Heavy Ion Accelerator of Lanzhou, Lanzhou 730000, China

(Received 11 December 2010; accepted 24 June 2011;

Counterions effects



Temperature effects



With the temperature rises, DNA structure changes to **(A-B) Mix-DNA**

Li⁺, K⁺, Rb⁺, Cs⁺ induced DNA conformation changes

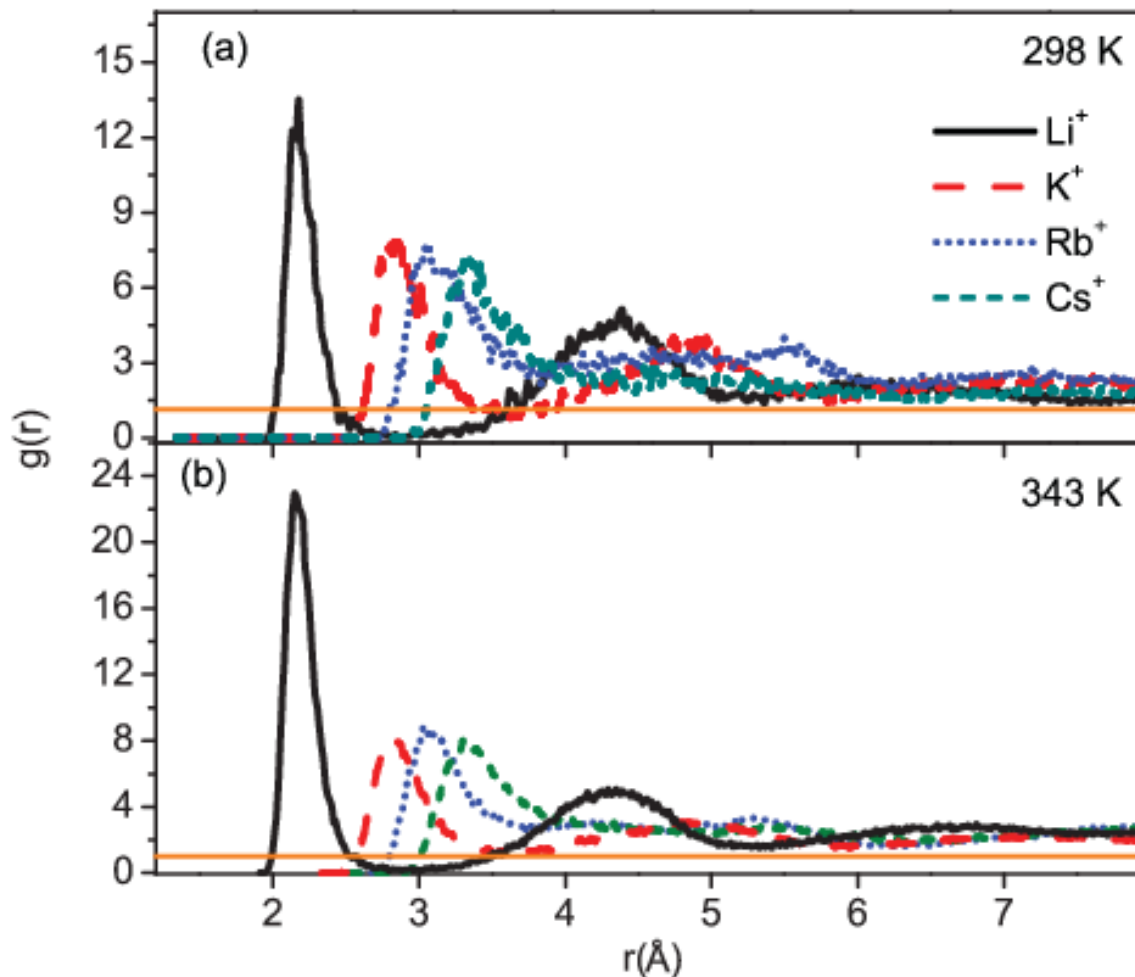


FIG. 8. RDFs of four ions around free phosphate oxygen atoms on the DNA backbones at two temperature. (a) ions-O⁻-(P) at 298 K. (b) ions-O⁻-(P) at 343 K.

Outline

1. Introduction

2. Applications

2.1 Cancer therapy

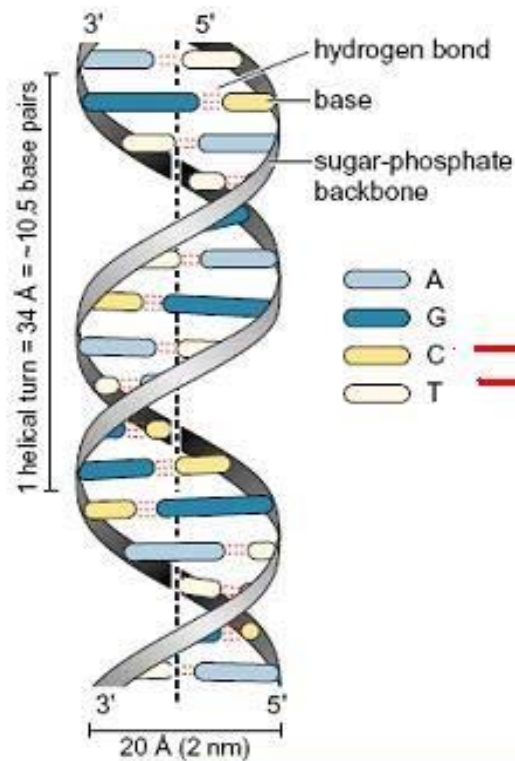
2.2 Seed breeding

2.3 Space radiation

2.4 Problems

3. A Multi-scale microscopic dynamical model

4. Conclusions



New Structure !

Physical process ($10^{-24} \sim 10^{-8} \text{s}$)

Chemical process (10^{-8}s)

Biological process (10^3s)

Nuclear process
($10^{-24} \sim 10^{-18} \text{s}$)

Electronic process
($10^{-18} \sim 10^{-12} \text{s}$)

Relaxation process
($10^{-12} \sim 10^{-8} \text{s}$)

Conclusions

- A preliminary version of:
A multi-scale microscopic dynamic approach to study interaction of heavy ions with biomolecules
- Smooth connections between different processes
Nucl. → Elec. → Relax. → Micro-dose
- Relationship between the structures and biological functions of biomolecules
- Your ideas, suggestions, comments ?

Collaborators:

X. Shen, J. Su, B. Gu, Z.P. Wang, H.Y. Zhou

Discussions:

Y. Su, T. Zhang, H.Z. Shang, J.H. Zhang, N. Y. Wang, CNST-BNU

G. F. Zhang, School of Life Sciences-BNU

W.J. Li, Z.G. Wang, H. Zhang, G.M. Jin, G.Q. Xiao, IMP-CAS

Z.Y. Zhu, Z. Y. Zhu, L. Yan, SINAP-CAS

Y.Z. Zhuo, K. Zhao, CIAE

B.A. Li, tamu-commerce-USA

Y.W. Zhang, ORNL-USA

P.M. Dinh, E. Suraud, Paul Sabatier University-France

R.M. Lynden-Bell, Queens/Cambridge University-UK

Funds:

- 1.National Natural Science Foundation of China under Grant No. 11025524
- 2.National Basic Research Program of China under Grant No. 2010CB832903
- 3.Sino-Ukraine Scientific Collaboration project under Grant No. CU08-04
- 4.Doctoral Station Foundation of Ministry of Education of China under Grant No. 200800270017
- 5.Beijing Beijing Radiation Center
- 6.Center of Theoretical Nuclear Physics, National Laboratory of Heavy Ion Accelerator of Lanzhou

Thank you for your attention !